The Role of Hexokinase II in the Regulation of Glycolysis and Cisplatin Sensitivity in Ovarian Cancer

Chae Young Han, M.Sc.

This thesis is submitted as a partial fulfillment of the Ph.D. program in Cellular and Molecular Medicine, Faculty of Medicine, University of Ottawa, Ottawa, Canada

Cellular and Molecular Medicine
Faculty of Medicine
University of Ottawa

Abstract

OVCA is the most lethal gynecological cancer, due primarily to late diagnosis and chemoresistance (Canada, 2014; Society, 2014b). CDDP resistance is a major hurdle to successful therapy (MayoClinic, 2014). The mechanism of chemoresistance is multi-factorial including defects in apoptotic pathway and key tumor suppressor as well as dysregulation of metabolism (Borst et al., 2000; Galluzzi et al., 2012a; Siddik, 2003). Elevated aerobic glycolysis is a major source for fulfilling high energy demand of cancer, but the role of metabolic reprogramming and its regulatory mechanism in OVCA cells remain unknown. p53 is a key tumor suppressor involved in apoptosis and frequent defect of p53 (> 80%) exist in epithelial OVCA. HKII is a key metabolic enzyme involved in the first step of glycolysis and its frequent presence in the mitochondria (80% >) has been reported in multiple cancers. We demonstrate here that CDDP-induced, p53-mediated HKII down-regulation and mitochondrial p53-HKII interaction are determinants of chemosensitivity in OVCA. CDDP decreased HKII (mRNA abundance, protein level), altered its cellular localization and glycolysis in p53-wt chemosensitive OVCA cells, a response loss or attenuated in p53 deficient cells. HKII depletion sensitized chemoresistant cells to CDDP -induced apoptosis in a p53- dependent manner. In addition, p53 binds to HKII and facilitates its nuclear localization. Mechanistically, our data suggest that CDDP-activated p53 (phosphorylated p53; P-p53 Ser15) interacts with HKII in the nucleus for its regulation. Upon entry to the nucleus, P-p53(Ser15) transcriptionally regulates HKII by promoter binding, contributing to the regulation of HKII and aerobic glycolysis, eliciting apoptosis in chemosensitive OVCA cells. Conversely, this response is compromised in p53 defect chemoresistant cells. Using proximity ligation assay (PLA) in human OVCA cell lines and primary tumor cells and tumor sections from OVCA patients, we have demonstrated that nuclear HKII-P-p53(Ser15) intracellular trafficking is associated with chemosensitivity *in vitro* and *in vivo*. Furthermore, the nuclear HKII-P-p53(Ser15) interaction may be useful as a biomarker for chemosensitivity in multiple epithelial subtypes of OVCA.

Table of Contents

List of Figures

List of Tables

List of Abbreviations

ABC	ATP binding cassette family
AIF	Apoptosis inducing factor
Akt	akaProtein Kinase B, PKB
Apaf-1	Apoptotic protease activating factor-1
ARF	Alternate open reading frame
ATM	Ataxia telangiectasia mutated
ATR	Ataxia telangiectasia mutated and Rad3-Related
ATRIP	ATR interacting protein
ATP	Adenosine triphosphate
BAD	Bcl-2 antagonist of cell death
BaK	Bcl-2 antagonist killer
Bax	Bcl-2-associated X protein
Bcl-2	B-cell lymphoma-2
Bcl-xL	B-cell lymphoma-extra large
BER	Base excision repair
BH3	Bcl-2 homology domain 3
Bid	BH3-interacting domain death agonist
Bim	Bcl-2 interacting mediator of cell death
BRAF	B-raf murine sarcoma viral oncogene homolog
BRCA	Breast cancer susceptibility gene
CA-125	Cancer antigen 125
CC	Clear cell ovarian carcinoma

CDDP	Cis-diamminedichloroplatinum (II) or cisplatin
CDK1	Cyclin dependent kinase 1
cDNA	Complementary deoxyribonucleic acid
Chk1	Checkpoint kinase 1
CI	Confidence Interval
Ctr1	Copper transporter homolog 1
DAPI	4´,6-diamidino-2-phenylindole
DDR	DNA damage response
DIABLO	Direct IAP binding protein with low pI
DMEM	Dulbecco's modified Eagle Medium
DMSO	Dimethyl sulfoxide
DNA	Deoxyribonucleic acid
DN-Akt	Dominant negative Akt
DR	Death Receptor
2-DG	2-Deoxy-D-Glucose
ERCC1	Excision repair cross-complementing rodent repair deficiency, complementation group 1
ECAR	Extracellular acidification rate
ER	Endoplasmic reticulum
Fas L	Fas ligand
FCCP	Carbonyl cyanide-4-(trifluoromethoxy)phenylhydrazone (FCCP)
FIGO	International Federation of Gynecology and Obstetrics
FITC	Fluorescein isothiocyanate

FLICE	Fas-associated death domain-like interleukin 1 β-converting enzyme
FLIP	FLICE-like inhibitory protein
FOXO-1	Forkhead transcription factor 1
GAPDH	Glyceraldehyde phosphate dehydrogenase
G-6-P	Glucose 6 Phosphate
GSH	Glutathione
HKII	Hexokinase II
HIF1	Hypoxia inducible factor
HR	Hazard Ratio
HRP	Horseradish peroxidase
IF	Immunofluorescence
IHC	Immunohistochemistry
IRB	Institutional Review Board
kD	Kilodalton
LDH	Lactate dehydrogenase
Mk	Monkey
KRAS	Kirsten rat sarcoma viral oncogene homolog
MAPK	Mitogen-activated protein kinase
MDM	Murine double minute
MDR	Multi drug resistance
Mito-HKII	HKII bound to mitochondria
MRP	Multi drug resistance protein
MOI	Multiplicity of infection

MOMP	Mitochondrial outer membrane permeabilization
mPTP	Mitochondrial permeability transition pore
mRNA	Messenger ribonucleic Acid
mTOR	Mammalian target of rapamycin complex
mTORC2	mTORC2 Mammalian target of rapamycin complex
NADH	Nicotinamide Adenine Dinucleotide Hydrogen
NADPH	Nicotinamide Adenine Dinucleotide Phosphate
NER	Nucleotide excision repair
NF- κB	Nuclear factor kappa B
NLS	Nuclear localization signal
NOXA	NADPH oxidase activator
OCR	Oxygen Consumption Rate
OPA1	Optic Atrophy
OS	Overall Survival
OSE	Ovarian surface epithelium
OVCA	Ovarian cancer
PAGE	Polyacrylamide gel electrophoresis
P-Akt	Phosphorylated Akt
PARP	Poly (adenosine diphosphate) polymerase
PBS	Phosphate buffered saline
PDC	Patient Derived Cells
PDK-1	Phosphatidylinositol-dependent protein kinase-1
PDX	Patient Derived Tumor Xenograft Model

PFK	Phosphofructose kinase
PFI	Progression Free Interval
PFS	Progression Free Survival
PH	Pleckstrin homology domain
PI3K	Phosphoinositide-3 kinase
PIP2	Phosphatidylinositol-4,5-bisphosphate
PIP3	Phosphatidylinositol-3,4,5-trisphosphate
PKB	Protein kinase B
PKM	Pyruvate kinase
PLA	Proximity ligation assay
PMSF	Phenylmethylsulfonyl fluoride
P-p53	Phosphorylated p53
PTEN	Phosphatase and tensin homolog
PUMA	p53-upregulated mediator of apoptosis
RIPA	Radioimmunoprecipitation assay buffer
RT	Reverse transcriptase
ROS	Reactive oxygen species
qPCR	Quantitative polymerase chain reaction
RPMI	Roswell Park Memorial Institute
RTK	Receptor tyrosine kinase
Ser	Serine
SDS	Sodium dodecyl sulfate
SEM	Standard error of the mean

siRNA	small interfering RNA
SMAC	Second mitochondria-derived activator of caspases
Thr	Threonine
TBS	Tris-buffered saline
TTBS	Tris-Tween Buffered Saline
TCA	Tricarboxylic acid
TNFR	Tumor necrosis factor receptor
TNFR1	Tumor necrosis factor receptor 1
TP53	p53 gene
TOM20	Translocase of outer membrane
TVUS	Transvaginal ultrasound
UNG2	Uracil DNA glycosylase 2
UV	Ultraviolet
Wt	Wild type
XIAP	X-linked inhibitor of apoptosis protein

Acknowledgment

I would like to sincerely thank my research mentor Professor Benjamin K Tsang for his relentless guidance, advice, energy, and passion for science which enables me to complete my doctoral studies. He motivated me when I was frustrated and always brought out the best in me throughout the past years. I would like to express appreciation for his mentorship, encouragement, and patience. I also appreciate his financial and intellectual support.

I would like to thank my committee members, Dr. Barbara Vanderhyden, Dr. Mary-Ellen Harper and Dr. Chantal Matar for their scientific advice and encouragement. Particularly, I am grateful to Dr. Harper and Dr. Vanderhyden for our research collaboration on cancer cell metabolism and for making primary human ovarian cancer cells available to my studies, respectively.

I would like to thank my collaborators locally and internationally, including Dr. David Patten, for the opportunity to work together, Professor Annie Cheung, University of Hong Kong and Professor Anne-Marie Mes-Masson, Institut du cancer de Montréal for providing clinical samples used in my studies, and special thanks to Dr. Yong Sang Song and his team for not only providing clinical samples for my studies but also the opportunity to work in their laboratory.

I would also like to thank the past and present members of Dr. Tsang lab, particularly Ahmed Ali and Jung Jin Lim for teaching me new techniques, their thoughtful critique of my experimental data, valuable ideas, and emotional support, as well as how best to adapt and survive in a culturally diverse laboratory environment and graduate student life.

I would like to thank the funding agencies for their financial support as an essential component of my project: Admission scholarship from University of Ottawa during Ph.D years and the Canadian Institute of Health Research (CIHR; MOP-126144).

I have to thank my parents for their support and encouragement, which helped me to complete this study. Special thanks to my husband, Chan Sik Uhm for helping me to remain motivated, his advice, and enjoyable moments with him.

Finally and most importantly, I would like to thank **God** who guided me through my academic journey during my Ph.D studies and in my life in Canada. His presence and plan for me encouraged me and led me in the right direction in good and difficult times.

Chapter 1. Introduction

1. 1 Ovarian Cancer

1.1.1 Incidence & Mortality

Ovarian cancer (OVCA) has a high mortality rate and is the fifth leading cause of cancer deaths in women (Siegel et al., 2017). In women diagnosed with OVCA, the prognosis is poor and with an average of 30-40% of patients surviving longer than 5 years after diagnosis. A woman's risk of developing OVCA is about 1 in 79, and the chance of dying from it is approximately 1 in 108 (CanadianCancerSociety, 2017). In 2017 in Canada, 2,800 women were diagnosed with OVCA and 1,800 patients died from it (CanadianCancerSociety, 2017).

1.1.2 Symptoms & Diagnosis

Unfortunately, late diagnosis and chemoresistance have become major hurdles to effective OVCA treatment. 75% of OVCA cases are diagnosed in advanced stages with no apparent symptoms (Ebell et al., 2016). The most common symptoms of OVCA include: bloating, pelvic or abdominal pain, trouble eating or feeling full easily, frequent and urgent needs to urinate, constipation or menstrual change, fatigue, and back pain. These symptoms can be easily ignored and are not organ specific which can be either caused by non-cancerous disease or cancer in other organs (Kurman and Shih Ie, 2008).

The diagnosis of OVCA often needs a physical pelvic exam, imaging test (e.g., transvaginal ultra sound), and blood test for cancer antigen 125 (Hennessy et al., 2009). However, these tests have limited applicability because other diseases and conditions such as endometriosis can cause false positive results (Benedet et al., 2000; Kurman and Shih Ie, 2008). Therefore, these tests are not specific enough to detect OVCA. Generally, confirmation of the diagnosis requires a biopsy where a sample is collected during a laparoscopic surgery. Thus, more reliable methods need to be developed for early and precise detection of OVCA (Society, 2018).

1.1.3 Risk Factors

A risk factor of cancer indicates any substance or condition that increases the likelihood of developing OVCA (Society, 2018). One major risk factor is genetics, which represents 20-25% of all cases. Mutation in one of two genes [breast cancer gene 1(BRCA1) or BRCA2] is responsible for 10-15% of OVCA (McLaughlin et al., 2007). Hereditary nonpolyposis colorectal cancer (HNPCC or Lynch Syndrome) also contributes to 12% of incidence of OVCA. A family history of OVCA elevates the risk of cancer development during a woman's lifetime by approximately 5-fold. Previous medical history of other cancers including breast, uterus, colon or rectal cancers, also increases the risk of developing OVCA. Having endometriosis increases the likelihood of developing endometroid OVCA by approximately 2 to 3-fold (Moll et al., 1990; Rosen et al., 2009). Age is another significant risk factor for the development of OVCA. Approximately half of all OVCA cases have been observed to occur in women that are 63 years of age or older (Prat and Oncology, 2015; Vang et al., 2009). In addition, obesity and reproductive history (no pregnancy or pregnancy in old age) can increase the risk of development of OVCA. Conversely, long-term use of (longer than 3-6 months) birth control pill or specific gynecological surgeries such as tubal ligation (tied fallopian tubes) or hysterectomy can lower the risk of developing OVCA by up to 60% (Cook et al., 2017; Narod et al., 1998). In case of germ cell tumor, risk factors are often associated with the disorder of sex development such as atypical gonadal or chromosomal development (e.g., presence of Y chromosome in female)(Cools et al., 2011). Individuals with rare genetic syndrome called "Peutz-Jeghers syndrome" are more susceptible to develop both epithelial ovarian cancer and stromal tumor. Peutz-Jeghers syndroms is caused by mutation of *STK11* and develops polyps in the stomach and intestine during their teenage years(Banno et al., 2013).

1.1.4 Stage & Grade of OVCA

Stage and grade of the OVCA are critical for determining the progression of the disease, effective treatment planning, and predicting prognosis of OVCA patients. Staging classifies cancer based on the size and its extent. According to the International Federation of Gynaecology and Obstetrics (FIGO), OVCA is divided into four stages which are confirmed based on the result of surgery as follows (Benedet et al., 2000; Prat and Oncology, 2015):

Stage I: The tumor is confined to one or both ovaries.

Stage II: The tumor involves one or both ovaries with pelvic extension and the presence of ascites or peritoneal washing containing malignant cells.

Stage III: The tumor involves both ovaries with peritoneal implants outside the pelvis or the tumor is limited to the pelvis.

Stage IV: The tumor involves one or both ovaries with distant metastases to other organs outside the abdomen & pelvis (e.g., lymph node and liver). There is a fluid build-up in the pleural cavity with an accumulation of ascites and cancer cells.

The grade of a cancer is a description of the morphology and growth rate of the cancer cells from the biopsy compared to normal cells under a microscope (Hennessy et al., 2009; McCluggage, 2011). Differentiation implies how different the cancer cells are compared to normal cells. In low grade cancers, the cancer cells are well differentiated, like normal cells, tend to grow slow and less likely to spread. Conversely, high grade serous cancer cells are poorly differentiated or undifferentiated with abnormal shape, with tendency to grow more quickly (Vang et al., 2009).

1.1.5 Histological Subtype of OVCA

The histological subtype of OVCA is usually defined by where the cancer cells originated in the ovary and tumor cell morphology. Over 90% of OVCA arises from the epithelial surface of

the ovary or the distal fallopian tube, the remaining 10% tend to originate from germ cells or stromal cells. The histologic subtypes differ in risk factors, biological action, and treatment response (Rosen et al., 2009) making this information important for the determination of treatment and prognosis **(Table 1.1).**

1.1.5.1 Epithelial OVCA

Epithelial OVCA is the most frequent subtype of OVCA, accounting for 90% of OVCA incidences. These tumors arise from the epithelial cells that line or cover the ovaries and fallopian tubes (Rosen et al., 2009; Vang et al., 2009). Epithelial ovarian tumors are classified into five histologic, subtypes [low grade serous, high grade serous (30-70% as serous subtype), endometrioid (10-20%), mucinous (5-20%), and clear cell (3-10%) with distinctive histology, molecular profiles, and pathogenesis (Rosen et al., 2009).These histologic subtypes are largely classified in type I tumors which is slow growing and genetically stable (low-grade serous, endometrioid, mucinous, and clear cell) and type II tumors which is genetically unstable (high-grade serous, undifferentiated carcinoma, and carcinosarcoma) with higher rate of *TP53* mutation (> 80%) (Kurman and Shih Ie, 2010; Shih and Kurman, 2004).

A. High grade & Low grade Serous Ovarian Carcinoma

Serous OVCA is the most common type and shows a mixture of cystic, papillary, and solid growth architecture. Its morphology resembles a fallopian tube. It is usually large, bilateral, and often invades through the ovarian capsule and the surface of the ovary. Serous can be further sub-divided into a high-grade and low grade (Rosen et al., 2009).

High grade serous OVCA accounts for the majority of epithelial OVCA cases observed in patients. Although high grade serous tumors are believed to originate from the ovarian surface epithelium, recent evidences suggest that the alternative origins of it is epithelial lining of the fimbrial segments of the fallopian tube which is near to the ovaries or mis-localized uterine tissue

(endometriosis) (Dubeau, 2008; Kurman and Shih Ie, 2011). High grade serious OVCA is frequently caused by *TP53* mutation (> 80%) with low incidences of mutations in Kirsten rat sarcoma viral oncogene homolog (*KRAS*), V-raf murine sarcoma viral oncogene homolog B *(BRAF),* or estrogen-related receptor beta type 2 (*ERRB2*) genes (Singer et al., 2002; Singer et al., 2003; Singer et al., 2005). High levels of chromosomal instability have also been reported in high grade serious OVCA (Vang et al., 2009). High grade serous carcinomas tend to be highly aggressive and initially respond to platinum-based chemotherapy, but frequently develop resistance.

Low grade serous OVCA is relatively rare, accounting for approximately 9% of all serous subtype OVCAs. These tumors are often slow growing, detected in a younger woman with good prognosis (75% survival rate). Despite its similar name, high grade and low grade subtypes are distinctive type of tumor with a different underlying molecular profile, pathogenesis, and responsiveness to therapy. Low grade serous carcinoma is characterized by frequent mutations (70%) of *KRAS*, *BRAF*, or *ERRB2* (Kaldawy et al., 2016). Being different from high grade serous, *TP53* mutations are uncommon in low grade serous OVCA (Singer et al., 2005).

B. Endometrioid Ovarian Carcinoma

The endometrioid subtype of OVCA is frequently diagnosed in early stages and tends to have a better prognosis. Most endometroid subtypes are low grade adenocarcinomas, often associated with endometriosis (McCluggage, 2011). Endometroid cancers exhibit microsatellite instability and frequent mutation of key tumor suppressor genes, including *TP53* (60%) and phosphatase tensin homolog (*PTEN*; 35-40%) (Sato et al., 2000). Due to the absence of functional PTEN, activating mutations of phosphatidylinositol 3-kinase (PI3K) frequently occur, leading to PI3KCA hyperactivation, activation of the akaProtein Kinase B, PKB (Akt) pathway and contributing to cancer progression.

C. Mucinous Ovarian Carcinoma

Mucinous tumors are usually large (average 18cm) and unilateral with multiloculate cystic mass with mucus-containing fluid. It is heterozygous in its cellular composition and differentiation (McCluggage, 2011). In mucinous ovarian tumors, *KRAS* mutations occur in approximately 75% of cases (Enomoto et al., 1991). Borderline and invasive mucinous tumors contain both papillae and solid areas. Necrosis & hemorrhage frequently occur in borderline and benign mucinous tumors.

D. Clear Cell Ovarian Carcinoma

Histology of clear cell ovarian carcinomas (CC) is characterized by the presence of clear cytoplasm rich in glycogen, resembling morphology of clear cell renal carcinomas (Bell, 2005; Kurman and Shih Ie, 2008). Unlike serous carcinoma, CC often presents as a large pelvic mass in early stages and thus tends to be diagnosed early. Advanced-stage CC tends to have a poor prognosis with resistance to CDDP-based chemotherapy (Rosen et al., 2009). Little is known about the development and progression of CC. Studies have shown that 5–10% of cases are associated with endometriotic lesions; however, there is little molecular evidence to support an ectopic origin of CC. The majority of CC occurs due to *PTEN* mutations/ deletion or PI3KCA activation (Rosen et al., 2009). Although *TP53* mutations are frequently found in various epithelial subtypes, particularly serous ovarian carcinoma, it is conspicuously absent in CC (Okuda et al., 2003; Skirnisdottir et al., 2005), implying that other molecular mechanisms are involved in CC. It is notable that the expression of the pro-apoptotic protein Bcl2-associated X protein (Bax) is higher in the early stage of CC, but the anti-apoptotic protein B-cell lymphoma **2 (**Bcl-2) is highly expressed in metastatic CC (Sheikh-Hamad et al., 2004; Simon et al., 2003). Lower relative ratio of Bcl-2/Bax is frequently observed in early stage whereas higher level of the ratio is found in advanced CC, associated with its prognosis.

1.1.5.2 Germ Cell Tumors

Ovarian germ cell tumors are malignancies that originate from the germ (egg) cells of the ovary. Ovarian germ cell tumors account for 5% of OVCA. Germ cell tumors often occur in teenage

girls or young women (Di Tucci et al., 2017). In many cases, including advanced stages, it is unilateral and curable (70%) with standard chemotherapy.

1.1.5.3 Stromal/Sex-Cord Tumors

Ovarian stromal/sex-cord tumors are also rare, accounting for 7% of OVCA. They originate from the cells composing the connective tissue that holds the ovary together and follicular cells (granulosa cells) which secrete sex hormones (Kurman and Shih Ie, 2008). The histopathologic character of stromal/sex-cord tumors is different from the prevalent epithelial ovarian tumors as they show low-grade disease with a good prognosis. Since the constituent cells of stromal tumors are engaged in the production of steroid hormones such as androgens, estrogens, and corticoids, these tumors are frequently associated with multiple hormone-mediated syndromes such as hyperandrogenism or hyper-estrogenic symptoms (Horta and Cunha, 2015).

Table 1.1 Histological subtypes of epithelial OVCA

Histological subtype of epithelial OVCA are described based on precursor lesions, pattern of spread, molecular abnormalities, chemotherapeutic response, prognosis. Abbreviation used in this table are as follows. [Clear cell carcinoma (CCC), Endometrial carcinoma (EC), Estrogen receptor (ER), high-grade serous carcinoma (HGSC), Low-grade serous carcinoma (LGSC), Mucinous carcinoma (MC), and serous borderline tumor (SBT)], Source: (Chris M.J. Conklin, 2013)

Table 1.1 Histological subtypes of epithelial OVCA

	HGSC	LGSC	MC	EC	CCC
Precursor lesions	Tubal intraepithelial carcinoma	SBT	Cystadenoma	Endometriosis	Endometriosis
Pattern of spread	Very early	Early	Often confined to ovary	Often confined to ovary	Often confined to pelvis
Molecular abnormalities	*TP53*; *BRCA1/2*; chromosomally unstable	*BRAF/KRAS*; chromosomally stable	*KRAS/HER-2*	*PTEN*, β-catenin; microsatellite instability	*PIK3CA*; *KRAS*; *PTEN*; *ARID1A*; microsatellite instability
Response to chemotherapy	High	Intermediate	Low	High	Low
Prognosis	Poor	Intermediate	Favorable	Favorable	Intermediate

CCC: Clear cell carcinoma; EC: Endometrial carcinoma; ER: Estrogen receptor; HGSC: High-grade serous carcinoma; LGSC: Low-grade serous carcinoma; MC: mucinous carcinoma; SBT: Serous borderline tumor.

Medscape Source: Expert Rev of Obstet Gynecol © 2013 Expert Reviews Ltd

1.1.6 Treatment

In order to effectively plan a treatment strategy for OVCA, multiple factors must be considered including: the stage, grade, the histologic subtype of the tumor, potential plan for pregnancy, patient age, and medical history (new or recurrent case and presence of another disease). There are several clinical end points to examine the effectiveness of treatment, including progression free interval (PFI), progression-free survival (PFS), and overall survival (OS) **(Fig. 1.1)**. PFI is the length of time from the termination of chemotherapy following surgery to first progression or relapse of cancer (Gallion et al., 2006). PFI is an indicator of chemo-responsiveness and the prognosis in OVCA patients (Covens et al., 2002; Rosen et al., 2009) and generally a 6 month (m) time defines the responsiveness to chemotherapy: chemosensitivity (PFI $\geq$ 6 m) and chemoresistance (PFI < 6 m). PFS is the length of time from diagnosis or starting date of treatment to first evidence of tumor progression (Ehmann et al., 2014; Matulonis et al., 2015). OS is the length of time from the date of diagnosis or the start of treatment to the last follow-up. Usually, 5 year survival rate is used to estimate the prognosis of a particular disease from the point of diagnosis (MayoClinic, 2014; Rosen et al., 2009).

The standard treatment approach is to surgically remove as much of the tumor as possible from the abdomen, known as surgical debulking followed by adjuvant chemotherapy (Rose et al., 2004; Society, 2014a) (Benedet et al., 2000). The purpose of surgery is also to confirm the stage of OVCA. In addition to debulking surgery, total hysterectomy (removing uterus without removing ovaries) and bilateral salpingo-oophorectomy (removing ovaries and fallopian tubes) surgeries are common methods with tissue removal of lymph nodes and/or omentum, depending on the condition (Cannistra SA, 2015). Conversely in patients with wide spread cancer who are unable to undergo standard debulking, interval debulking surgery after three cycles of short neoadjuvant chemotherapy has become a possible alternative treatment option (Chang and Bristow, 2012). Although neoadjuvant chemotherapy does not significantly improve either PFS or overall survival

rates compared with conventional debulking followed by chemotherapy, they do exhibit significantly lower adverse effect and mortality rates (Rose et al., 2004; Sato and Itamochi, 2014; Vergote et al., 2010).

Regardless of the surgical option used to treat the OVCA, further treatment with chemotherapy is required in most cases to kill any remaining cancer cells and to prevent further growth. Usually, platinum compounds, such as cisplatin (CDDP; Cis-diammineddichloroplatinum) or carboplatin, combined with tubulin targeting drugs, including Paclitaxel (Taxol) or Docetaxel are commonly used. The typical course of chemotherapy for OVCA involves 3 to 6 cycles of intravenous injection (1 month per cycle). In some cases, chemotherapy can be directly injected into the abdominal cavity (intraperitoneal) with the most concentrated dose of the drugs (Cannistra SA, 2015; Society, 2014a). Although 75% of patients in advanced stage OVCA initially respond to the platinum/taxol based chemotherapy, majority of them (> 90%) experience recurrence within two years, resulting in treatment barrier and cancer death. On the other hand, 25% of rest of patients did not respond to chemotherapy at all. Therefore, more effective chemotherapy and strategies are urgently needed (Agarwal and Kaye, 2003).

Figure 1.1 Schematic diagram of clinical endpoints in course of cancer therapy

Length of progression free survival (PFS, from starting of 1st treatment to recurrence of cancer), progression free interval (PFI, from the end of 1st chemotherapy to recurrence of cancer), and overall survival (OS, from starting of 1st treatment to last follow up) are illustrated based on its definition during the course of treatment (Benedet et al., 2000; Hennessy et al., 2009).

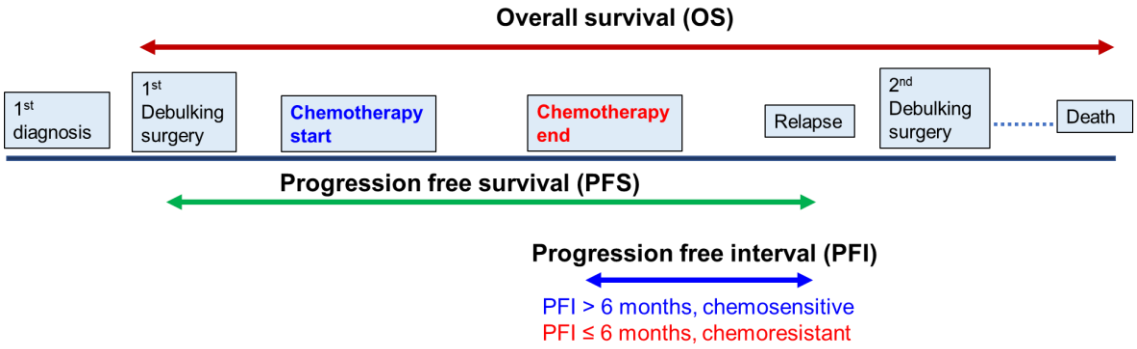
Overall survival (OS)
1st diagnosis
1st Debulking surgery
Chemotherapy start
Chemotherapy end
Relapse
2nd Debulking surgery
Death
Progression free survival (PFS)
Progression free interval (PFI)
PFI > 6 months, chemosensitive
PFI ≤ 6 months, chemoresistant

1.2 Chemoresistant OVCA

1.2.1 Cisplatin & Mechanism of Action

Cisplatin (CDDP; Cis-diammineddichloroplatinum) analogues (e.g., carboplatin and oxaliplatin) exhibiting the similar mechanism of action of its parent compound, are the most commonly used platinum-based chemotherapy for OVCA treatment. CDDP, $[Pt(NH_3)_2Cl_2]$ consists of double charged platinum ion connected to two amino and two chloride ligands, in cis configuration (Galluzzi et al., 2012a; Siddik, 2003). CDDP causes DNA damage by irreversibly intercalating DNA strands by forming inter- and intra-strand DNA adducts **(Fig.1.2).** Mechanistically, upon entering the cell, the chloride atoms of CDDP are displaced by water (aquation reaction), creating a positively charged electrophile. This enables the platinum atom to bind to negatively charged DNA, forming CDDP-DNA adducts (Jamieson and Lippard, 1999). The majority of CDDP-DNA adducts are intra-strand 1,2-ApG, 1,2-CpG, and 1,3-GpXpG crosslinks [Guanine (G) or Adenine (A), Cytosine (C)], which cause distortion of the DNA helix and initiate DNA damage response (Crul et al., 2002; Kelland, 2000b; Moggs et al., 1997). The cross-linking induced by the CDDP-DNA adducts distorts and abnormally unwinds the DNA duplex, interfering with DNA replication and/or transcription. This results in DNA damage and subsequently activates the apoptosis pathway, leading to cancer cell death (Lovejoy et al., 2008; Wang and Lippard, 2005).

Figure 1.2 Formation and effects of CDDP-DNA adducts

Cisplatin undergoes aquation reaction to hydrolyze chloride ions, forming positively charged CDDP $[Pt(NH3)2Cl(OH2)]^{+}$ and $[Pt(NH3)2(OH2)2]^{2+}$ inside the cell. Positively changed platinum atom of CDDP covalently binds to the N7 position of purines [Guanine (G) or Adenine (A)], forming intra- and inter-strand crosslinks and leading to distortion of DNA helices. CDDP-DNA adducts cause various cellular responses including replication arrest, transcription inhibition, cell cycle arrest, DNA repair and apoptosis (Adapted from Lippard 2005) (Wang and Lippard, 2005).

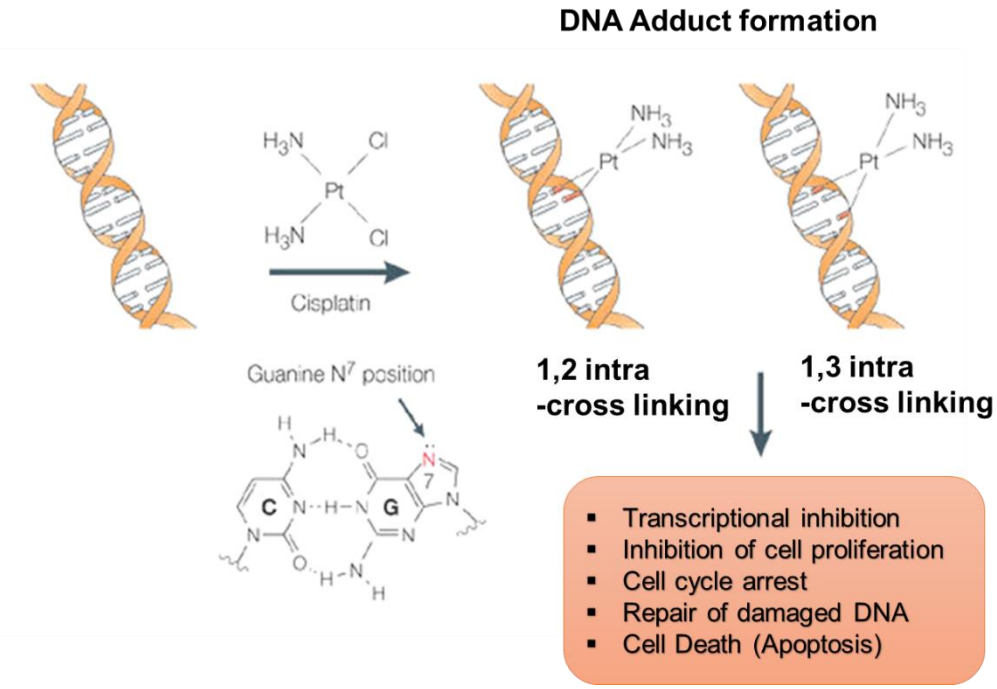
DNA Adduct formation
H3N
Cl
Pt
H3N
Cl
Cisplatin
NH3
NH3
Pt
NH3
NH3
Pt
Guanine N7 position
1,2 intra
-cross linking
1,3 intra
-cross linking
Transcriptional inhibition
Inhibition of cell proliferation
Cell cycle arrest
Repair of damaged DNA
Cell Death (Apoptosis)

1.2.2 Multiple Mechanisms of CDDP Resistance

In OVCA, chemoresistance is a major hurdle to effective therapy. Chemoresistance is usually determined based on clinical recurrence occuring within 6 months after the completion of platinum-containing chemotherapy (Benedet et al., 2000). Although first-line chemotherapy works effectively for more than 80% of OVCA, recurrence occurs in a majority of patients approximately 15 months from the time of diagnosis. Therefore, chemoresistance severely limits the effectiveness of OVCA treatment (Hennessy et al., 2009). The underlying mechanism of CDDP chemoresistance is multifactorial, partly due to the defects in cancer cells including **(Fig. 1.3)**: 1) increased DNA repair (Hu et al., 2016),; 2) increased activity of efflux pumps leading to decreased intracellular drug accumulation (Borst et al., 2000; Jekunen et al., 1994; Lovejoy et al., 2008); 3) enhanced drug detoxification and increased metabolism, and 4) dysregulation of drug-induced apoptosis (Galluzzi et al., 2012a; Shen et al., 2012; Wang and Lippard, 2005).

A. Elevated DNA Repair

Elevated DNA repair contributes to CDDP resistance in response to CDDP-induced cell damage. DNA repair mechanisms include nucleotide excision repair (NER), mismatch repair, homologous recombination (HR), and base excision repair. NER, one of DNA repair mechanism is strongly associated with CDDP resistance in OVCA (Li et al., 1998). DNA adducts induced by CDDP are primarily repaired by the NER pathway; damaged nucleotides are excised from DNA on both sides of adducts followed by DNA synthesis to restore the genetic integrity. The NER pathway involves multiple proteins, including the excision repair cross-complementing 1 (ECRR1) and a single-strand DNA endonuclease which removes the bulky DNA adducts. High ECRR1 expression is associated with elevated DNA repair and leads to poor CDDP responsiveness in OVCA as a result (Dabholkar et al., 1992; Li et al., 1998).

CDDP-induced inter-strand adducts also lead to double-strand breaks mainly repaired by homologous recombination (HR). HR involves two critical proteins BRCA 1 and BRCA2, which

are frequently mutated in inherited ovarian and breast cancers (Narod and Foulkes, 2004; Venkitaraman, 2002; Venkitaraman, 2014). Although BRCA1/2 deficient tumors tend to be hypersensitive to DNA crosslinking agents such as CDDP, BRCA2 restoration by secondary mutation could cause CDDP resistance in OVCA cells (Edwards et al., 2008; Sakai et al., 2008)

B. Reduced CDDP Accumulation

Decreased CDDP accumulation plays an important role in determining the resistance of OVCA to CDDP. CDDP enters cells by passive diffusion across the plasma membrane because the uptake of CDDP is relatively slow (Kelland, 2000a). A highly conserved ATPase cooper transporter (Ctr1) functions to uptake in cells as a major transporter of platinum-based drugs. *In vivo* Ctr1 knockout mouse model, intracellular accumulation of CDDP is decreased by approximately 80%, leading to platinum resistant phenotypes (Ishida et al., 2002; Lee et al., 2011). High Ctr1 expression is positively associated with CDDP sensitivity and longer survival rate in OVCA patients (Lee et al., 2011). On the other hand, increased expression of the ATP-dependent efflux pump, ATP Binding Cassette Subfamily B Member (ABCB1) which encodes the membrane drug transporter P-glycoprotein (also known as multi drug resistance protein, MDR1), is responsible for drug resistance (Shen et al., 1986). MDR1 controls the drug efflux, thereby reducing the intracellular concentrations of CDDP preventing it from acting upon the DNA to induce apoptosis (Arts et al., 1999).

C. Increased Drug Detoxification & Metabolism

Drug detoxification and increased metabolism mediated by metabolic enzymes also affect the responsiveness of OVCA to CDDP treatment. Glutathione (GSH) is a highly abundant small peptide in the cell and functions to maintain cellular oxidative balance as a free radical scavenger. GSH is associated with CDDP resistance in multiple types of cancer. The intracellular concentrations of GSH have been demonstrated to be higher in many chemoresistant cancer cells (Godwin et al., 1992; Zhang et al., 2001). GSH has a high affinity for CDDP and forms GSH-

adduct, which interferes with CDDP action. GSH conjugates organic substances and the metabolites of CDDP catalyzed by cytochrome 450, facilitating export of these substances via transmembrane pumps such as MDR1 and multidrug resistance protein 2 (MRP2) (Zhang et al., 2001). In cancer cells, GSH serves as a cofactor for multidrug resistance protein 2- (MRP2), which provides protection against oxidative stress (Myint et al., 2015). Glutaminolysis is a series of biochemical reactions by which glutamine is broken into multiple amino acids including glutamate, aspartate, CO_2, pyruvate, lactate, alanine, and citrate. Glutaminolysis also increases CDDP resistance through activation of the mammalian target of rapamycin complex 1 (mTORC1) cascade, which triggers cell growth and inhibits autophagy (Zhao et al., 2013).

D. Dysregulation of Oncogene and Apoptosis

Suppression of apoptosis is a determinant in chemoresistance in cancer cells. Many death and survival genes including oncogenes, which are regulated by extracellular factors, are involved in apoptosis. An oncogene has potential to transform a normal cell into a cancer cell when mutated; activated oncogenes can drive normal cells destined for apoptosis to abnormal cell proliferation and survival as a consequence of genetic alterations (Croce, 2008). On the other hand, tumor suppressor genes act to inhibit prevent tumor development. In many tumors, these genes are frequently inactivated or lost. Due to frequent genetic mutations of tumor suppressors (e.g., p53) and hyperactivation of oncogenes (e.g., PI3K and Akt), apoptotic responses are decreased in response to various chemotherapeutic drug or external stimuli (Antoun et al., 2018; Yuan et al., 2000). Moreover, malfunction of pro-apoptotic proteins [e.g., Bax, Bcl-2-associated death promoter **(**Bad)] or elevated anti-apoptotic proteins including inhibitor of apoptotic proteins (IAP) or Bcl-2 also result in decreased apoptosis (Fraser et al., 2003; Skirnisdottir et al., 2002).

Figure 1.3 Reprogramming tumor metabolism in chemoresistant OVCA

Metabolic reprogramming of cancer cells contributes to their transformation. The Warburg effect (see main text) often allows cancerous cells to maintain energy production in otherwise energy poor conditions. Genetic and environmental factors may transform normal cells to either chemosensitive or chemoresistant OVCA. However, the majority of chemoresistant cells stem from chemosensitive cancer cells that acquire their resistance due to multiple factors: increased DNA Repair, CDDP detoxification, increased metabolism, and the upregulation of multi-drug resistance and copper transporters. As a result, chemoresistant cells have markedly higher rates of proliferation, and their metabolism is less sensitive to bouts of chemotherapeutics. We and other, have also demonstrated that the recovery of defective p53 and PTEN can sensitize chemoresistant cells to chemotherapy.

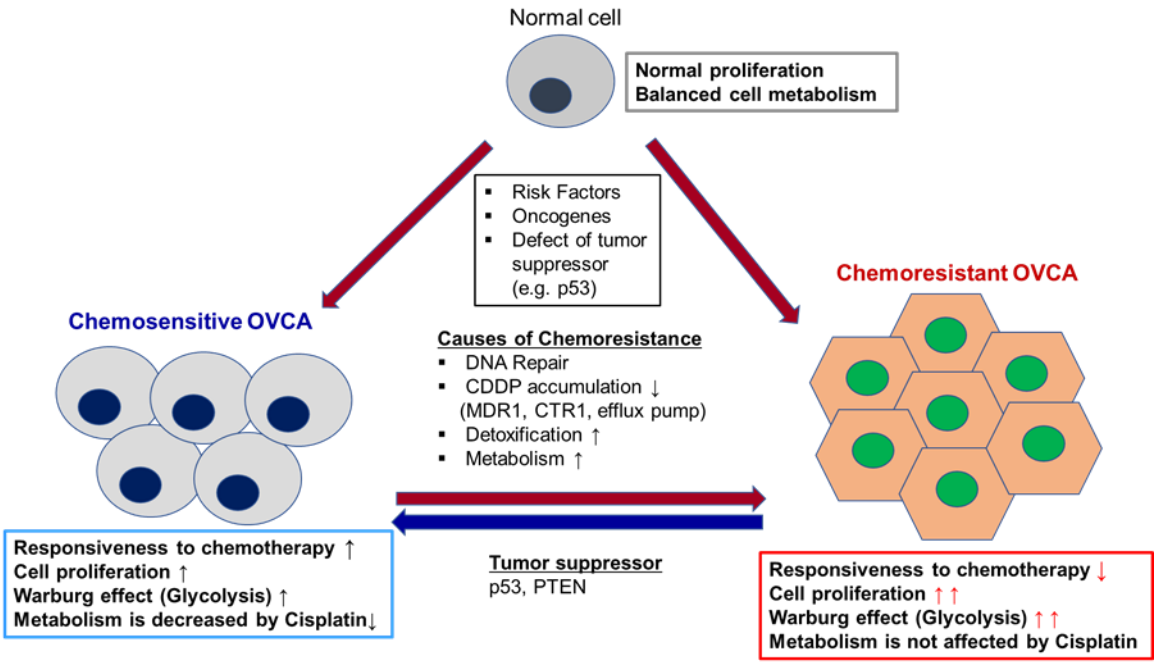
Normal cell
Normal proliferation
Balanced cell metabolism
Risk Factors
Oncogenes
Defect of tumor suppressor (e.g. p53)
Chemosensitive OVCA
Chemoresistant OVCA
Causes of Chemoresistance
DNA Repair
CDDP accumulation ↓ (MDR1, CTR1, efflux pump)
Detoxification ↑
Metabolism ↑
Responsiveness to chemotherapy ↑
Cell proliferation ↑
Warburg effect (Glycolysis) ↑
Metabolism is decreased by Cisplatin↓
Tumor suppressor
p53, PTEN
Responsiveness to chemotherapy ↓
Cell proliferation ↑↑
Warburg effect (Glycolysis) ↑↑
Metabolism is not affected by Cisplatin

1.3 Apoptosis of OVCA

1.3.1 Apoptosis

Apoptosis or programmed cell death, is the major form of cellular suicide. Apoptosis is required to maintain cellular homeostasis, to respond to chemotherapy, and to adapt to various physiological stimuli (Kerr et al., 1972). Cells undergoing apoptosis show well-defined morphological changes including plasma membrane blebbing, chromatin condensation, the loss of mitochondrial membrane potential, nuclear fragmentation, and the formation of apoptotic bodies (Galluzzi et al., 2012b; Gorman et al., 1996). Apoptosis can be induced by extrinsic factors through the death receptor (DR)- mediated pathway, or intrinsic factors through the mitochondrial pathway. Both extrinsic and intrinsic factors will cause apoptosis through a proteolytic cascade involving a family of cysteine-aspartic acid proteases (caspases) (Denault and Boatright, 2004; Elmore, 2007). The molecular events of apoptosis are divided into three major steps: 1) initiation by an apoptotic inducing agent; 2) activation of the caspase by a signal transduction cascade, and 3) proteolytic cleavage of cellular components. The intrinsic mitochondrial mediated apoptotic pathway is activated by exogenous and endogenous stimuli such as DNA damage, ischemia, and oxidative stress (Danial and Korsmeyer, 2004). The intrinsic pathway is initiated by the loss of mitochondria membrane potential, increased mitochondrial outer membrane permeabilization (MOMP), and the subsequent release of mitochondrial death proteins including cytochrome c (Vieira et al., 2000). Cytochrome c and deoxyadenosine triphosphate (dATP) bind to apoptotic peptidase activating factor (Apaf-1) to form multimeric complex which recruits and activates procaspase-9. Procaspase 9 proteolytic cleaves and activates caspase 3, resulting in apoptosis (Taylor et al., 2008).

Extrinsic pathway is initiated by the ligation of membrane-associated DR, which are First apoptosis signal (Fas) and tumor necrosis factor receptor family (TNF-) receptor, or TNF related

apoptosis inducing ligand (TRAIL) (Peter et al., 1995; Tartaglia et al., 1993). The ligation of DR-4 and DR-5 with Fas ligand (FasL) or TRAIL results in oligomerization of the receptors and recruitment of the adaptor protein, Fas-associated death domain (FADD) and caspase-8. This forms an active death-inducing signaling complex (DISC) which can bind effector molecules including procaspase-8, leading to induction of caspase cascade for the execution of apoptosis and the death of the cell (Chan et al., 2000; Jin and El-Deiry, 2005)

Recent evidence suggests that apoptosis can occur through a caspase-independent pathway involving the endoplasmic reticulum (ER) and apoptosis inducing factor (AIF) (Tabas and Ron, 2011). The ER is the cellular site of polypeptide folding and modification. Ca^{2+} is mainly localized in the ER of the cell and high concentration of Ca^{2+} is required for proper folding of proteins in ER. Mitochondria are highly sensitive to Ca^{2+} release upon ER activation (Berridge et al., 2000). When proper folding is prevented due to cellular damage, an unfolded protein response (UPR) is activated (Berridge et al., 2000), initiating apoptotic process (Breckenridge et al., 2003). UPR stimulates inositol 1,4,5-triphosphate receptor (IP3R), and cytosolic Ca^{2+} is released from ER (Nakamura et al., 2000; Rao et al., 2004). It leads to the activation of transcription factors, and in turn induces the release of cytochrome c from mitochondria and apoptosome formation. On the other hand, transport of Ca^{2+} between ER and mitochondrial membranes sensitize mitochondria to the pro-apoptotic Bcl-2 family members (e.g., Bid and Bim) (Kale et al., 2018). Caspase -2 and 12 were proposed as an initiator caspase, as the key molecules in ER mediated apoptotic process (Rao et al., 2004). High concentration of Ca^{2+} induces cell death in caspase dependent and independent pathways. Ca^{2+} also activates calpain, calcium-dependent cysteine proteases, which mediates release and cleavage of AIF (Polster et al., 2005).

AIF, a mitochondrial flavoprotein is cleaved by calpain during the induction of apoptosis (Polster et al., 2005; Susin et al., 1999). Cleaved AIF is released following MOMP and translocates to the nucleus where it causes caspase-independent DNA fragmentation and chromatin

condensation, playing a critical role in apoptosis (Tabas and Ron, 2011; Yang et al., 2008).

1.3.2 Key Molecule Determinants in Apoptosis

In OVCA cells, many genes with oncogenic characteristics are associated with CDDP resistance. These include: the Bcl-2 family members (Tomita et al., 2006), Akt (Yang et al., 2006), Fas-associated death domain like interleukin 1β-converting enzyme (FLICE) -like inhibitory protein (FLIP) (Abedini et al., 2004), X-linked inhibitor of apoptosis protein (Xiap) (Sasaki et al., 2000), and Protein phosphatase magnesium/manganese-dependent 1D (PPM1D)(Ali et al., 2012). In contrast, key tumor suppressor genes, which protects cells from becoming cancer such as p53, PTEN, and BRCA1/2 are frequently lost or mutated in advanced OVCA. Defects of key tumor suppressor suppressed cellular responses including DNA damage and apoptosis.

1.3.2.1 p53

p53 is a key tumor suppressor, encoded by *TP53* gene in humans, can induce apoptosis in transcription -dependent and -independent manners (Moll et al., 2005; Vousden and Lu, 2002). In response to external stimuli or internal cell stress, p53 can induce cells cycle arrest, apoptosis, senescence, DNA repair and the regulation of metabolism (Skirnisdottir et al., 2002). Dysfunctional intracellular localization and/or inactivation of p53 contributes to the development of chemoresistance in OVCA (Atlas et al., 2016; Fraser et al., 2003). *TP53* mutation occurs in 70% of cases of OVCA and in more than 90% in high-grade serous epithelial OVCA, closely associated with chemoresistance (Marabese et al., 2008). DNA damaging agents such as CDDP require activation of functional p53 signaling in order to induce apoptosis in cancer cells (Wang and Lippard, 2005). p53 is activated by major molecular sensors of DNA damage including ataxia telangiectasia mutated protein (ATM) and ataxia telangiectasia mutated and Rad3-related (ATR) (Jackson et al., 2000). In response to DNA damage, these proteins are recruited to the site

of DNA damage, activating downstream checkpoint kinases 1 and 2 for DNA repair (Chk1 and Chk2) (Ou et al., 2005; Zhao and Piwnica-Worms, 2001).

p53 contains multiple serine residues (15, 27, 33, 37 and 46), which can be phosphorylated by ATM or ATR following cellular stresses (Ashcroft et al., 2000; Banin et al., 1998; Ou et al., 2005). CDDP increases p53 phosphorylation at Ser15 and Ser20 by Chk1 in chemosensitive, but not in chemoresistant OVCA cells (Fraser et al., 2003; Kong et al., 2014; Yang et al., 2006). Biochemically, phosphorylation of Ser15 is critical for the activation of carboxy terminal of p53 and the association of p53 with histone/lysine acetyltransferases (HATs), such as p300 and CREB-Binding Protein (CBP) for its DNA binding (Lambert et al., 1998; Loughery et al., 2014). Mouse double minute 2 homolog (Mdm2), an E3 ubiquitin of ligase of p53, interacts with p53, causing its ubiquitination and repression of its transcriptional activity (Ren et al., 2012; Skirnisdottir et al., 2002). Conversely, phosphorylation of p53 at Ser15 and Ser20 suppresses its interaction with Mdm2, stabilizing p53 by preventing its ubiquitination. In chemosensitive OVCA cells, CDDP induces p53-dependent ubiquitination and proteasomal degradation of the anti-apoptotic FLIP by interacting with the E3 ubiquitin ligase, whereas this process is attenuated by Akt in chemoresistant cells (Abedini et al., 2008; Abedini et al., 2004).

Accumulating evidence demonstrates that p53 mediates the intrinsic apoptosis pathway by interacting with members of the pro-apoptotic Bcl-2 family, Bax and Bcl-2 homologous antagonist/killer (Bak), to induce MOMP. Upon cellular stress, p53 rapidly translocates to the outer mitochondrial membrane (OMM) and directly interacts with Bcl-2 family members to neutralize the anti-apoptotic member Bcl-xL and Bcl-2 by forming an inhibitor complex (Marchenko et al., 2000; Mihara et al., 2003). The formation of this inhibitor complex stimulates the changes of mitochondrial membrane potential, the release of cytochrome c, and caspase activation (Erster et al., 2004; Marchenko et al., 2000). This process also causes the release of pro-apoptotic proteins associated with mitochondrial death which are modulators of apoptosis (PUMA), Nicotinamide

adenine dinucleotide phosphate (NADPH) oxidase activation (NOXA) , Bcl-2 family members, Bax and Bid (Miyashita and Reed, 1995; Nakano and Vousden, 2001; Park et al., 2012; Riley et al., 2008; Sax et al., 2002). Defects of p53 prevent the interaction of p53 with Bcl-2, leading to suppressed mitochondrial permeabilization (Tomita et al., 2006). Based on the multiple roles of p53 in both transcriptional activation and in the mitochondria, the function of p53 is critical in facilitating apoptosis and regulating tumor growth in OVCA.

1.3.2.2 PI3K-AKT

The PI3K/Akt pathway is a critical signaling cascade linked to oncogenes, regulation of cancer progression, and metabolism (Manning and Toker, 2017; Neary and Pastorino, 2013). PI3Ks are heterodimers with separate regulatory (p85) and catalytic (p110) subunits. PI3Ks are activated upon recruitment of the inactive p85-p110 complex to receptor tyrosine kinases (RTKs). Interaction of the Src-homology 2 (SH2) domain of p85 with consensus phosphotyrosine residues at the RTKs in response to external stimuli (e.g., Growth factor) results in PI3Ks activation (Cheng et al., 2002).

Previous studies support that multiple tumor suppressor/oncogenes affect glucose metabolism (Hay, 2005; Hay, 2016; Vousden and Ryan, 2009). The PI3K/Akt axis is a key oncogenic cell signaling pathway in cell survival and tumor progression, suppression of apoptosis and may promote glycolytic reprogramming (Altomare et al., 2004; Hay, 2005). For example, acute insulin treatment leads to the trafficking of glucose transporter in a PI3K/Akt-dependent manner (Kotani et al., 1995). PI3K is a phospholipid kinase which phosphorylates the 3’ hydroxyl group (OH) of the inositol ring of phosphoinositide lipids. Stimulation of RTK or G-protein-coupled receptors (GPCR) induces the recruitment and activation of PI3K family, leading to downstream effectors of PI3K-Akt activation (Vanhaesebroeck et al., 2010). PI3K phosphorylates the membrane lipid phosphatidylinositol 4,5-bisphosphate (PIP_2) to form phosphatidylinositol 3,4,5-triphosphate (PIP_3), whereas this process is regulated by tumor suppressors PTEN to dephosphorylate PIP3 (West et al., 2002).

Akt is a serine/threonine (S/T) kinase and highly upregulated in cancer cells (Scheid and Woodgett, 2001). PI lipids serve as plasma membrane docking sites for proteins harboring pleckstrin-homology (PH) domains, including Akt and its upstream activator Phosphoinositide-dependent protein kinase (PDK1). After recruitment to the plasma membrane PIP3, PDK1 phosphorylates Thr^{308} and Ser^{473}(Stokoe et al., 1997) leading to activation of Akt, whereas mTORC2 phosphorylates Akt for full enzymatic activity (Vanhaesebroeck and Alessi, 2000). DNA-protein dependent kinase and members of the PI3K-related kinase (PIKK) family can also phosphorylate Akt at Ser^{473}. On the other hand, protein phosphatase 2A (PP2A) is used to promote phosphprlyation of Akt whereas PH-domain leucine rich-repeat containing protein phosphatase (PHLPP1/2) dephosphorylate it (Sarbassov et al., 2005). In OVCA, aberrant Akt 2 hyperactivation has been observed in 40% of OVCA patients (Bellacosa et al., 1995; Yuan et al., 2000). Akt activation promotes the survival of chemoresistant cells by attenuating p53 activation and subsequent pro-apoptotic signaling (Fraser et al., 2008; Fraser et al., 2003).

Akt phosphorylates residues of S and T in target molecules including lipid kinases, transcription factors, metabolic enzymes, E3 ubiquitin ligases, cell cycle regulators, and many other proteins. Akt phosphorylates proteins by recognizing a consensus sequence of R-X-R-X-X-S/T (where X represents any amino acid) on target proteins (Rust and Thompson, 2011; Sarbassov et al., 2005). However, approximately 25% of Akt target substrates do not have this consensus sequence required for Akt-mediated phosphorylation. How Akt phosphorylates these targets remains unknown and needs to be further investigated (Manning and Toker, 2017).

Akt has three isoforms (Akt1, Akt2, and Akt3) which all share high sequence homology with similar domain structures, N-terminal PH, and its kinase activities (Franke et al., 1997). Akt1 is reported to be involved in cell survival and inhibition of apoptosis whereas Akt2 is required for glucose transport (Staal et al., 1977; Zhang and Yang, 2013). In OVCA, aberrant Akt 2 activation

has been observed in 40% of OVCA patients (Bellacosa et al., 1995; Yuan et al., 2000). The function of Akt3 still remains unclear.

Akt suppresses apoptosis through phosphorylation of B-cell lymphoma **2 (**Bcl)-2 family members. Akt phosphorylates pro-apoptotic Bcl-2-associated death promoter (Bad) at Ser136. This phosphorylation inhibits Bad from binding with Bcl-xL, resulting in the suppressed release of mitochondrial death proteins (Datta et al., 1997). Akt phosphorylates fork head transcription factor 1 (FOXO-1) which facilitates the export and sequestration of FOXO1 out of the nucleus, thereby suppressing its transcriptional action on multiple proapoptotic molecules (e.g., BIM, and PUMA), cell cycle arrest (e.g., p21 and p27), and tissue-specific metabolic changes (van der Vos and Coffer, 2011; Webb and Brunet, 2014). In addition, Akt directly phosphorylates mTOR at S2448, leading to mTORC1 activation (Sekulic et al., 2000). By phosphorylating procaspase-9, Akt inhibits the cleavage of both procaspase-3 and -7, preventing the caspase cascade and apoptosis (Cardone et al., 1998)

Akt decreases p53 protein stability through phosphorylation of Mdm2 at Ser166 and Ser186. This facilitates nuclear translocation of Mdm2, where it causes proteasomal degradation of nuclear p53 (Mayo and Donner, 2001; Ogawara et al., 2002). Conversely, p53 decreases Akt activity by promoting transcription of the PIP3 inhibitor, PTEN and thereby enhancing negative expression of PI3K and its downstream Akt (Mayo et al., 2002). In addition, Akt activation confers resistance to OVCA cells via inhibition of caspase-dependent apoptosis (Yang et al., 2006).

1.4 Energy Metabolism of Cancer

1.4.1 Multiple Aspects of Tumor Metabolic Reprogramming

Metabolic reprogramming enables cancer cells to be highly proliferative and promotes cell survival (Hay, 2016). Demonstrated by Otto Warburg in 1923, cancer cells show accelerated aerobic glycolysis (Warburg, 1956). The previous perspective of Warburg effect specifically proposes that glycolysis is the main metabolic pathway for ATP generation and that oxidative

phosphorylation (OXPHOS) is impaired in cancer cells; however, recent research has demonstrated that both pathways are relatively elevated in cancer cells compared to normal cells (Hay, 2016; Pfeiffer and Morley, 2014). Moreover, it may be that the ability of cancer cells to switch between energy substrates and metabolic pathways (termed bioenergetic flexibility) is associated with poor prognosis, including metastasis (Andrzejewski et al., 2017; St-Pierre et al., 2006). Glycolysis works as precursor pathway, since its metabolites and products are required for downstream pathways including the tricarboxylic acid (TCA) cycle and OXPHOS; pentose phosphate pathway (PPP) for ribonucleotide synthesis and NADPH, glycosylation and gluconeogenesis, amino acid biosynthesis, and fatty acid synthesis (Hay, 2016; Pedersen, 2007). In addition to glycolysis, the PPP pathway is highly elevated in cancer (Catanzaro et al., 2015; Zheng et al., 2017), providing anabolic substrates for cancer growth and reductive intermediates (NADPH) for glutathione synthesis and protection from oxidative damage.

Fatty acid metabolism is similarly altered in cancer. Unsaturated lipids are increased in OVCA (Li et al., 2017b; Zhang et al., 2015), which induces stemness, whereas lipid desaturation impairs cancer stemness which has characteristics of tumor initiation and self-renewal (Li et al., 2017b). Cellular glycogen accumulation is observed as a feature of clear cell, a sub-type of epithelial OVCA, which frequently develops chemoresistance (Iida et al., 2012). Also, glycogen accumulation is elevated in hypoxic conditions, a core component of the solid tumor microenvironment (Iida et al., 2012; Uekuri et al., 2013). These findings suggest that specific metabolic phenotypes enhance chemoresistance in OVCA. By increasing aerobic glycolysis over respiration, cancer cells are provided with several benefits: 1) an environment high in lactic acid which facilitates tumor evasion; 2) higher generation of NADPH which provides protection from chemotherapeutic drugs; and, 3) production of glycolytic intermediates meeting the need for further anabolic demands (Vander Heiden et al., 2009; Zhao et al., 2013).

1.4.2 Warburg Effect & Glycolysis Metabolism in Cancer

Accelerated glycolysis is a key hallmark of tumorigenesis (Mathupala et al., 2006; Mathupala et al., 2001; Warburg, 1956). Glycolysis is the first metabolic pathway converting glucose to pyruvate. Beyond their metabolic functions, key glycolytic enzymes have been shown to enhance the survival and progression of tumors associated with drug resistance **(Fig. 1.4)**. Metabolic adaptation of excessive glycolysis in cancer is mediated by hyperactive glycolytic enzymes, and this is primarily due to dysregulation of tumor suppressors or activation of oncogenes (Annibaldi and Widmann, 2010).

The first step of glucose metabolism is the transport of glucose across the plasma membrane by GLUT (Glucose transporter), which is often dysregulated or overexpressed in malignant cells (Macheda et al., 2005; Younes et al., 1995). GLUT 1, 2, and 3 among the 14 isoforms of GLUT are considered as possible metabolic targets for cancer therapy (Thorens and Mueckler, 2010; Zhao et al., 2013). Lactate dehydrogenase (LDH) is responsible for converting pyruvate to lactate. LDH has been observed to induce paclitaxel/trastuzumab resistance in breast cancer cells (Xie et al., 2009; Zhou et al., 2010). Excessive activity of LDH in glycolysis also leads to local acidification of tumor microenvironment, which facilitates more favorable conditions for tumor invasion and metastasis (Gatenby et al., 2006; Gatenby and Gillies, 2004). Pyruvate kinase is responsible for the last irreversible reaction of glycolysis, where it converts phosphoenolpyruvate to pyruvate. One isoform of pyruvate kinase, pyruvate kinase muscle (*PKM2*), enables cancer cells to adapt an altered tumor metabolic condition. Depletion of *PKM2* in a mouse model reversed the Warburg effect and inhibited tumor growth in a breast cancer (Christofk et al., 2008). Collectively, this evidence suggests that the glycolytic metabolism of cancer cells is associated with the development of chemoresistance in addition to facilitating energy production and promoting cancer cell survival.

1.4.3 Hexokinase II, Key Glycolytic Enzymes Involved in Chemoresistance

Hexokinase (HK) is the enzyme involved in the first committed and irreversible step in glycolysis, converting glucose to glucose-6-phosphate (G-6-P). There are five HK isoforms including recently discovered HKV (HKI, II, III, IV, and V) (Guo et al., 2015). HKI to HKIII have high substrate affinity, while HKIV has low glucose affinity and serves as an important glucose sensor (e.g., to control β-cell insulin release). The fifth HK as novel isoform was recently found, and it remains to be further explored (Guo et al., 2015). HKI and HKII are found in many cellular compartments, including being bound to the OMM, and localized within mitochondria (Kabir and Wilson, 1994). The product of HKII, G-6-P, is a precursor used for other downstream pathways including pentose phosphate (NADPH and ribulose-5-P), glycogenesis (glycogen), and the hexosamine pathways (UDP-GlcNAc). This suggests the universal involvement of HKII in the regulation of anabolic and catabolic cellular metabolism (Pedersen, 2007; Robey and Hay, 2006). Both HKI and HKII are inhibited by G-6-P, its catalytic product via feedback inhibition (Vander Heiden et al., 2009). HKII, a predominant isoform in insulin sensitive tissues (adipose, skeletal and cardiac muscles), is highly expressed in multiple tumors (Roberts and Miyamoto, 2014). Recent research demonstrates that HKII is highly associated with tumorigenesis and cancer cell survival (Majewski et al., 2004a; Mathupala et al., 2006). In mouse models, deletion of HKII significantly decreased tumor burden and prolonged survival, suggesting that HKII is a critical factor involved in tumor progression (Patra et al., 2013). HKII depletion restored balanced rate of glycolysis and OXPHOS pathway as well as mitochondrial biogenesis in glioblastoma (Wolf et al., 2011). HKII depletion also increased intrinsic apoptosis by increased mitochondrial permeability in chemoresistant glioblastoma cells (Wolf et al., 2011). Lysophosphatidic acid (LPA), a lipid growth factor and G protein-coupled receptor (GPCR) ligand are significantly increased in OVCA, triggering the activation of hypoxia inducible factor 1α (HIF1α) and inducing GLUT1 and HKII, thus shifting cells towards a glycolytic metabolism (Ha et al., 2018).

Figure 1.4 The regulation of HKII and other glycolytic enzymes in OVCA cells

Enhanced glycolysis in cancer cells, through a combination of metabolic pathways, drives glucose utilization to fulfill high anabolic demands. In this schematic diagram of the glycolysis pathway, metabolites are shown as square boxes. Key regulatory molecules which either promote (yellow box) or suppresses (Purple box) glycolytic enzymes and metabolites such as G-6-P are shown. GLUT (glucose transporter), G-6-P (glucose-6-phosphate), F-6-P (fructose-6-phosphate), F-1,6-BP (fructose-1,6-bisphosphate), PFK (phosphofructokinase), TIGAR (TP-inducible glycolysis and apoptosis regulator), 1,3-BPG (1,3-bisphosphoglycerate), 2-PG (2-phosphoglycerate), 3-PG (3-phophosphoglycerate); PEP (phosphoenolpyruvate), ENO (enolase), MCT (monocarboxylate transporter). mTORC1 (mTOR complex 1), Mutant p53 (defect p53), PFKFB (6-phosphofructo 2-kinase/fructose-2,6-bisphosphatase), Akt (Protein Kinase B), HIF1α (Hypoxia Inducible Factor 1α), c-Myc (v-myc avian myelocytomatosis viral oncogene homolog), and LPA (Lysophosphatidic acid) (Adapted from Hay et al. 2016) (Hay, 2016).

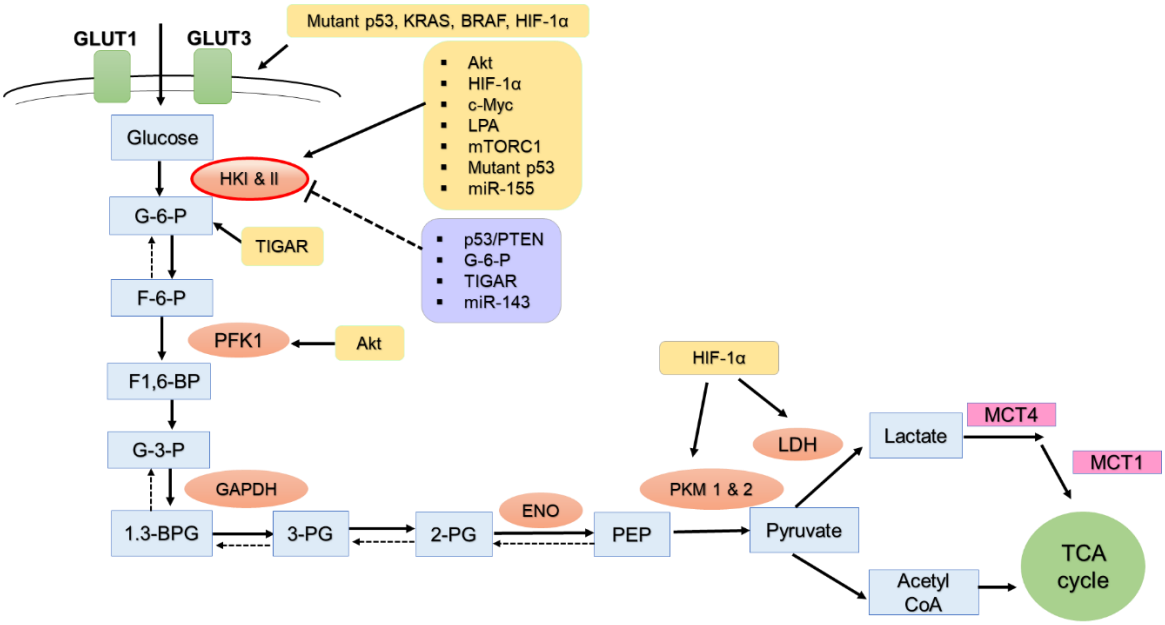
GLUT1
GLUT3
Mutant p53, KRAS, BRAF, HIF-1α
Akt
HIF-1α
c-Myc
LPA
mTORC1
Mutant p53
miR-155
Glucose
HKI & II
G-6-P
TIGAR
p53/PTEN
G-6-P
TIGAR
miR-143
F-6-P
PFK1
Akt
F1,6-BP
G-3-P
GAPDH
1.3-BPG
3-PG
2-PG
ENO
PEP
HIF-1α
LDH
PKM 1 & 2
Pyruvate
Lactate
MCT4
MCT1
Acetyl CoA
TCA cycle

1.4.4 The Influence of HKII Mediated Glycolysis on Intrinsic Apoptosis in OVCA

Intrinsic (mitochondria-mediated) apoptosis is initiated by the loss of mitochondrial membrane potential, increased MOMP, and the subsequent release of mitochondrial death proteins including cytochrome c (Vieira et al., 2000). In addition to its role in glycolysis, HKII is involved in protecting mitochondria and the suppression of intrinsic apoptosis (Suh et al., 2014), whereas its depletion of HKII enhances apoptosis and sensitivity to external stimuli **(Fig.1.5)**. Hay et al. showed that ectopic expression of mitochondrial binding-deficient HKII failed to restore cell proliferation and tumorigenesis, emphasizing the pivotal role of mitochondria-bound HKII (DeWaal et al., 2018). Ectopic expression of HKII protects lung cancer cells and renal epithelial cells from oxidative injury or cell death (Ahmad et al., 2002; Bryson et al., 2002).

In line with its role in regulating MOMP, HKI and HKII can bind to voltage-dependent anion channel 1 (VDAC1), a likely component of the mitochondrial permeability transition pores (mPTP) (Mathupala et al., 2006; Vyssokikh and Brdiczka, 2003). Approximately 80% of HKII is localized with mitochondria in cancer cells (Kabir and Wilson, 1994). Accumulating studies showed that Mito-HKII enhances the tight coupling of glucose phosphorylation to mitochondrial ATP generation (Corona et al., 2010; Sun et al., 2008). Mitochondrial Ca^{2+} overload and reactive oxygen species (ROS) induce the opening of mPTP and consequent rupture. Mito-HKII provides cellular protection against this Ca^{2+} overload and mPTP opening (Majewski et al., 2004a).

The interaction of HKII with Bcl-2 members also affects apoptotic processes, particularly the execution of intrinsic apoptosis. Some anti-apoptotic molecules of Bcl-2 family [e.g., Bcl-2 and B-cell lymphoma-extra large (Bcl-xL)] stay in the OMM, whereas pro-apoptotic members, Bcl-2-associated death promoter (Bad), Bax, and BH3 interacting-domain death agonist (Bid) are translocated from the cytosol to the OMM upon initiation of apoptotic signaling (Gross et al., 1999; Harris and Thompson, 2000). In mitochondrial-mediated cell death, activated Bax/Bak forms a pore at the OMM, induces MOMP, and results in the release of apoptotic factors such as

cytochrome c from the inter-membrane space (Harris and Thompson, 2000), which then accelerates the opening of VDAC (Vander Heiden et al., 2000). Conversely, anti-apoptotic Bcl-2 family members, such as Bcl-xL interact with VDAC, inhibiting cytochrome c release by modulating OMM integrity or MOMP (Gogvadze et al., 2006; Gross et al., 1999). Mito-HKII inhibits binding of Bax to Bcl-2 through competitive inhibition and antagonizes truncated Bid (tBid)-mediated apoptosis (Majewski et al., 2004b; Pastorino et al., 2002). Upon cell stress (e.g., glucose restriction or treatment with Metformin, Clotrimazole, Flavonoid-429, 2-DG, or 3-Bromopyruvate, HKII is detached from VDAC (Chen et al., 2009; Neary and Pastorino, 2013; Salani et al., 2013; Zhou et al., 2016), inducing dysregulation of mitochondria by opening the mPTP, increasing the MOMP, and subsequent inducing of mitochondrial-mediated apoptosis (Krasnov et al., 2013; Pastorino et al., 2002). HKII dissociation from mitochondria using an artificial peptide also was shown to induce apoptosis without changing mitochondrial membrane potential, ROS production, or OXPHOS (Chen et al., 2009). This suggests that detachment of HKII from mitochondria is critical for intrinsic apoptosis. However, the molecular mechanism of HKII detachment and its relationship to chemoresponsiveness remain to be elucidated.

1.4.5 Regulatory Mechanism of Glycolytic Metabolism in OVCA

Accumulating evidence suggests that multiple tumor suppressors and oncogenes affect HKII and its role in glucose metabolism. The interplay of these molecules with HKII affect its enzymatic function, cellular metabolism, and survival of cancer cells **(Fig. 1.4).** (Hay, 2005; Hay, 2016)

Figure 1.5 The regulation of mitochondrial-HKII associated with intrinsic apoptosis in OVCA

A hypothetical model demonstrating mechanisms regulating the mitochondrial localization of HK II and apoptosis. **(A) In chemosensitive OVCA cells,** CDDP-induced detachment of mitochondrial bound HK II (mito-HKII) from VDAC is required for the induction of apoptosis. Chemotherapy such as CDDP induces the phosphorylation of p53 at Ser 15 (S15) and Ser 20 (S20), which suppresses phosphorylation of Akt, and promotes binding of HKII to mitochondria. In the absence of mito-HKII, proapoptotic Bcl-2 family proteins (Bax and Bad) interact with VDAC, increasing mPTP, ROS, MOMP, and Ca^{2+} in the OMM where AIF and cytochrome c are released. **(B) In chemoresistant OVCA cells,** CDDP-induced apoptosis is attenuated due to defective p53. Through increased GLUT1 & 3 membrane trafficking, glucose is transported into the cell. Activated PI3-kinase phosphorylates lipids in the plasma membrane where Akt is recruited for activation. Activated Akt phosphorylates HKII (P-HKII), facilitates the translocation of Bcl-xL and promotes binding of P-HKII to VDAC on the OMM, thus preventing apoptosis. Bcl-xL directly interacts with VDAC, closing the mitochondrial ion channel and decreasing MOMP, while HKII inhibits apoptosis by competing for the binding sites for Bax and Bad of VDAC. Solid line indicates activated molecular action whereas dashed line indicates suppressed signaling. Arrows indicates direct action whereas blocked line indicates inhibition. (Mathupala et al., 2006).

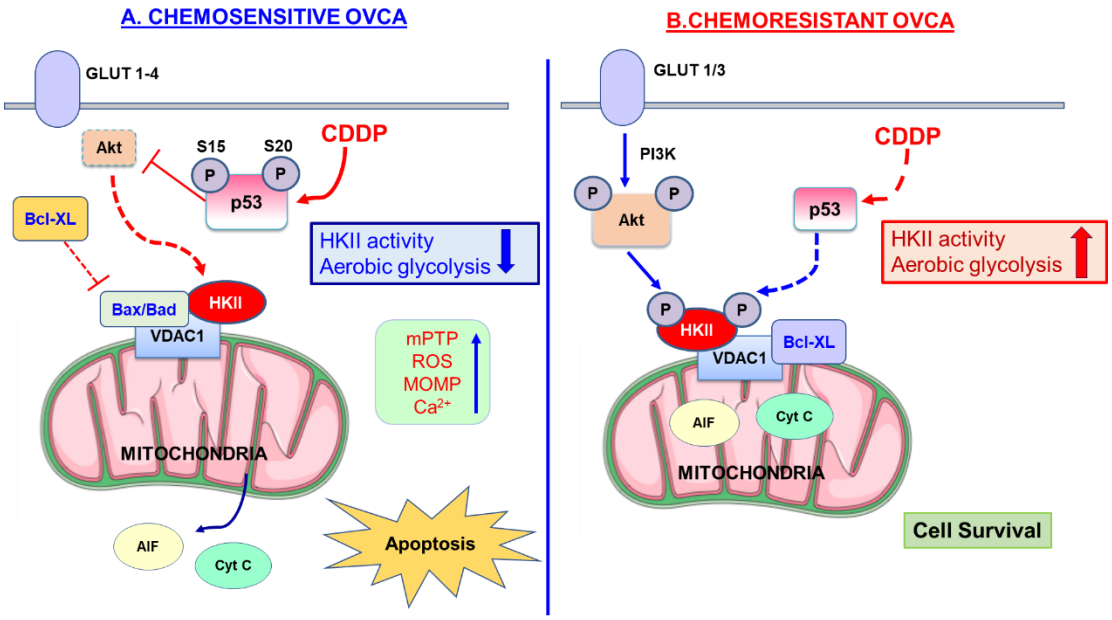
A. CHEMOSENSITIVE OVCA
B.CHEMORESISTANT OVCA
GLUT 1-4
GLUT 1/3
Akt
S15
S20
P
p53
CDDP
Bcl-XL
HKII activity
Aerobic glycolysis
Bax/Bad
HKII
VDAC1
mPTP
ROS
MOMP
Ca2+
MITOCHONDRIA
AIF
Cyt C
Apoptosis
PI3K
Cell Survival

A. PI3K/Akt

PI3K/Akt signaling cascade promotes glycolysis, suppresses apoptosis, and elicits cell survival via multiple mechanisms (Miyamoto et al., 2008; Roberts and Miyamoto, 2014; Roberts et al., 2013). PI3K pathway activation or mutational changes in genetic and function were common in OVCA (Cheaib et al., 2015). Effect of inhibition of *AKT* depends on genetic heterogeneity of cancer. Inhibition of *AKT1* selectively caused cancer growth in a subset of OVCA cells lines, but not applied to all of OVCA subset, due to high expression of other *AKT* isoforms (Gasparri et al., 2017; Hanrahan et al., 2012). Akt enhances mitochondrial HKII activity and in turn OMM stability, thereby increasing its anti-apoptotic action. Akt directly phosphorylates HKII at the consensus binding site of (RARQKT*) at Thr473. Phosphorylated-HKII (P-HKII) is more stably associated with mitochondria, by inhibiting opening of mPTP (Gottlob et al., 2001; Miyamoto et al., 2008). Akt facilitates binding of Bcl-xL and HKII to VDAC in OMM. Apoptosis induction and mPTP formation by Bax/Bak are prevented, largely due to pre-occupied Bax binding site by HKII for OMM permeability (Majewski et al., 2004a; Roberts et al., 2013). Treatment of brain cancer cells with a PI3K inhibitor (LY294002) decreased P-Akt, causing decreased association of mitochondrial HKII fraction (Ahn et al., 2009; Pastorino et al., 2002). Also, Akt activates PFK1 by the phosphorylation and activation of PFKFB2 (Ros and Schulze, 2013). In breast cancer, FV-429 inhibits glycolysis by attenuating Akt-mediated phosphorylation of HKII, resulting in apoptotic induction (Zhou et al., 2016). As oncogenes, *KRAS* and *BRAF* activate Akt and its mutation enhance the expression and plasma membrane trafficking of GLUT1 (Barthel et al., 1999; Foran et al., 1999; Yun et al., 2009). Still, it remains unclear how the interplay of Akt/p53 affects the HKII-mediated glycolysis and other metabolic processes in cancer.

B. c-MYC

c-MYC (v-myc avian myelocytomatosis viral oncogene homolog) is an oncogene and transcription factor that regulates multiple genes involved in cell proliferation, metabolism, and apoptosis (Eilers

and Eisenman, 2008). Constitutive activation of c-MYC is frequently found in human cancer (Ischenko et al., 2013). In OVCA, protein expression of c-MYC is higher in chemosresistant cells compared with its counterpart sensitive cells (Lawrenson et al., 2011; Reyes-Gonzalez et al., 2015). High c-MYC expression is also associated with decreased overall survival and disease free survival rate (Reyes-Gonzalez et al., 2015). c-MYC contributes to chemoresistance of cancer in part by controlling metabolism (Kim et al., 2007). c-MYC binds and activates the promoters of key metabolic enzymes including GLUT1, HKII, PFK, and enolase 1 (ENO1), leading to an activation of the glycolysis pathway (Kim and Dang, 2006; Kim et al., 2006; Osthus et al., 2000). In addition, c-MYC cooperates with HIF 1α to promote HKII and PDKI, again shifting metabolic pathway to glycolysis (Kim et al., 2007).

C. mTOR

mTOR is a serine/threonine kinase involved in promoting energy metabolism, cell growth and proliferation. Elevated mTOR suppresses the induction of autophagy and frequently leads to the development of tumors (Hay, 2005; Roberts and Miyamoto, 2014). mTOR is composed of two distinct functional complexes, mTOR complex 1 and 2 (mTORC1 and mTORC2), with their respective defining components Raptor and Rictor (Vousden and Ryan, 2009). Akt activates mTOR, promoting anabolic metabolism and fatty acid synthesis, whereas AMPK represses mTOR, leading to catabolic energy production and fatty acid oxidation. In response to glucose deprivation, HKII can bind to mTORC1 by its TOS motif, decreasing TORC1 activity and positively regulate autophagy (Roberts et al., 2014). Under glucose depletion, inhibition of HKII is attenuated, while overexpression of HKII elevates glucose deprivation-induced autophagy (Roberts and Miyamoto, 2014; Roberts et al., 2014). This indicates that cells increase their adaptability and survival by mTOR-HKII interaction under varied energy conditions.

C. p53 & PTEN

Our lab has demonstrated that activation of functional p53 signaling is required for apoptosis in response to chemotherapy such as CDDP (Fraser et al., 2008; Yang et al., 2006). In addition to its fundamental role in apoptosis, p53 is shown to negatively regulate glycolysis (Berkers et al., 2013), as its mutation may lead to the reliance on glycolysis of cancer cells (Richardson, 2013). Moreover, the co-deletion of p53/PTEN in prostate cancer can further increase HKII levels (Wang et al., 2014). For example, PTEN deletion increases HKII mRNA translation via activation of the AKT-mTOR-4EBP1 pathway, whereas p53 loss enhances HKII mRNA stability by inhibiting miR-143 biogenesis (Wang et al., 2014). p53 plays a critical role in maintaining mitochondrial integrity and function, potentially through modulating SCO2 (the synthesis of cytochrome c oxidase protein) and cytochrome oxidase II (COX II) (Assaily and Benchimol, 2006; Matoba et al., 2006). SCO2 is required for the OXPHOS, mitochondrial respiration, and the assembly of the mitochondrial complex with COX II. Therefore, depletion of p53 impairs mitochondrial structure and respiration, shifting cells toward glycolytic metabolism. p53 can also induce the protein TIGAR (*TP53*-inducible glycolysis and apoptosis regulator) (Cheung et al., 2012). TIGAR has dual functions in suppressing or activating glycolysis to maintain homeostatic balance system in the cell depending on varied condition. In normal conditions, TIGAR leads to the accumulated production of G-6-P, preventing glycolysis. However, under hypoxic conditions, TIGAR is translocated to mitochondria and binds to HKII, decreasing ROS, promoting glycolysis, and providing cell protection from apoptosis (Cheung et al., 2012; Cheung and Vousden, 2010). Also, it has been reported that defect of p53 promotes the plasma membrane trafficking of GLUT1 via Rho-associated protein kinase (ROCK) signalling (Zhang et al., 2013). Despite p53's regulatory role in metabolism, detailed molecular and temporal mechanisms remain to be further elucidated.

D. HIF1α

Hypoxia inducible factors (HIFs) are master transcription factors required for metabolic and survival adaptations to hypoxia (Semenza, 2013). Active HIF1 is a heterodimer of an oxygen

sensitive HIF1α and constitutively expressed HIF1β. HIF1α stability in hypoxia allows for the transcription of many HIF-dependent genes, including multiple glycolytic genes (Ivan et al., 2002; Wang et al., 1995). For example, HIF1α promotes the expression of pyruvate dehydrogenase kinase (PDK) 2 and PDK4 which inactivates PDH. PDH is responsible for converting pyruvate to acetyl-CoA, which is used in TCA cycle (Kim et al., 2006). However, excessive PDK inactivates PDH and results in the suppression of TCA cycle and OXPHOS activities, shifting the generation of ATP toward glycolysis (Gogvadze et al., 2008). Under hypoxic conditions, HIFα is stabilized by inhibiting hydroxylation mediated by HIF1α prolyl hydroxylase (PHD). Decreased oxygen protects HIF1α from VHL-mediated HIF1α degradation. In non small cell lung cancer (NSCLC), aberrant expression of HIF1α stimulates HKII expression, contributing to elevated glycolysis (Ma et al., 2016). In turn, PKM2 function as an upstream effector and binds to HIF1α, promoting glycolysis metabolism and tumorigenesis (Wang and Semenza, 1995). HIF1α cooperates with c-Myc, an oncogenic transcription factor, and induces key metabolic genes, HK2 and PDK1 to promote glycolysis (Kim and Dang, 2006; Kim et al., 2007; Kim et al., 2006). HIF1α increases the expression of GLUT1, glucose uptake, and glucose phosphorylation (Assaily and Benchimol, 2006; Chen et al., 2001).

Chapter 2. Objectives & Hypotheses

2.1 Background and Rationale

OVCA is the most lethal gynecological cancer, due primarily to late diagnosis and chemoresistance (Canada, 2014; Society, 2014b). CDDP resistance is a major hurdle to successful therapy (MayoClinic, 2014). The mechanism of chemoresistance is multi-factorial including defects in apoptotic pathway and key tumor suppressor as well as dysregulation of metabolism (Borst et al., 2000; Galluzzi et al., 2012a; Siddik, 2003). p53, a key tumor suppressor for exerting apoptosis in cancer cells, are frequently mutated (> 80%) in OVCA patients (Cheung and Vousden, 2010; Farrand et al., 2013).

Cancer cells preferably obtain energy via aerobic glycolysis (Warburg effect) (Ahn et al., 2009; Gatenby and Gillies, 2004). The key glycolytic enzyme, HKII is responsible for the first glycolysis pathway, conversion of glucose to glucose-6-phosphate. HKII is shown to be highly expressed in multiple cancers, associated with tumorigenesis (Mathupala et al., 2006; Patra et al., 2013; Suh et al., 2014). HKII binds to VDAC in OMM of mitochondria, resulting in maintenance of mitochondrial membrane integrity thereby impairing the release of apoptotic molecules (e.g., Cytochrome c and AIF) (Roberts et al., 2013; Wolff et al., 2008). HKII is highly localized in mitochondria in cancer cells (80%), and mito-HKII contributes to protecting cells from intrinsic apoptosis beyond its metabolic function. Upon external stress, HKII is dissociated from VDAC, resulting in opening of mPTP, increase in MOMP, and subsequent induction of intrinsic apoptosis, but the causative mechanism of HKII dissociation remains elusive (Krasnov et al., 2013; Pastorino et al., 2002).

In the present study, we examine the 1) role of HKII in cancer cell survival and its mediated glycolysis in OVCA; 2) whether and how it is associated with dysregulation of chemosensitivity; 3) p53 mediated regulatory mechanism of HKII, and 4) its potential implementation as a biomarker in OVCA. Through mechanistic and translational approaches with clinical implication, we will

better understand the underlying causes of CDDP resistance associated with cellular metabolism and potentially develop effective therapeutic strategy in treatment of OVCA.

2.2 Overall Objective

The overall objective of present studies is to improve our understanding of the role and molecular mechanism (s) of HKII in cellular metabolism and cell survival of chemoresistant OVCA and its potential clinical implication for determining chemoresponsiveness and decision making in chemotherapeutic regimen.

2.3 Overall Hypothesis

CDDP-activated P-p53(Ser15) regulates intracellular trafficking and transcription of HKII, affecting metabolic reprogramming and chemosensitivity in OVCA.

2.4 Specific Hypotheses & Objectives

1. **Hypothesis:** CDDP-mediated down-regulation of protein and mRNA abundance of HKII is associated with chemosensitivity of OVCA.

   Objective i) Compare the responsiveness of protein and mRNA abundance HKII level in sensitive and its counterpart resistant OVCA cells upon CDDP treatment and determine if this is associated with CDDP-induced apoptosis

   Objective ii) Examine whether HKII depletion is associated with CDDP-induced apoptosis in chemoresistant OVCA cells

2. **Hypothesis:** CDDP down-regulates HKII-mediated glycolysis in chemosensitive, but not in chemoresistant cells.

   Objective: Compare altered cellular glycolytic metabolic levels in chemosensitive and chemoresistant cells upon the CDDP treatment

3. **Hypothesis:** CDDP-activated P-p53(Ser15) facilitates intracellular translocation of mito-HKII to the nucleus in chemosensitive OVCA cells, leading to loss of mito-HKII enzymatic function and decreased glycolytic metabolism.

   Objective: Examine the role of mito-HKII contributing to chemoresistance and cellular metabolism and regulatory role of p53

4. **Hypothesis:** Through direct binding of activated p53 to HKII promoter, CDDP decreases HKII expression at the transcriptional level and its mediated glycolysis in chemosensitive OVCA cells.

   Objective: Examine the role of p53 in transcriptional regulation of HKII and its influence on cellular metabolism

5. **Hypothesis:** CDDP induces the interaction of HKII-AIF with P-p53(Ser15), translocating it from mitochondria to the nucleus for induction of apoptosis in chemosensitive OVCA.

   Objective: Establish the molecular mechanism and interaction of HKII and CDDP-activated P-p53(Ser15) in sensitive OVCA cells, associated with AIF-induced apoptosis

6. **Hypothesis:** p53 and HKII interaction in the nucleus are required for its regulation and this may serve as a potential biomarker for determining the chemosensitivity in different subtypes of epithelial OVCA patients.

Objective: Determine nuclear and mitochondrial HKII-P-p53(Ser15) interaction in OVCA and its potential as a biomarker in a different epithelial subtypes of tumor in OVCA patients apoptosis

Chapter 3. Materials & Methods

3.1 Reagents & Chemicals

CDDP, DMSO, Hoechst 33258, lactacystin, epoxomicin, formaldehyde, 2-Deoxy-D-glucose (2-DG), Oligomycin, FCCP, Rotenone, Antimycin A, and D-glucose were purchased from Sigma-Aldrich (MO, USA). Hexokinase activity assay kit was purchased from Abcam (MA, USA). p53 siRNA, and HKII siRNA were purchased from Santa Cruz Biotechnology (TX, USA). Scramble siRNA, Lipofectamine 2000 transfection reagent, Prolong Gold Anti fade Reagents (DAPI), RPMI 1640 medium, penicillin/streptomycin (10,000/U/mL), Amphotericin B, fetal bovine serum (Origin: Canada), Dynabeads A, TEMED, and Ultrapure Trizol were purchased from Thermo Fisher Scientific (MA, USA). SYBR Green I mixture, Mini protease inhibitor mixture tablets, Phosphostop phosphatase inhibitor mixture tablets were obtained from Roche Life Science (QC, CANADA). Bio-Rad DC protein assay kit and 30% Acrylamide/Bis solution were purchased from Bio-Rad. Glucose colorimetric assay kit was purchased from Biovision (CA, USA) and XF96 well plates were purchased from Seahorse Bioscience (MA, USA). LacZ, and p53-GFP adenoviruses were from Applied Biological Materials (BC, CANADA). An Adenoviral construct containing kinase-dead dominant negative Akt (DN-Akt) was a gift from Dr. Kenneth Walsh (St. Elizabeth's Medical Centre, Boston, MA). Adenoviruses were amplified at the lab of Dr. Robin Parks (Regenerative Medicine program), Ottawa Hospital Research Institute. Detailed information of reagent and antibodies is stated in table 3.1.

3.2 Cell Lines and Culture

CDDP sensitive A2780s (wild type-p53), and -resistant [A2780cp (mutant-p53), Hey (wild type-p53), SKOV3 (p53-null), OVCAR3 (mutant-p53), ES2 (mutant-p53), PA-1 (wild type-p53) human OVCA cell lines] were gifts from Drs. Rakesh Goel and Barbara Vanderhyden (Ottawa Hospital

Research Institute, Ottawa, ON, Canada), and Dr. Yong Sang Song (Seoul National University Hospital). Cell lines were cultured in RPMI1640 medium supplemented with 10% heat-inactivated fetal bovine serum, penicillin/streptomycin (10,000 U/mL), Amphotericin B at 37°C with 5% CO_2. Detailed information of cell lines was stated in Appendix 1.

3.3 Primary Human OVCA Cells

Primary human OVCA cells were obtained from Dr. Barbara Vanderhyden (Ottawa Ovarian Cancer Tissue Bank) and Dr. Yong Sang Song and Ja-Lok Ku (Korean cell line bank, Seoul National University Hospital, SNU). Under IRB-approved protocols (SNU: 1409-1540-616 and OHSN-REB 1999540-01H) with patient informed consent. Tumor ascites or primary ovarian tumor cells were collected from patients with serous and clear cell OVCA. Ascites from SNU were centrifuged at 800 g for 20 minutes. Ascites-derived OVCA cells were maintained in either DMEM or RPMI supplemented with 10% FBS. Detailed information of primary human cell OVCA cells is stated in table 4.1.

3.4 Apoptosis (Hoechst Nuclear Staining)

Apoptosis was morphologically assessed using Hoechst staining (Abedini et al., 2008). Cells were harvested by trypsinization, washed with PBS, fixed in neutral-buffered 10% formalin and stained at 4°C overnight with the nuclear dye Hoechst 33258 (12.5ng/ml). 10-20 μl of cells were spotted onto a slide and assessed for typical apoptotic nuclear morphology (nuclear shrinkage, condensation, and fragmentation) using fluorescence microscopy (DAPI filter). At least 400 cells were counted for each treatment group, and the process was blinded to avoid experimental bias.

3.5 Western Blot

Protein extraction and Western blot were performed as previously described (Cepeda et al., 2007).

Cells were pelleted and lysed in ice-cold Radioimmunoprecipitation (RIPA) lysis buffer (pH 7.4) containing 20mM Tris-HCl, 150 mM NaCl, 1 mM EGTA, 1 mM Na2EDTA, 1% sodium deoxycholate, 2.5mM sodium pyrophosphate, and 1% NP-40. Mini protease inhibitors or Phosphostop (phosphatase inhibitors) were added to the lysis buffer freshly. Cell lysates were sonicated briefly, incubated on ice for 1 hr and pelleted by centrifugation (11,000 *g*; 20 min). The supernatant was taken as whole-cell lysate and stored at −20°C for subsequent analyses. Protein concentration was determined using Bio-Rad DC protein assay kit. Equal amounts of proteins (30–50 μg) were loaded and resolved by 8-10% SDS-PAGE and electro transferred (100 V, 90 mins) onto nitrocellulose membranes (Bio-Rad). Membranes were blocked (room temperature, 1 hr) with 5% skim milk blocking buffer [Tris-HCl (10 mM; pH 8.0), NaCl (150 mM), Tween 20 (0.05%, v/v; TBS-Tween 20), and skim milk (5%; w/v)]. Membranes were incubated overnight 4°C with primary antibodies as indicated dilution factor (Table 3.1). On the second day, membrane was washed with Tris-Tween Buffered Saline (TTBS) and incubated with fluorescence conjugated goat-anti rabbit (1:10,000) or anti-mouse secondary antibodies (1:8,000) followed by quantification and analysis using LI-COR (Odyssey Imager, Nebraska, USA) or Image J.

3.6 Immunofluorescence Microscopy

Immunofluorescence microscopy was performed as previously described (Farrand et al., 2013; Kong et al., 2014). Cells were seeded on 8 chamber slides (BD Biosciences) 1 day before and treated as indicated. Cells were fixed with 4% paraformaldehyde overnight (4°C), washed with PBS, incubated with 0.5 % Triton X-100 (5-10mins), and blocked with 3% BSA followed by incubation with primary antibodies (1: 200, rabbit-anti-HKII), (1:150, mouse anti-P-p53, Ser15), (1:250, mouse anti-TOM20). Cells were then incubated with fluorescence-conjugated secondary antibodies (1:400; Alexa Fluor 488, Alexa Fluor 555) and mounted with Prolong Gold Antifade Reagents for DAPI. The images were obtained with a ZEISS LSM510 confocal scanning

microscope. Original magnification was (640x) for all panels, respectively. At least 100 cells were analyzed per experimental group.

3.7 Adenoviral Infection

Cells were infected with adenoviral constructs (Adv) containing wt-p53 (multiplicity of infection, MOI =0.5-1.0 , 12h), Lac Z (MOI=, 24h), and DN-Akt (MOI = 0-40, 12h) as previously described (Yang et al., 2008). Adv-LacZ was served as a control. Total MOI was maintained constant for all treatment groups between Adv and LacZ. Adenovirus infection efficiency was > 80% determined based on GFP expression [Adv-p53 (MOI = 1.0, 24h), DN-AKT (MOI = 40, 24h)].

3.8 siRNA Transfection

OVCA cells were cultured (60% confluence) and transfected using Lipofectamine 2000 for 16-24h, following the manufacturer's instruction. p53 siRNA (0-100 nM) and HKII siRNA (0-100 nM) were used whereas scramble siRNA was used as a negative control. Detailed information of siRNA is stated in table 3.1C.

3.9 Quantitative Real Time-PCR (RT-qPCR)

qPCR was performed as previously described (Kong et al., 2014). Total RNAs were isolated using TRIzol (Thermo Fisher Scientific), following the manufacturer's instructions. cDNA was synthesized from 1μg total RNA using reverse transcriptase and oligo(dT) primers. mRNA abundances of target genes were analyzed with quantitative real time PCR (qPCR) using Light Cycler 480 SYBR Green I master mix (Roche Life Science) at Light Cycler 480 machine (Roche Life Science). The data were analyzed by $2^{-\Delta\Delta CT}$ method and normalized by expression of the GAPDH or actin as housekeeping gene. Primer information stated is in table 3.2.

3.10 Chromatin Immunoprecipitation (ChIP) Assay

Chromatin immunoprecipitation assay was performed as previously described (Liefke et al., 2010; Lim et al., 2017). Briefly, OVCA cells were cross linked, lysed, and sonicated as 150-250 bp size using an ultra-sonicator (Covaris S220, MA, USA). After sonication (Peak PW: 140.0, Duty Factor: 10.0, Cycle Burst: 200), the lysate was centrifuged and diluted with dilution buffer. 5% volume of the supernatant was removed for input. After preclearing the protein with 30µl of protein A conjugated Dynabeads, immunoprecipitation was conducted with a mixture of Protein A dynabeads and a mixture of 2-3 µg antibodies. Amount of antibodies are decided based on the experimental optimization: 2µg of p53, 3µg of p-p53 Ser 15, 3µg of p-p53 Ser 20, and 1µg of normal rabbit IgG, overnight at 4°C with rotation. Immunoprecipitates were washed, heated for reverse crosslinking. DNA fragments were then purified using phenol: chloroform: isoamyl alcohol (15593031, Thermo Fisher Scientific) and subjected to qPCR using primers stated in table 3.2. Data are presented as an enrichment of the precipitated target sequence as compared with input DNA.

3.11 Glucose Colorimetric Assay

Glucose consumption was measured using the colorimetric glucose assay kit (K606-100, Biovision). Upon the treatment, media was collected and diluted in 1:100 in dilution assay buffer as number of live cells were counted by Trypan blue assay. The amount of glucose in the media and standards were detected following the manufacturer's instruction. Glucose consumption was determined by subtracting the amount of glucose in each sample from the total amount of glucose in the blank media (without cells). The detection was performed by reading absorbance values at 570 nm with a microplate reader.

3.12 HKII Enzymatic Assay

HK enzymatic activity of OVCA cells was measured using a Hexokinase Assay Kit (ab 136957, Abcam). In this assay, HK converts glucose into G-6-P. G-6-P is oxidized by G-6-P dehydrogenase to form Nicotinamide adenine dinucleotide (NADH), which reduces a transparent colorless probe to generate a colored product (Red) with strong absorbance at 450nm. Cultured cells were counted and collected as 1 X 10^6 cells, and dissolved with 200 µl of provided assay buffer. Supernatants of each cell lysate were collected after washing, homogenization, and centrifugation at 12,000 rpm (13,200g) for 5 mins at 4°C. 1µl of sample and 49µl of assay buffer were added to sample well in 96 well plate, followed by addition of colorimetric reaction mixture. Also, NADH standard with 50 µl colorimetric reaction mix was added. Reaction mixtures were incubated at room temperature for 30-60 mins. At the end of incubation period, optical density at 450 nm was determined using a microplate reader. Hexokinase activity (expressed as nmol NADH produced) was calculated according to the manufacturer's instructions.

3.13 Extracellular Flux Assays (Sea Horse)

Metabolic measurements of the oxygen consumption rate (OCR) and the extracellular acidification rate (ECAR) were performed on OVCA cell lines using the Seahorse XF96e Extracellular Flux Analyzer (Agilent, USA). Cells were evenly seeded with a density of 20,000 cells/well (experimentally determined) on XF96e cell culture microplate 24 h before experiments. The mitochondrial stress test was utilized to assess OCR. Prior to each experiment, the culture medium was replaced with XF96 DMEM (supplemented with 25 mM D-glucose, 4 mM L-glutamine, 1 mM sodium pyruvate, pH 7.4) and incubated in a non-CO_2 incubator (37°C, 1 h). OCR was measured over a 3 min period. Oligomycin A (1µM; for ATP synthase inhibition), FCCP (0.5µM; for maximal respiratory capacity), antimycin A [(0.5µM)/ rotenone(1µM) for terminating mitochondrial respiration] were sequentially added into each well for the assessment of resting respiration, ATP-linked OCR, and maximal respiratory capacity, respectively.

The glycolytic stress test was utilized to determine ECAR. Prior to each experiment, the culture medium was replaced with XF96e glucose-free DMEM (4 mM L-glutamine, 1 mM sodium pyruvate, pH 7.4) and incubated in a non-CO_2 incubator (37°C, 1 h). Glycolytic flux (basal glycolysis, glycolytic capacity, and glycolytic reserve), as assessed by ECAR, was analyzed by the sequential addition of glucose (10 mM), oligomycin (1.0 μM), and 2-DG (50 mM) in an XF96e flux analyzer. ECAR was measured over a 3 min period. OCR and ECAR values were normalized to the protein concentration in each well, as determined by the Bradford assay.

3.14 Immunohistochemistry (IHC)

Under institutional review board (IRB) or Institutional Ethics Committee (IEC) approved protocols with patient consent forms, tissues were collected from Formalin-Fixed-Paraffin-Embedded (FFPE) ovarian tumors from SNU (IRB No.:H-1711-142-904), University of Hong Kong (IRB UW16_107), and the Centre hospitalier de l'Université de Montréal (CHUM), Division of Gynecologic Oncology (IEC No. 2005-1893, BD 04.002 – BSP). The stage was determined at the time of surgery by a gynecologic oncologist. Histology and tumor grades were determined by a gynecologic-oncology pathologist using criteria consistent with the International Federation of Gynecology and Obstetrics (FIGO) classification. Pre-chemotherapy ovarian tumor sections were obtained at primary debulking surgery and post-chemotherapy ovarian tumor sections were obtained at the second debulking surgery. 4-5 micron thick pre- and post- chemotherapy ovarian tumor IHC sections were cut and deparaffinized. For antigen-retrieval, slides were heated at citrate buffer (10mM sodium citrate, 0.05% Tween 20, pH 6.0; 90°C, 20 min) followed by incubation with primary antibodies for PLA assay.

3.15 Proximity Ligation Assay (PLA)

Proximity ligation assay (PLA) was performed as previously described (Lin et al., 2014; Soderberg et al., 2006). PLA enables us to detect the direct interaction between two adjacent proteins in fixed cell or tissues. The interaction between two proteins is detected using the corresponding two primary antibodies raised in different species. When the PLA probes are in close proximity (< 40 nm), species-specific secondary antibodies as PLA probes with attached unique short DNA strand bind to the primary antibodies. Then, these two DNA strands can interact via a subsequent addition of two other circle-forming DNA oligonucleotides. Cells were grown on 8 well chamber slides, treated with DMSO or CDDP, and subjected to PLA using the Duolink Detection kit (Sigma, USA), according to the manufacturer's instructions. Cells were fixed, permeabilized, blocked, and incubated with antibodies directed against either HKII and P-p53, or HKII and AIF, followed by incubation with or without PLA probes conjugated to oligonucleotides. Ligation and amplification steps were followed by counterstaining of TOM20 as a mitochondrial marker. Images were obtained by confocal microscopy using LSM510 and the quantification and analysis were conducted by Duolink Image tool program (Sigma). The mean of number of PLA signal per cell were determined. At least 50 cells were analyzed per experimental group.

Kaplan-Meier curves were stratified according to PLA signal intensity [HKII-P-p53(Ser15)] in ovarian tumor sections, with low intensity signal assigned a median value of score ≤ 1.0, and high intensity signal assigned a score > 1.

3.16 Statistical Analysis

Results are expressed as the mean $\pm$ SEM of at least three independent experiments. Statistical analysis was carried out by one-way (one variable), two-way (two variables), three-way (three variables) ANOVA to examine the interaction/difference among groups more than two using PRISM (version 7.0; Graph Pad, San Diego, CA) or Sigma Plot (version 12. Systat Software,

Chicago, IL). Differences between multiple experimental groups were determined by the Bonferroni post-hoc test. Correlations were analyzed by the Pearson correlation method using Prism. Kaplan-Meier curves were analyzed using log rank test for hazard ratio (HR), confidence interval (CI), and *P* value. Statistical significance was inferred at $*P < 0.05$.

Table 3.1 List of Primary Antibodies

A. Primary antibodies

Antigen	Species Cross-Reactivity	Host species	Dilution	Company	Catalogue Number	Application
Hexokinase 2	H, M, R, Mk	Rabbit mAb	1/2000 (WB) 1/200 (IF)	Cell Signaling	2867	WB, IF, ChIP
Hexokinase 2	H	Mouse mAb	1/80 (PLA)	Santa Cruz	sc-374091	IF, PLA
P-p53(Ser15)	H, M, R, Mk	Rabbit pAb	1/2000 (WB) 1/100 (IF) 1/100 (ChIP) 1/80 (PLA)	Cell Signaling	9284	WB, IF, ChIP
P-p53(Ser15)	H	Mouse mAb	1/80	Cell Signaling	9286	IF
P-p53 (Ser20)	H, Mk	Mouse pAb	1/100 (ChIP)	Santa Cruz	sc-18079	ChIP
P53(DO-1)	H	Mouse mAb	1/2000 (WB)	Santa Cruz	sc-126	WB, IF
PFK1	H, M, R	Rabbit mAb	1/1000	Santa Cruz	sc-166722	WB
LDH	H	Mouse mAb	1/1000	Santa Cruz	sc-137243	WB
PKM2	H, M, R, Mk	Rabbit mAb	1/1000	Cell Signaling	4053	WB
AIF	H, M, R	Mouse mAb	1/80	Santa Cruz	sc-55519	PLA
TOM20	H	Mouse mAb	1/200	Santa Cruz	sc-17764	IF
β-Actin	H, M, R, Mk	Mouse mAb	1/4,000	Ab cam	Ab8226	WB
GAPDH	H, M, R, Mk	Rabbit mAb	1/10,000	Ab cam	Ab181602	WB

B. Secondary antibodies

Host / Conjugate	Dilution	Company	Catalogue	Application
Goat Anti-Rabbit Alexa Fluor 555	1/400	Thermo Fisher Scientific	A21428	IF
Goat Anti-Mouse Alexa Fluor 488	1/400		A11001	IF
Goat Anti-Rabbit Alexa Fluor 647	1/400		A27040	IF
Goat-Anti Rabbit Alexa Fluor 680	1/10,000		A27042	WB(Li-cor)
Goat-Anti Mouse Alexa Fluor 800	1/8000		A32730	WB(Li-cor)

C. siRNA

Name	Conc (nM)	Gene Accession	Company	Catalogue
HKII siRNA (h)	0-100 nM	NM_000189	Santa Cruz	sc-35621
p53 siRNA (h)	0-100 nM	NM_000546	Santa Cruz	sc-29435

*Western Blotting (WB), ImmunoFluorescence (IF), Monoclonal Antibody (mAb), Polyclonal Antibody (pAb), H (Human), R (Rabbit), M (Mouse), Mk (Monkey), Cell Signaling Technology (Danvers, MA, USA), Santa Cruz Biotechnology (Santa Cruz, CA, USA), Abcam (Cambridge, MA, USA), LifeSpan BioSciences (Seattle, WA, USA), BD Biosciences (San Jose, CA, USA), Thermo Fisher Scientific (Waltham, MA, USA).

Table 3.2 List of Primers

Experiment	Primer	Sequence (5' → 3')	Amplicon size (bp)	Annealing Tm (°)
qPCR	HKII	F: TTGACCAGGAGATTGACATGGG R: CAACCGCATCAGGACCTCA	248	62
	Actin	F: GACAGGATGCAGAAGGAGATTACT R: TGATCCACATCTGCTGGAAGGT	137	62
	p53	F: ACC AGC TCT ATG CGG TCT R: TCC ATC GAA TGA CCT TCT CA	141	61
ChIP	HKII	F: TCACTTGAGGTTAGGAGTTTGAG R: GCCTCAGCCTCCCAAATAG	128	62

Chapter 4. Results

1. CDDP-induced apoptosis is associated with decreased HKII protein in OVCA cells.

To identify which metabolic enzyme(s) in the glycolysis pathway is associated with chemoresistance, established paired chemosensitive A2780s and chemoresistant A2780cp cells were cultured with or without CDDP (10 μM, 24 h) and the protein contents of various metabolic enzymes in the glycolysis pathway were determined by Western blot (WB). We used physiological reliable concentration (0-10μM) and optimal culture duration (24h) for CDDP. CDDP markedly decreased the protein content of HKII and Phosphofructokinase 1 (PFK1) and to a lesser extent of PKM2 while it had no significant effect on lactate dehydrogenase (LDH) or Glyceraldehyde-3-phosphate dehydrogenase (GAPDH) in A2780s cells, In contrast, none of these glycolytic enzymes in the chemoresistant counterpart (A2780cp) were affected by CDDP, suggesting that HKII and PFK1 maybe involved in both cellular metabolism and chemosensitivity (Fig. 4.1A). Based on these results and previous reports that HKII is a key enzyme involved in tumor formation (Patra et al., 2013), HKII was selected for further investigation. We also examined the influence of various concentrations of CDDP (0-10 μM, 24 h) on HKII content and apoptosis in cell lines with different p53 mutational status: chemosensitive OVCA (A2780s; p53-wild type), its counterpart resistant cell (A2780cp; p53-mutant), and other resistant variants (Hey; p53-wild type, and SKOV3; p53-null) (Fig.4.1B).

As shown in Fig.4.1B, CDDP down-regulated HKII protein content in a concentration-dependent manner (Fig.4.1B ; ** $P < 0.01$), with significant decrease detectable in chemosensitive A2780s at 5μM CDDP, but not in A2780cp cells and other resistant variants with different p53 status. A significant increase in CDDP-induced apoptosis was also observed at 5μM in chemosensitive cells but not in chemoresistant cells at all concentrations examined (Fig. 4.1B, Right panel; *** $P <$ 0.001). Time course experiments indicate that CDDP slightly although not significantly decreased

HKII protein content in A2780s cells in 12 hours, but the effect was more pronounced and significant at 24 hours (Fig. 4.1C *** $P < 0.001$). Irrespective of the culture duration (0-24 h), CDDP (10 μM) had no effect on HKII content in A2780cp cells *in vitro*.

Figure 4.1 CDDP-induced apoptosis in OVCA is associated with decreased HKII protein

(A) Chemosensitive OVCA cells A2780s (p53-wild type) and its chemoresistant counterpart A2780cp (p53-mutant) were cultured in the presence or absence of CDDP (10μM, 24 h) and protein contents of HKII, PFK1, PKM2, LDH, GAPDH, and actin (loading control) were measured by Western blot, WB (n = 3). **(B)** Chemosensitive [A2780s (p53-wild type)], and chemoresistant [A2780cp (p53-mutant), Hey (p53-wild type), and SKOV3 (p53-null)] OVCA cells were cultured in different concentration of CDDP (0-10μM) for 24 h and changes in the protein contents of HKII, p53, P-p53(Ser15) and actin (loading control) and apoptosis were assessed by WB and Hoechst nuclear staining, respectively. **(C)** A2780s and A2780cp cells were cultured with different culture duration (0, 1.5, 3, 6 12 h, and 24h) in the absence or presence of CDDP (10 μM) and the protein contents of HKII and actin (loading control) were determined by WB. Results are expressed as mean ± SEM (n = 4) and analyzed by 2-way ANOVA and Bonferroni post-hoc test (** $P < 0.01$, *** $P < 0.001$, **** $P < 0.0001$ vs. CTL). Control, CTL

Fig.4.1

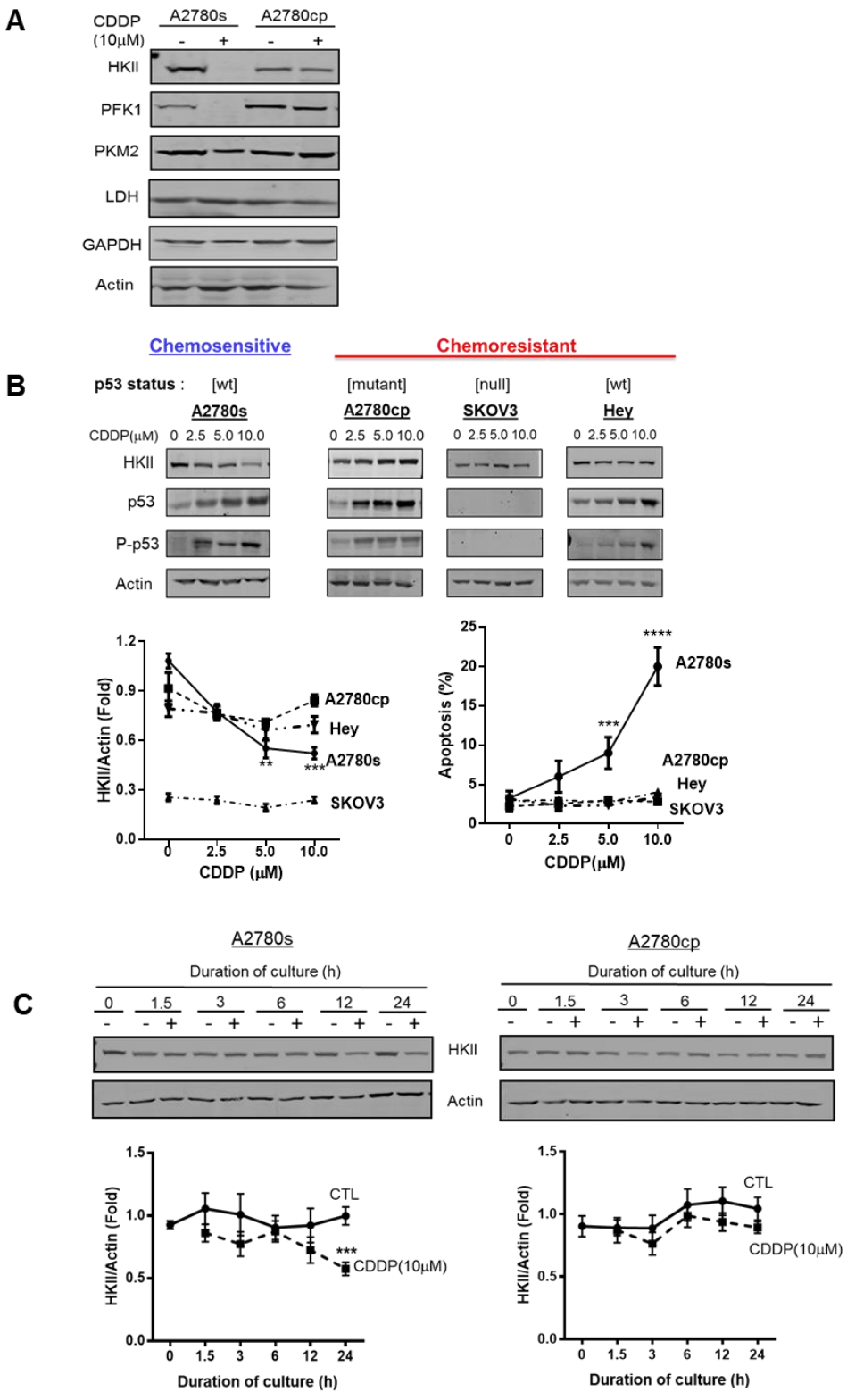
A
CDDP (10μM)
A2780s
A2780cp
HKII
PFK1
PKM2
LDH
GAPDH
Actin
B
Chemosensitive
Chemoresistant
p53 status :
[wt]
[mutant]
[null]
[wt]
A2780s
A2780cp
SKOV3
Hey
CDDP(μM) 0 2.5 5.0 10.0
HKII
p53
P-p53
Actin
HKII/Actin (Fold)
CDDP (μM)
Apoptosis (%)
CDDP(μM)
C
A2780s
A2780cp
Duration of culture (h)
0 1.5 3 6 12 24
HKII
Actin
CTL
CDDP(10μM)
HKII/Actin (Fold)
Duration of culture (h)

2. CDDP transcriptionally decreases HKII in chemosensitive but not in chemoresistant OVCA cells.

To investigate the mechanism by which CDDP decreased HKII content, we first determined if this response was associated with changes in HKII mRNA abundance (Fig. 4.2A). As observed in HKII protein content, HKII mRNA abundance during a 24h culture period was significantly suppressed by the presence of CDDP in A2780s but not in A2780cp (Fig. 4.2A; * $P < 0.05$ & ** $P < 0.01$). To determine whether the CDDP-induced changes in HKII protein levels in chemosensitive cells were due to proteasomal degradation, A2780s cells were pre-treated with the proteasomal inhibitors Lactacystin (2 μM) and epoxomicin (5 nM), at optimized concentrations, previously demonstrated to suppress proteasomal protein degradation in A2780s cells (Abedini et al., 2004) 3 h prior to and during CDDP treatment. Although CDDP markedly and significantly decreased HKII protein content (Fig 4.2 B, * $P < 0.05$, CTL vs. CDDP) as shown in my previous studies, this response was not affected by the presence of either inhibitor, suggesting that CDDP-induced changes in HKII protein level could be caused by downregulation of mRNA, likely at the transcriptional level.

Figure 4.2 CDDP transcriptionally decreases HKII in chemosensitive but not in chemoresistant OVCA cells.

(A) A2780s and A2780cp cells were cultured with different concentration of CDDP (0-10μM, 24 h) and changes in mRNA abundance of HKII and actin (loading control) were determined by qPCR. **(B)** A2780s cells were pre-treated with proteasomal inhibitors Lactacystin (Lacta; 2 μM) and Epoxomycin (Epo; 5 nM) for 3 h prior to and during CDDP treatment (10μM, 24 h). Changes in HKII content and GAPDH (loading control) were assessed by WB. DMSO was used as a vehicle. Results are expressed as mean ± SEM (n= 4) and analyzed by 2-way ANOVA and Bonferroni post hoc test (* $P < 0.05$, ** $P < 0.01$, and *** $P < 0.001$ vs. CTL).

Fig.4.2

A qPCR

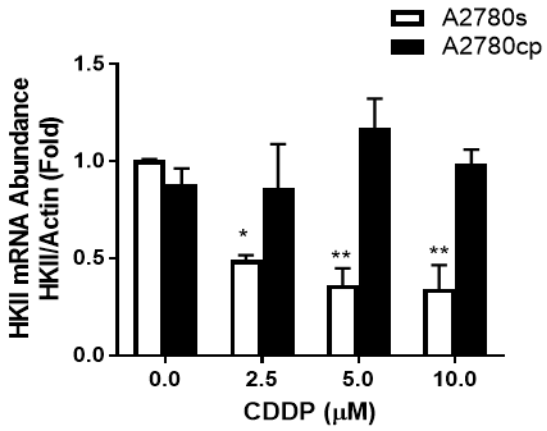

B WB (Proteasomal degradation)

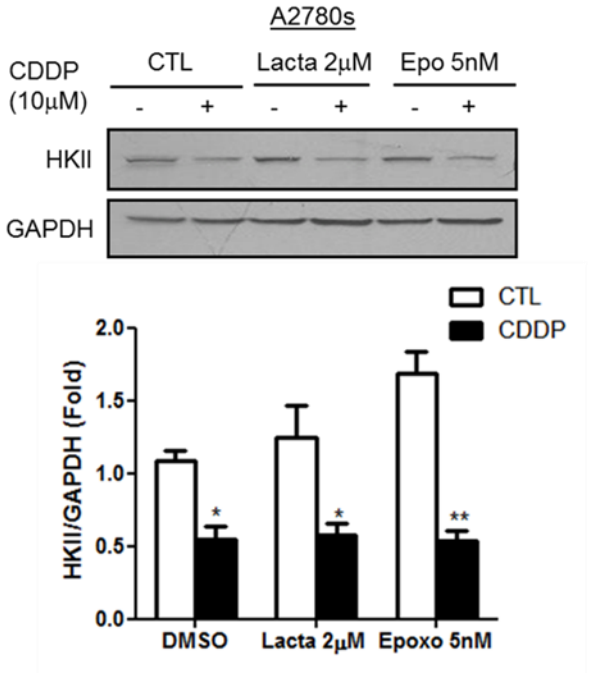

3. CDDP decreases HKII-mediated glycolysis in chemosensitive but not chemoresistant OVCA cells.

Elevated aerobic glycolysis is a key hallmark of multiple cancer cells, including OVCA (Dang, 2012). To examine whether CDDP differently influences aerobic glycolysis and cellular metabolism in chemosensitive and chemoresistant cells, A2780s and A2780cp cells were cultured with different concentrations of CDDP (0-10 μM, 24 h) and glycolysis and multiple metabolic indicators were assessed. To firstly examine metabolic profiles, we conducted extracellular flux analysis (using the XFe96 Seahorse): oxygen consumption rate (OCR; an indicator of mitochondrial oxidation pathway) and extracellular acidification rate (ECAR; an endpoint associated with lactic acid in the glycolysis pathway). As shown in Fig. 4.3A, CDDP markedly decreased the level of resting OCR, glycolysis (resting ECAR), and adenosine triphosphate (ATP)-linked OCR as CDDP concentration was increased in chemosensitive A2780s cells but not in resistant A2780cp cells (Fig.4.3A; ** $P < 0.01$, *** $P < 0.001$ vs. CTL; $^{\#}$ $P < 0.05$, $^{\#\#\#}$ $P < 0.001$, A2780s vs. A2780cp). Interestingly, CDDP affects both resting OCR and ATP-linked OCR starting at a minimal concentration of CDDP at 5 μM in sensitive A2780s cells (Fig.4.3A; **$P < 0.01$, *** $P < 0.001$), whereas ECAR of chemosensitive cells were only affected at the highest concentration examined (10 μM; Fig.4.3A; ** $P < 0.01$), suggesting that OXPHOS is more sensitive than glycolysis to CDDP treatments in chemosensitive OVCA cells. CDDP treatment resulted in a significant decrease in resting and maximal OCR rate over time in chemosensitive cells (Fig.4.3B; ** $P < 0.01$). Notably, chemoresistant A2780cp cells demonstrated higher resting and maximal ECAR rates than that of A2780s cells, implying highly activated glycolysis in chemoresistant OVCA cells. In addition, we indirectly measured glucose consumption using spent medium of A2780s and A2780cp cells treated with CDDP and observed that CDDP significantly decreased glucose consumption of chemosensitive cells starting from 5 μM and showed maximal decrease (~50%) at 10 μM (Fig 4.3C; *** $P < 0.001$, CTL vs. CDDP; $^{\#\#\#}P < 0.001$, A2780s vs. A2780cp)

compared with A2780cp cells. Similarly, CDDP significantly downregulated HK activity to a maximum of 40% at 10 μM CDDP (Fig 4.3D; ** $P < 0.01$) in A2780s cells, but not in chemoresistant cells.

Figure 4.3 CDDP downregulates HKII-mediated aerobic glycolysis in chemosensitive OVCA cells.

(A) A2780s and A2780cp cells were seeded on 96-well plate, treated with CDDP (10μM, 24 h; DMSO as a vehicle), and resting oxygen consumption rate (OCR), glycolysis as resting extracellular acidification rate (ECAR), and ATP-linked OCR were measured after exposure to biomodulators as indicated (dashed vertical line) using an XF96e Extracellular Flux Analyzer. **(B)** OCR and ECAR measurements were obtained over time (72 min) in A2780s and A2780cp cells cultured with minimal (0 μM) and maximal concentration of CDDP (10 μM). **(C)** A2780s and A2780cp cells were cultured with CDDP (0-10μM, 24 h) and glucose consumption from the spent medium, and **(D)** HK activity from cell lysates were measured. For all experiments described, DMSO was used as a vehicle control. Results are expressed as mean ± SEM (n = 4) and analyzed by 2-way ANOVA and Bonferroni post-hoc test. (* $P < 0.05$, ** $P < 0.01$, *** $P < 0.001$, and **** $P < 0.0001$, CTL vs. CDDP; $^{\#}P < 0.05$, $^{\#\#}P < 0.01$, $^{\#\#\#}P < 0.001$, A2780s vs. A2780cp).

Fig.4.3

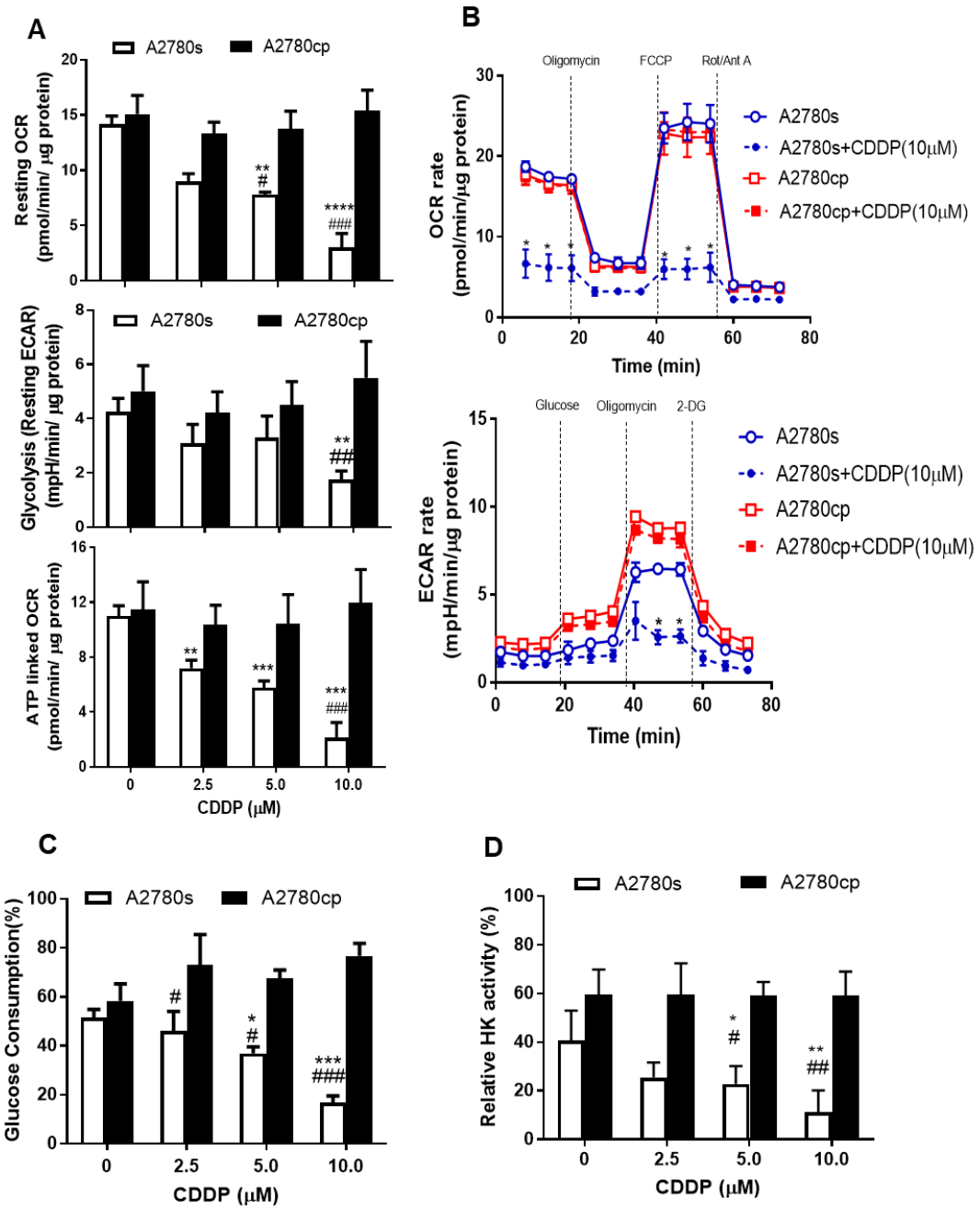
A
A2780s
A2780cp
Resting OCR (pmol/min/ μg protein)
Glycolysis (Resting ECAR) (mpH/min/ μg protein)
ATP linked OCR (pmol/min/ μg protein)
CDDP (μM)
B
Oligomycin
FCCP
Rot/Ant A
OCR rate (pmol/min/μg protein)
A2780s+CDDP(10μM)
A2780cp+CDDP(10μM)
Time (min)
Glucose
Oligomycin
2-DG
ECAR rate (mpH/min/μg protein)
C
Glucose Consumption(%)
D
Relative HK activity (%)

4. CDDP induces HKII nuclear localization where P-p53(Ser15) is co-localized.

HKII bound to mitchondria (mito-HKII) is important for cell survival during external stress and intrinsic apoptosis (Pastorino et al., 2002; Roberts et al., 2013), but if and how mito HKII contributes to chemoresistance remain unclear. To this end, we examined whether CDDP treatments (10 μM, 0-24 h) affected the cellular localization of HKII in chemosensitive A2780s cells and its counterpart chemoresistant A2780cp OVCA cells. Remarkably, in chemosensitive A2780s cells, nuclear localization of HKII was significantly increased from 28% to 55% in 24 hrs following CDDP treatment (Fig.4.4A, ** $P < 0.01$). In contrast, only 17% of HKII in the nuclear region was observed in chemoresistant A2780cp cells and was not changed with CDDP treatment (Fig.4.4A, P = NS). Notably, the basal level of nuclear HKII is marginally higher in A2780s cells than A2780cp cells. Conversely, HKII localization was significantly decreased from mitochondria from 60% to 35% at 24h in A2780s and this change is maintained as peak up to ~24 h (Fig.4.4A; ** $P < 0.01$) in A2780cp cells. In contrast, HKII was predominantly localized to mitochondria (70%) and unaffected by CDDP treatment (Fig 4.4A; P = NS), suggesting that intracellular trafficking of HKII is associated with responsiveness to CDDP.

Nuclear localization of P-p53 (Ser 15) is important for its apoptotic function and DNA binding activity as a transcription factor (Moll et al., 2005; Vousden and Lu, 2002). In response to CDDP, we reported that Ser15 and Ser20 are important for facilitating apoptosis in OVCA. We then examined whether CDDP facilitates the co-localization of P-p53 (Ser15) and HKII in the nucleus in later section. In the absence of CDDP, P-p53(Ser15) localizes minimally to the nucleus in chemosensitive A2780s cells but rapidly accumulates in 60% of the cells 24 hours after CDDP treatment in (Fig.4.4B; **** $P < 0.0001$, CTL vs. CDDP). However, this response was significantly attenuated in chemoresistant cells (Fig.4.4B; $^{\#} P < 0.05$, A2780s vs. A2780cp). In addition, HKII-P-p53(Ser15) co-localization was observed starting from 3 h and reached a peak at 6 h in chemosensitive cells (Fig.4.4B; ** $P < 0.01$, CTL vs. CDDP), but this phenomenon is evidently

compromised in chemoresistant cells with defective p53. Although HKII nuclear localization has been previously reported, this data suggests that nuclear HKII localization maybe mediated by P-p53(Ser15), which will be examined more conclusively below.

We also confirmed that high mitochondrial HKII localization occurs in other epithelial subtypes of OVCA cells including high grade serous and clear cell carcinoma. A2780s and A2780cp are reported to be originated from ovarian endometrioid adenocarcinoma (Anglesio et al., 2013; Beaufort et al., 2014). Similar to previous observation in chemoresistant A2780cp cells, 70% HKII is highly localized in mitochondria in other chemoresistant OVCAR3 cells (p53-mutant) as a high grade serous subtype and 60% HKII in ES2 (p53-mutant) as a clear cell carcinoma, respectively (Fig. 4.5).

Figure 4.4 CDDP facilitates translocation of HKII to the nucleus in chemosensitive but not in chemoresistant cells.

(A) A2780s and A2780cp cells were cultured with CDDP (10 μM, 0-24 h; DMSO as a vehicle), fixed, stained, and subjected to confocal microscopy. Cellular localization HKII (Red) as % of total cells with TOM20 (Green: Mitochondrial Marker), DAPI (Blue: Nucleus marker) was analyzed followed by quantification using Image premier program. **(B)** In A2780s and A2780cp cells, same treatment as above in (A) was subjected to confocal microscopy with HKII, P-p53 antibody, and DAPI. Co-localization of HKII and P-p53 were quantitatively analyzed by Image premier program. Results are expressed as mean ± SEM (n = 4) and analyzed by 2-way ANOVA and Bonferroni post-hoc test (* $P < 0.05$, ** $P < 0.01$, *** $P < 0.001$, CTL vs. CDDP; $^{\#\#} P < 0.01$ $^{\#\#\#} P < 0.001$, $^{\#\#\#\#} P < 0.0001$, A2780s vs. A2780cp). Yellow inserted box represents response of single cells. Scale bar: 10 μm

Fig 4.4

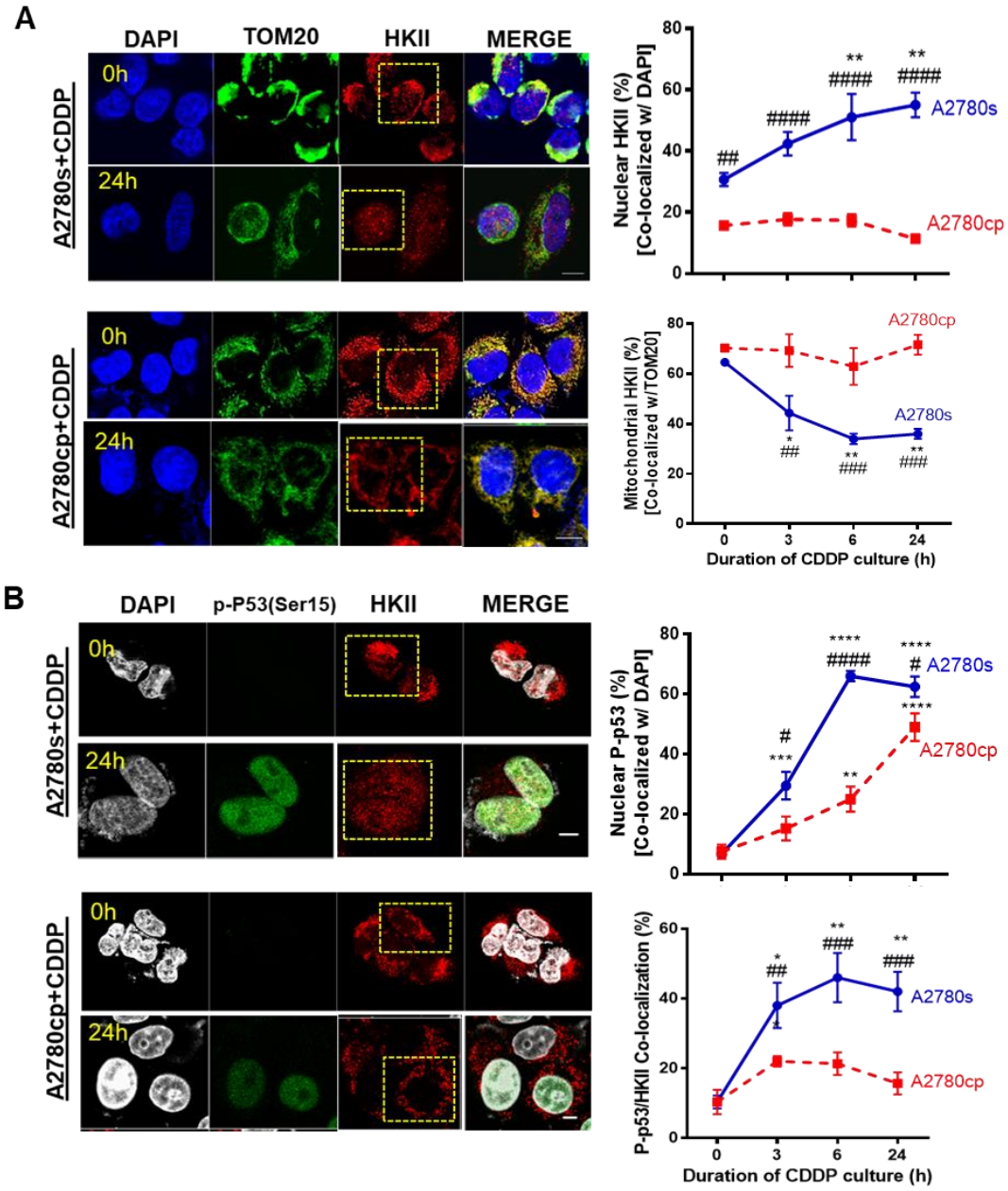
A
DAPI
TOM20
HKII
MERGE
A2780s+CDDP
A2780cp+CDDP
0h
24h
Nuclear HKII (%) [Co-localized w/ DAPI]
A2780s
A2780cp
Mitochondrial HKII (%) [Co-localized w/TOM20]
Duration of CDDP culture (h)
B
DAPI
p-P53(Ser15)
HKII
MERGE
Nuclear P-p53 (%) [Co-localized w/ DAPI]
P-p53/HKII Co-localization (%)

Figure 4.5 HKII is highly localized in mitochondria in different subtypes of chemoresistant OVCA cells.

(A) OVCAR 3 (High grade serous, p53 wild-type) and **(B)** ES2 cells (Clear cell, p53 mutant) were cultured with CDDP (10 μM, 24 h), fixed, stained, and subjected to confocal microscopy. Cellular localization of HKII (Red) as % of total cells was analyzed using TOM20 (Green: mitochondrial Marker) and DAPI (Blue: nucleus marker) followed by quantification using Image premier program. **(C)** OVCAR3 and ES2 cells cultured as above were also subjected to apoptosis measurement using Hoechst staining. Results are expressed as mean ± SEM (n =3) and analyzed by 2-way ANOVA and Bonferroni post hoc test. (No significance: NS). Scale bar: 10 μm

Fig.4.5

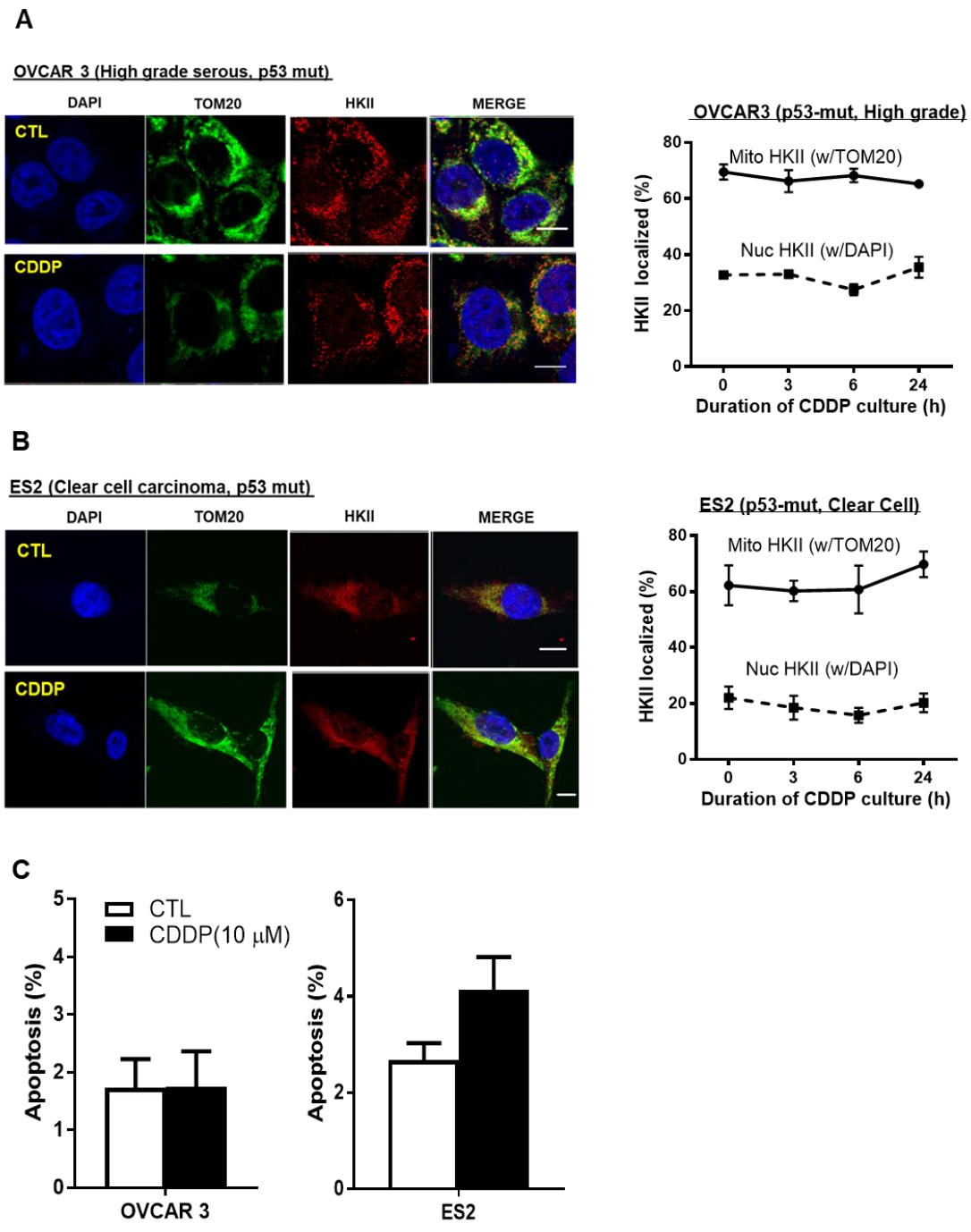
A
OVCAR 3 (High grade serous, p53 mut)
DAPI
TOM20
HKII
MERGE
CTL
CDDP
OVCAR3 (p53-mut, High grade)
Mito HKII (w/TOM20)
Nuc HKII (w/DAPI)
HKII localized (%)
Duration of CDDP culture (h)
B
ES2 (Clear cell carcinoma, p53 mut)
ES2 (p53-mut, Clear Cell)
C
CTL
CDDP(10 μM)
Apoptosis (%)
OVCAR 3
ES2

5. p53 is required for modulating HKII intracellular trafficking and aerobic glycolysis.

We next sought to determine if and how the detachment of HKII from the mitochondria affects its metabolic function and aerobic glycolysis. Based on our previous findings, activated P-p53 is a likely inducible factor which enables the nuclear localization of HKII. Thus, A2780cp cells (p53-mutant) were infected with an adenoviral construct (Adv) containing Adv-LacZ as a control (MOI = 1.0, 24 h) or functional p53 (Adv-p53) alone or together followed by treatment with CDDP (10 μM, 24h). We observed that HKII nuclear localization was markedly increased from 20% to 40% (Fig. 4.6A; ** $P < 0.01$) in A2780cp cells infected with Adv-p53 treated with CDDP compared with cells infected with Adv-LacZ (MOI = 1.0, 24 h) alone. In addition, nuclear co-localization of P-p53(Ser15) and HKII were significantly increased from 23% to 45% (Fig. 4.6A; ** $P < 0.01$), but this phenomenon was attenuated in A2780cp with Adv-LacZ only, possibly due to defective p53. Notably, neither Adv-p53 alone or nor Adv-LacZ as counterparts without CDDP elicited such responses (Fig. 4.6A; *P*=NS), suggesting that CDDP-activated P-p53 is required for modulating HKII cellular localization.

We then tested if detachment of HKII from mitochondria by P-p53 affects glycolytic metabolism. Glycolysis (as measured by resting ECAR) and ATP-linked OCR were measured in A2780cp cells infected with Adv-p53, or CTL, followed by CDDP treatment (10 μM, 24 h). Adv-p53 infection in A2780cp cells treated with CDDP decreased glycolysis (Resting ECAR; Fig. 4.6B; ** $P < 0.01$) and ATP linked OCR (Fig. 4.6B; ** $P < 0.01$). However, p53 infection alone also significantly decreased resting ECAR (Fig. 4.6B; $^{\#\#}P < 0.01$, LacZ vs. Adv-p53), suggesting that both p53 and P-p53 (Ser15) enforces this metabolic regulation (Fig.4.6B; $^{\#\#}P < 0.01$). Similarly, HK activity and glucose consumption were significantly decreased in p53 infected cells with identical treatment (Fig. 4.6C; * $P < 0.05$). Overall, these results suggest that P-p53 is specifically involved in the

detachment of HKII from mitochondria and attributes dysregulation of HKII enzyme activity and its mediated glycolysis.

Conversely, we also performed the experiment by downregulating p53 expression in chemosensitive A2780s cells and assessed HKII localization in cellular bioenergetics. As expected, we observed that mito HKII localization was markedly decreased from 60% to 40% and nuclear HKII localization was increased from 30% to 45% in control cells (scramble) with CDDP treatment, but not in p53 knocked down A2780s cells. (Fig. 4.7A; ** $P < 0.01$), confirming p53 is involved in the regulation of intracellular HKII localization.

We then examined whether p53 depletion increases HKII-mediated glycolysis in the presence of CDDP. Consistent with previous findings, CDDP-induced downregulation of glycolysis, ATP linked OCR, and glucose consumption was recovered in p53 depleted groups irrespective of CDDP treatment (Fig. 4.7B; $^{\#}P < 0.05$, $^{\#\#}P < 0.01$, scramble vs. p53 siRNA). Notably, p53 knockdown itself significantly increased the basal level of glycolysis, ATP linked OCR, and glucose consumption (Fig. 4.7B; $^{\#\#}P < 0.01$, scramble vs. p53 siRNA). This may indicate that p53 is required for facilitating HKII nuclear localization and HKII-mediated glycolysis.

Figure 4.6 p53 is required for detachment of HKII from mitochondria, resulting in attenuated aerobic glycolysis.

(A) A2780cp cells were transfected with either Adv-LacZ (multiplicity of infection**,** MOI = 1.0, 24 h) or Adv-p53 with GFP tag (MOI = 1.0, 12h) and cultured with or without CDDP (10 μM, 24 h; DMSO as a vehicle). Total MOI was constant for all treatment groups as MOI 1.0. Cellular localization of HKII (Red) as % of total cells with P-p53 with GFP tag (Green), and DAPI (Blue) was obtained by confocal microscopy and quantified with Image premier program. **(B)** Glycolysis (resting ECAR) and ATP-linked OCR were measured with an XF96e Extracellular Flux Analyzer. **(C)** HK activity and glucose consumption were measured using cell lysate and spent medium from A2780cp cells treated as in (A). Results are expressed as mean ± SEM (n =3) and analyzed by 2-way ANOVA and Bonferroni post-hoc test (* $P < 0.05$, ** $P < 0.01$, CTL vs. CDDP; $^{\#\#} P < 0.05$, $^{\#\#} P < 0.01$, $^{\#\#\#} P < 0.001$, Adv-LacZ vs. Adv-p53). Scale bar: 10 μm

Fig 4.6

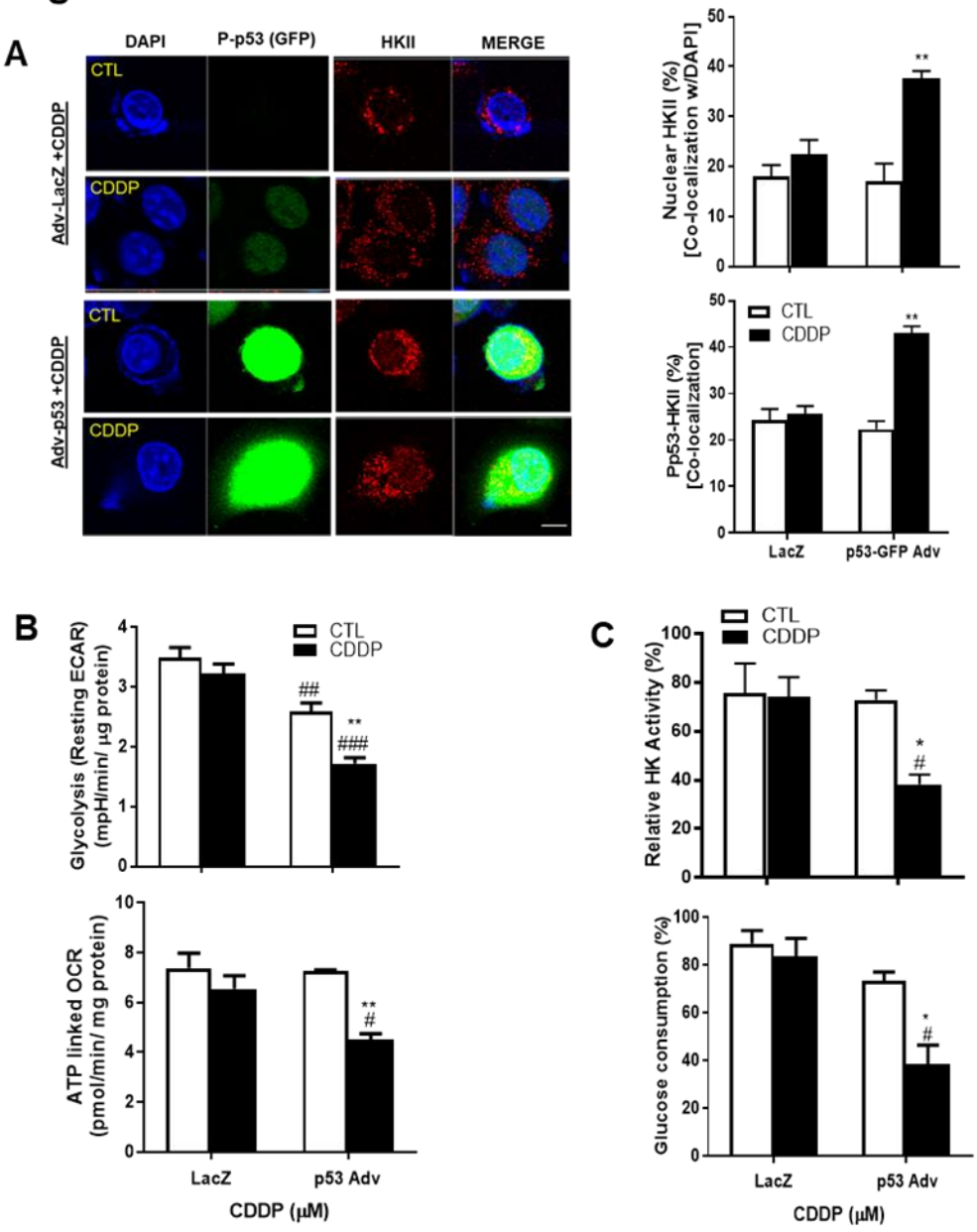
A
DAPI
P-p53 (GFP)
HKII
MERGE
CTL
CDDP
Adv-LacZ +CDDP
Adv-p53 +CDDP
Nuclear HKII (%) [Co-localization w/DAPI]
Pp53-HKII (%) [Co-localization]
LacZ
p53-GFP Adv
B
Glycolysis (Resting ECAR) (mpH/min/ µg protein)
ATP linked OCR (pmol/min/ mg protein)
LacZ
p53 Adv
CDDP (µM)
C
Relative HK Activity (%)
Glucose consumption (%)
LacZ
p53 Adv
CDDP (µM)

Figure 4.7 p53 depletion promotes mito-HKII localization and aerobic glycolysis.

(A) A2780s cells were knocked down using either scramble or p53 siRNA (100 nM) and cultured with CDDP (0, 10μM 24; DMSO as a vehicle). Cellular localization of HKII (Red) as % of total cells, TOM20 (Green, mitochondrial marker), and DAPI (Blue, nucleus marker) were obtained using confocal microscopy and analyzed by Image premier program **(B)** Glycolysis (Resting ECAR) and ATP-linked oxygen consumption rate (OCR) were measured in A2780s cells transfected with p53 siRNA (100 nM), seeded on 96-well plate, treated with CDDP (10μM, 24 h), and analyzed using an XF96e Seahorse Analyzer. Glucose consumption was measured using the spent medium of cells seeded on 12-well plate, and treated with CDDP (10μM, 24 h). Results are expressed as mean ± SEM (n =4) and analyzed by 2-way ANOVA and Bonferroni post hoc test (* $P < 0.05$, ** $P < 0.01$, CTL vs. CDDP; $^{\#} P < 0.05$, $^{\#\#} P < 0.01$; Scramble vs. p53 siRNA). Scale bar: 10 μm

Fig.4.7

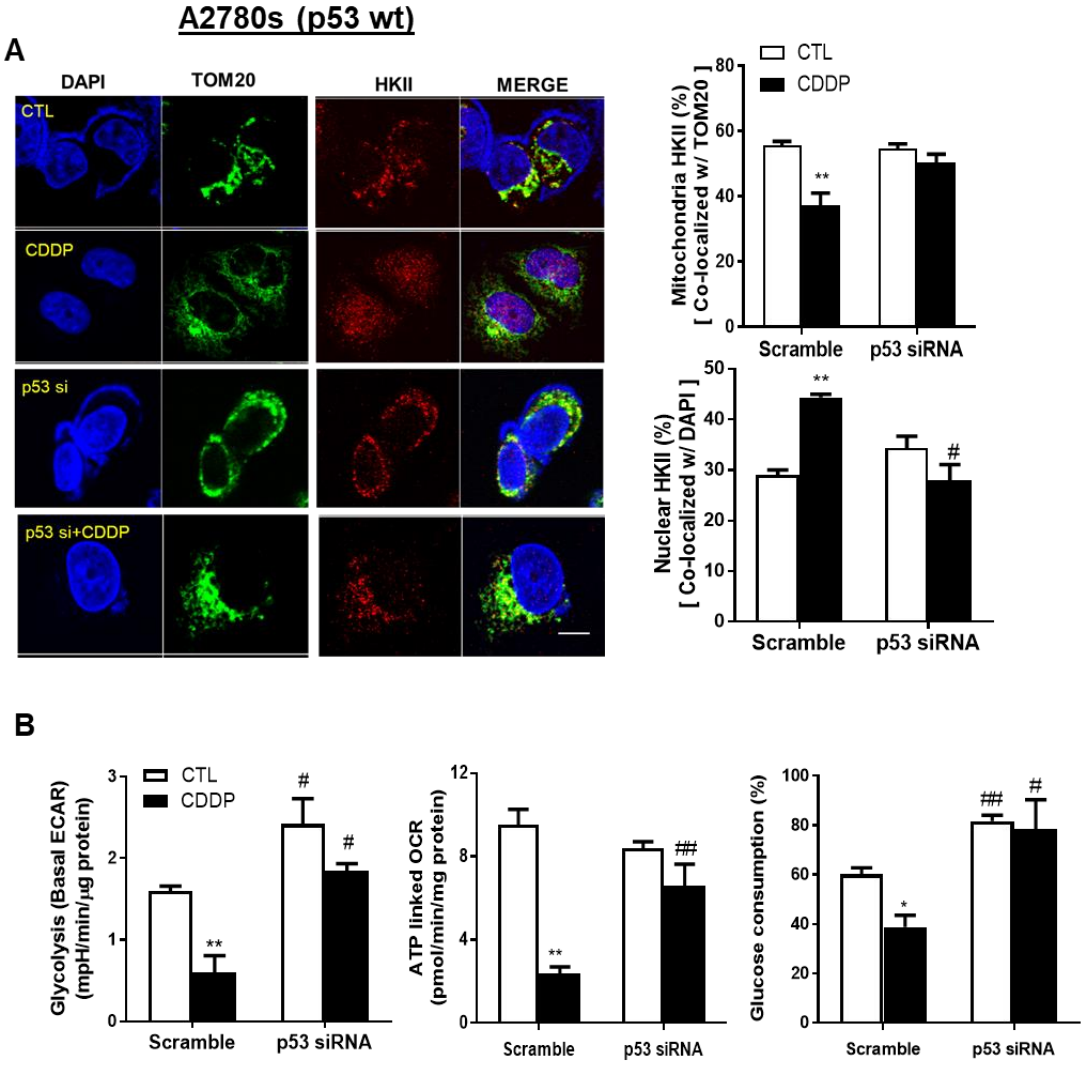
A2780s (p53 wt)
A
DAPI
TOM20
HKII
MERGE
CTL
CDDP
p53 si
p53 si+CDDP
CTL
CDDP
Mitochondria HKII (%)
[Co-localized w/ TOM20]
Scramble
p53 siRNA
Nuclear HKII (%)
[Co-localized w/ DAPI]
Scramble
p53 siRNA
B
Glycolysis (Basal ECAR)
(mpH/min/μg protein)
CTL
CDDP
Scramble
p53 siRNA
ATP linked OCR
(pmol/min/mg protein)
Scramble
p53 siRNA
Glucose consumption (%)
Scramble
p53 siRNA

6. p53 re-constitution and Akt suppression cooperatively facilitate translocation of HKII.

Previous research reported that activated phosphorylated Akt (P-Akt) promotes binding of HKII to OMM of mitochondria (Roberts et al., 2013). On the other hand, our previous findings (Fig. 4.6 and 4.7) also showed that P-p53(Ser15) facilitates detachment of HKII from the mitochondria. Based on that, we examined whether Akt suppression with dominant negative Akt (DN-Akt) and P-p53 together detach HKII from OMM of mitochondria, associated with chemosensitivity. Thus, A2780cp (p53-mutant) cells were infected with an adenoviral construct containing Adv-LacZ as a control (MOI = 0.5, 12 h) or functional p53 (Adv-p53, MOI = 1.0, 24 h), DN-Akt (Adv-DN Akt, MOI = 40, 24 h) alone, or together followed by treatment with CDDP (10 μM, 24 h) as indicated. We observed that CDDP significantly decreased mito HKII localization from 43% to 27% in A2780cp cells infected with p53 and DN-Akt adenovirus together. In A2780cp cells re-constituted with Adv-p53 and Adv-DN-Akt, CDDP significantly decreased mito HKII localization from 40 % to 31 % (** $P < 0.01$ vs. CTL, Fig. 4.8A), but nuclear HKII is significantly increased from 15% to 45% (**** $P < 0.0001$ vs. CTL, Fig. 4.8A). However, DN-Akt infection alone or together with CDDP did not significantly change nuclear HKII localization (NS. Fig 4.8A).

In Fig. 4.8B, we used the same treatment group above as successful infection was confirmed using WB, shown as increased p53 and Akt protein content. Interestingly, our WB analysis showed that the protein content of HKII was not decreased with A2780cp infected with either functional p53 (Adv-p53), DN-Akt alone regardless of CDDP treatment. However, DN-Akt and p53 together decreased the protein content of HKII irrespective of CDDP treatment. Along with that, we examined the apoptosis rate. In A2780cp cells infected with LacZ, p53, DN-Akt alone did not show a significant increase in apoptosis rate, but p53 and DN-Akt together followed by CDDP treatment showed an increase in 20% of apoptosis rate (** $P < 0.01$ vs. CTL, Fig 4.8A). In Fig. 4.8 D & E, A2780cp cells infected with Adv-p53 and Adv-DN-Akt together significantly synergized to

decrease both ECAR as well as OCR. Collectively, these data suggest us that functional p53 and Akt depletion cooperatively facilitate nuclear localization of HKII in chemoresistant OVCA cells, associated with apoptotic induction and metabolic activity.

Figure 4.8 p53 re-constitution and Akt depletion together facilitate detachment of HKII from mitochondria.

(A) A2780cp cells were transfected with either Adenoviral constructs (Adv)- LacZ (MOI:0.5, 12 h) or Adv-p53 with GFP tag (MOI = 0.5, 12h), Dominant Negative (DN)-Akt Adv with GFP tag (MOI = 40), and cultured with CDDP (0, 10μM 24h; DMSO as vehicle). Total MOI was constant for all treatment groups as MOI 40.5. Cellular localization of HKII (Red) as % of total cells, and p53/P-p53 w GFP tag (Green) with TOM20 (Blue), and DAPI (Grey) were measured using confocal microscopy and quantitatively analyzed with Image premier program. **(B)** A2780cp cells transfected as mentioned above were cultured with CDDP (10μM, 24h) followed by WB and **(C)** apoptosis measurement using Hoechst staining. **(D)** OCR and **(E)** Glycolysis (Resting ECAR) were measured in A2780cp cells infected with Adv-LacZ (MOI:0.5 or 40.0, 24 h) or Adv-p53 with GFP tag (MOI = 0.5, 12h), Adv-DN-Akt with GFP tag (MOI = 40, 12h) alone or together, seeded on 96-well plate, treated with CDDP (10μM, 24 h), and analyzed using an XF96e Extracellular Flux Analyzer. Results are expressed as mean ± SEM (n =4) and analyzed by 2-way ANOVA and Bonferroni post hoc test (* $P < 0.05$, ** $P < 0.01$, **** < 0.0001, CTL vs. CDDP; $^{\#} P < 0.05$, Adv-LacZ vs. Adv-p53). Scale bar: 10 μm

Fig.4.8

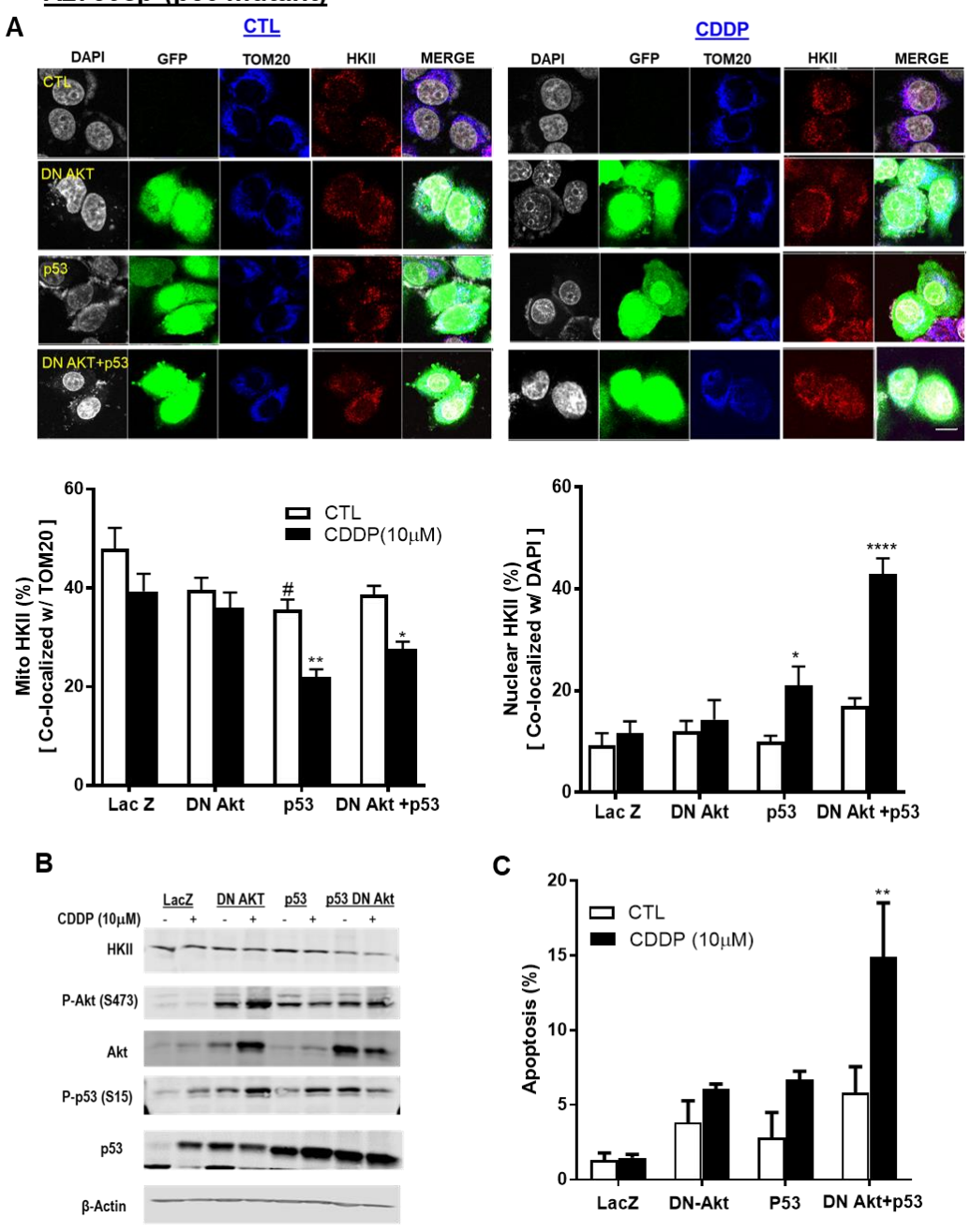
A2780cp (p53 mutant)
A
CTL
CDDP
DAPI
GFP
TOM20
HKII
MERGE
CTL
DN AKT
p53
DN AKT+p53
Mito HKII (%)
[Co-localized w/ TOM20]
CTL
CDDP(10μM)
Lac Z
DN Akt
p53
DN Akt +p53
Nuclear HKII (%)
[Co-localized w/ DAPI]
B
LacZ
DN AKT
p53
p53 DN Akt
CDDP (10μM)
HKII
P-Akt (S473)
Akt
P-p53 (S15)
p53
β-Actin
C
Apoptosis (%)
CTL
CDDP (10μM)
LacZ
DN-Akt
P53
DN Akt+p53

Fig.4.8

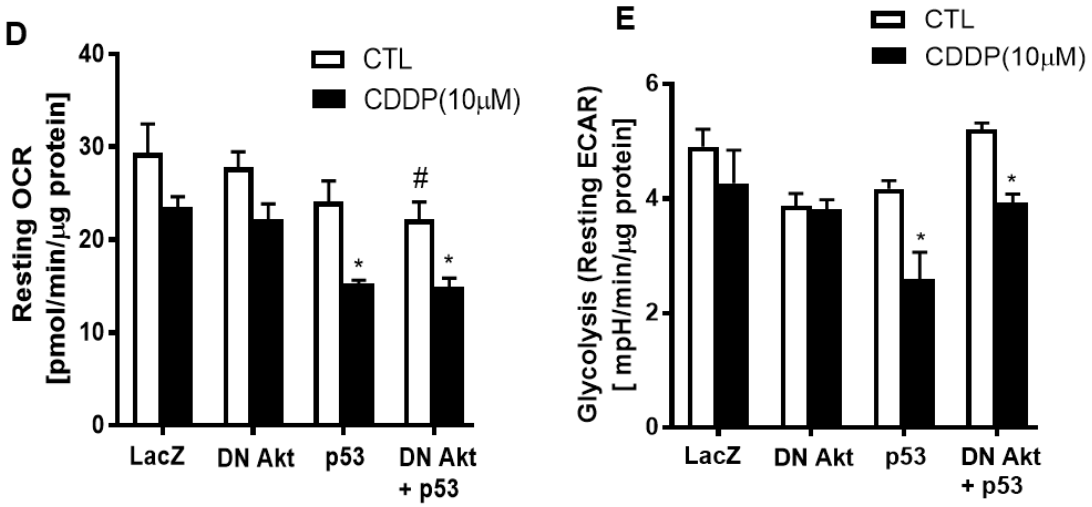
D
Resting OCR
[pmol/min/μg protein]
40
30
20
10
0
CTL
CDDP(10μM)
#
*
*
LacZ
DN Akt
p53
DN Akt
+ p53
E
Glycolysis (Resting ECAR)
[mpH/min/μg protein]
6
4
2
0
CTL
CDDP(10μM)
*
*
LacZ
DN Akt
p53
DN Akt
+ p53

7. p53 is required for CDDP-induced apoptosis in HKII depleted cell.

To further understand the role of HKII in chemoresistance, we examined the effect of HKII depletion on the apoptotic response of chemoresistant OVCA cells to CDDP. Various chemoresistant OVCA cell lines, including A2780cp (p53-mutant), Hey (p53-wild type), and SKOV3 (p53-null) cells were treated with either pharmacologic HK inhibitor (2-Deoxy-D-Glucose: 2-DG) or HKII siRNA. 2-DG treatment markedly sensitized Hey cells to CDDP-induced apoptosis starting from 12% (5 mM; Fig. 4.9A; $*P < 0.01$) and maximally up to 20% (20 mM; Fig.4.9A; $***$ $P < 0.001$), but not in other p53 defective chemoresistant cells (A2780cp and SKOV3). Consistent with previous findings, HKII siRNA facilitates increase CDDP-induced apoptosis from 8% (50 nM) to 11% (100 nM) (Fig. 4.9A; $***$ $P < 0.001$) of p53-wild type Hey cells, but not in other p53 defective chemoresistant cells. To confirm that p53 is required for the induction of apoptosis in HKII depleted cells, chemoresistant A2780cp cells were re-constituted with an Adv-p53 (MOI = 0.5 or 1.0, 12 h) followed by HKII knock-down and CDDP treatment (10μM, 24h). In HKII-depleted A2780cp cells, infection with Adv-p53 markedly enhanced apoptosis rate to 10% (MOI = 0.5) and maximally up to 20% at highest MOI (MOI = 1.0, 12h) in response to CDDP (Fig.4.9B; $***$ $P < 0.001$). These data demonstrate that HKII depletion is not sufficient, but the functional p53 is required for the synergistic induction of apoptosis in chemoresistant OVCA cells.

We then investigated the role of HKII in glycolysis metabolism in cancer cells. HKII knockdown significantly decreased glycolysis (resting ECAR) compared with control (Fig. 4.9 C; $^{\#}P < 0.05$). Similarly, HKII knockdown in chemoresistant A2780cp cells exhibited a significant 40% decrease in glucose consumption (Fig. 4.9C, Right panel; $^{\#\#}$ $P < 0.01$) compared with control transfected with a scramble. However, HKII knockdown did not cause any significant difference between control and CDDP (10μM, 24h) treatment group (Fig. 4.9 C: P = NS). As expected, HKII knockdown caused a significant decrease in both ECAR and glucose consumption while no further

decrease was observed in CDDP treated cells, suggesting that HKII mediates aerobic glycolysis. On the other hand, HKII depletion significantly decreased cell viability in various chemoresistant cells (Hey, A2780cp, and SKOV3), suggesting that HKII depletion is sufficient for decreasing cell proliferation or cell viability, but p53 is required for apoptosis induction (Fig.4.9D).

Figure 4.9 p53 is required for CDDP-induced apoptosis of chemoresistant OVCA cells when HKII is depleted.

(A) Hey (p53-wt), A2780cp (p53-mutant), and SKOV3 (p53-null) were treated with the HK inhibitor, 2-deoxy-D-glucose (2-DG, 0 - 20 mM, 6 h; Upper panel) or transfected with 0 ~100 nM of HKII siRNA (16 h; Bottom panel), treated with CDDP (10 μM, 24h; DMSO as a vehicle), and apoptosis was assessed morphologically with Hoechst staining. For successful transfection, HKII protein content (actin as loading control) was assessed by WB. **(B)** p53 re-constitution sensitizes chemoresistant OVCA cells with HKII knocked-down to CDDP-induced apoptosis. A2780cp cells were transfected with HKII siRNA (100 nM, 16 h), infected with p53 adenovirus (MOI = 0 - 1.0, 12 h) or Lac Z as control and then treated with CDDP (10 μM, 24 h) followed by apoptosis measurement. Total MOI was constant for all treatment groups as MOI 1.0. For successful transfection, the protein content of HKII, P-p53(Ser15), p53 and actin were assessed by WB. **(C)** Glycolysis (resting ECAR) was measured with A2780cp cells transfected with 0-100 nM of HKII siRNA and subjected to CDDP treatment (10 μM, 24 h) on 96 wells. Glucose consumption was also measured using same cells seeded on to 12-well plate followed by CDDP treatment (10 μM, 24 h) (**D**) Hey, A2780cp, and SKOV3 cells were transfected with HKII siRNA (0 ~100 nM, 16 h), treated with CDDP (10 μM, 24 h) followed by cell viability assay with Trypan blue. Results are expressed as mean ± SEM ($n \geq 3$) and analyzed by 2-way ANOVA and Bonferroni post-hoc test (** $P < 0.01$, and *** $P < 0.001$, CTL vs. CDDP, $^{\#}$ $P < 0.05$, $^{\#\#}$ $P < 0.01$, Scramble vs. HKII siRNA).

Fig.4.9

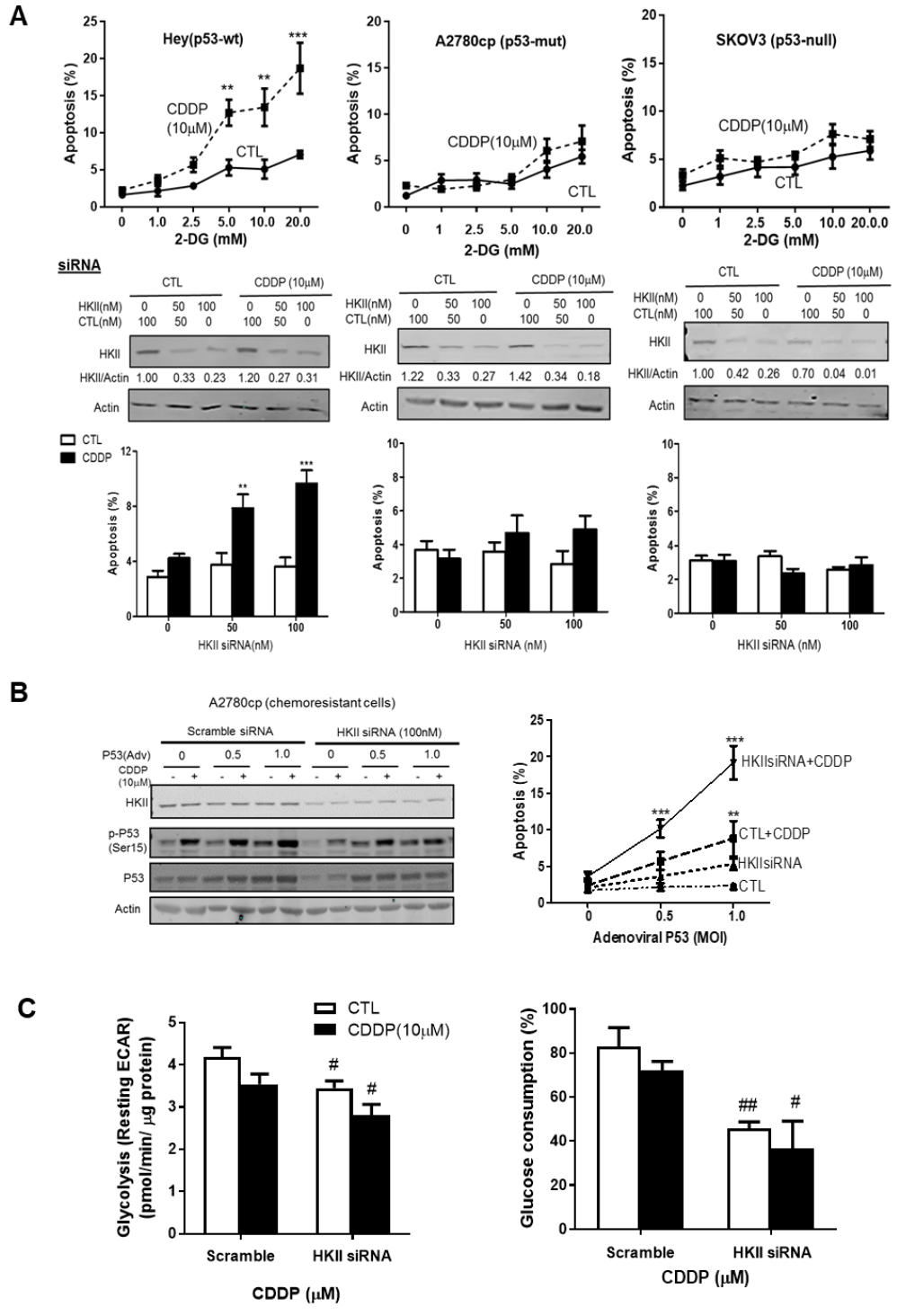
A
Hey(p53-wt)
A2780cp (p53-mut)
SKOV3 (p53-null)
Apoptosis (%)
CDDP (10μM)
CTL
2-DG (mM)
siRNA
HKII(nM)
CTL(nM)
HKII
HKII/Actin
Actin
HKII siRNA(nM)
B
A2780cp (chemoresistant cells)
Scramble siRNA
HKII siRNA (100nM)
P53(Adv)
p-P53 (Ser15)
P53
HKIIsiRNA+CDDP
CTL+CDDP
HKIIsiRNA
Adenoviral P53 (MOI)
C
Glycolysis (Resting ECAR) (pmol/min/ μg protein)
Glucose consumption (%)
Scramble
HKII siRNA
CDDP (μM)

Fig.4.9

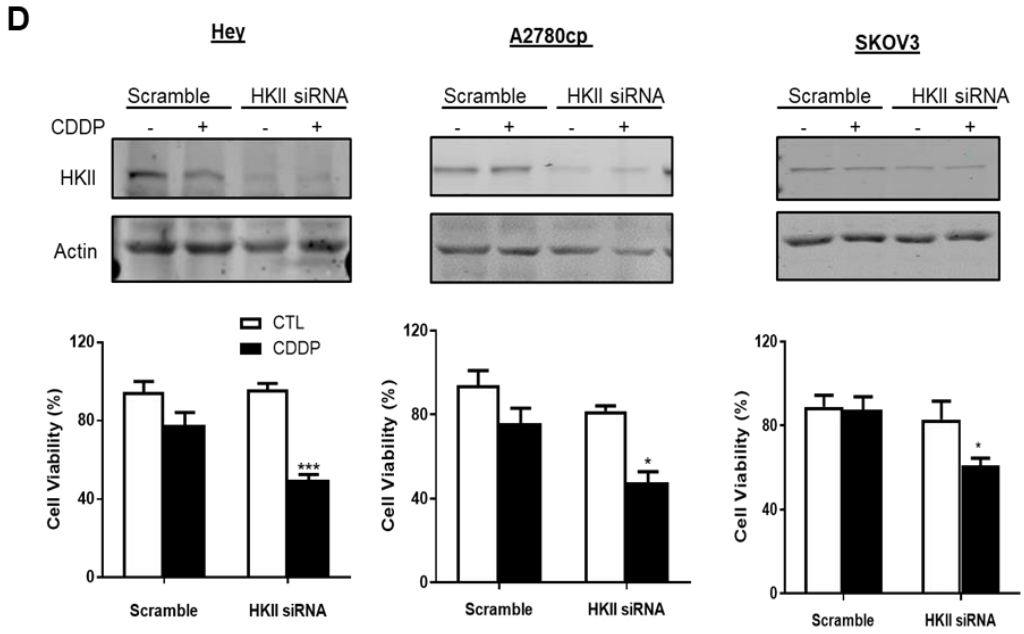
D
Hey
A2780cp
SKOV3
Scramble
HKII siRNA
CDDP
HKII
Actin
CTL
CDDP
Cell Viability (%)
120
80
40
0
***
*
Scramble
HKII siRNA

8. p53 transcriptionally regulates HKII and aerobic glycolysis

Based on that role of p53 demonstrated in HKII nuclear localization, we next investigated a second way in which p53 may regulate its expression at the transcriptional level in the nucleus and subsequent effect on glycolysis metabolism. Our lab previously demonstrated that CDDP promotes phosphorylation of p53 (Ser15 & Ser20) and DNA binding affinity of P-p53 in OVCA cells (Fraser et al., 2008; Kong et al., 2014). To examine if p53 or P-p53 transcriptionally represses HKII expression and HKII-mediated glycolysis in OVCA cells, p53 was knocked down in chemosensitive A2780s cells, the cells were treated with CDDP (10 μM, 24 h) and HKII mRNA abundance and protein levels were assessed. CDDP treatment significantly decreased mRNA abundance of HKII, but this downregulation was largely attenuated in p53-knockdown cells (Fig. 4.10A; $^{*}P$ <0.05, $^{\#}P$ < 0.05, $^{\#\#}P$ < 0.01), indicating that p53 is required for transcriptional suppression of HKII. Consistent with that, HKII mRNA downregulation led to a decrease of HKII protein content in chemosensitive cells treated with CDDP but recovered in p53-knocked down A2780s cells (Fig.4.10B). Also, p53 downregulated decreased CDDP-induced apoptosis rate from 13% to 6% (Fig.4.10C; ** $P < 0.01$, $^{\#}P < 0.05$).

To demonstrate a direct role of p53 in HKII transcriptional repression via promoter binding, we performed chromatin immunoprecipitation (ChIP) assays in A2780s and A2780cp cells with and without CDDP treatment (10 μM, 24 h). Using qPCR analysis of p53 immunoprecipitates, we determined that p53 binding to the HK promoter is prominently increased in CDDP treated chemosensitive A2780s cells (~20 fold) compared with untreated control. Conversely, this response was largely compromised in chemoresistant cells, irrespective of CDDP treatment (Fig. 4.10D; *** $P < 0.001$). Our data exhibited that P-p53(Ser15), but not P-p53 (Ser20) is involved in the regulation of HKII DNA by promoter binding (Fig. 4.10D; Ser15: ** $P < 0.01$; Ser20: $P > 0.05$), supporting that activated form of P-p53 at site of Ser15 is specifically involved in the transcriptional suppression of HKII.

Figure 4.10 p53 transcriptionally regulates HKII and aerobic glycolysis.

(A) A2780s cells were transfected with either scramble or p53 siRNA (100 nM, 16 h), treated with CDDP (10 μM, 24 h) followed by measurement of mRNA abundance (qPCR) for HKII, p53, and actin as house keeping gene. **(B)** WB and **(C)** apoptosis assessment was conducted using the same samples. **(D)** CDDP activated P-p53 (Ser15), but not P-p53 (Ser20) regulates HKII via promoter binding in chemosensitive, but not in chemoresistant OVCA cells. A2780s and A2780cp cells were treated with CDDP (10 μM, 24 h), and ChIP assay was conducted using p53, P-p53(Ser15), and P-p53 (Ser20) antibody followed by DNA purification. DNA was subjected to qPCR for quantification. Results are expressed as mean ± SEM (n = 4) and analyzed by 2-way ANOVA and Bonferroni post hoc test (* $P < 0.05$, ** $P < 0.01$, *** $P < 0.001$, CTL vs. CDDP, $^{\#} P < 0.05$, $^{\#\#} P < 0.01$, Scramble vs. p53 siRNA). **(E)** Schematic map of the p53 binding to the human HKII promoter region showing potential p53 consensus binding site (Grey color), and primers used for ChIP assay (Arrow). p53 consensus binding sequence was located at the promoter region from -1 to -1,000 upstream, and the amplicon targeting p53 bound to HKII was designed in the region of (-265 to -137 bp).

Fig.4.10

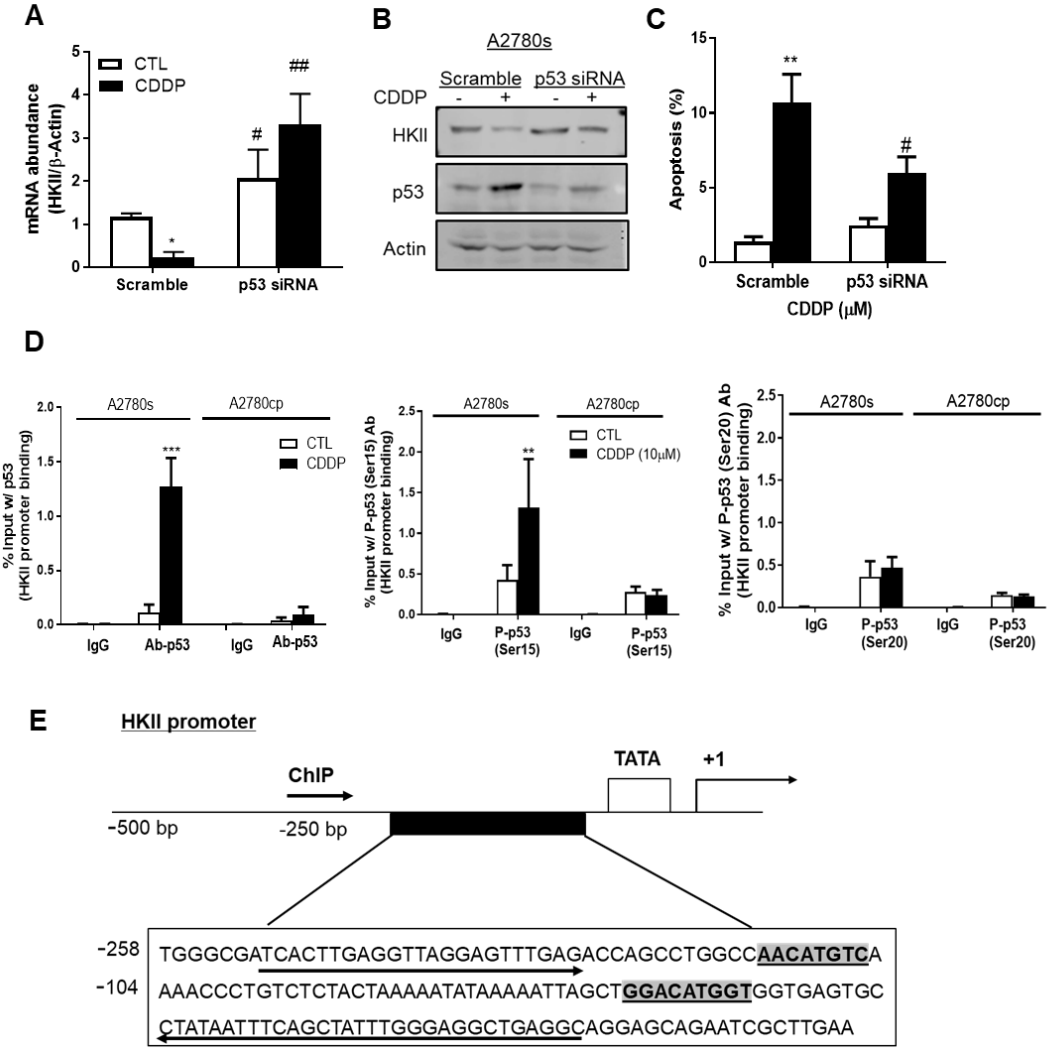
A
mRNA abundance (HKII/β-Actin)
CTL
CDDP
Scramble
p53 siRNA
B
A2780s
Scramble
p53 siRNA
CDDP
HKII
p53
Actin
C
Apoptosis (%)
Scramble
p53 siRNA
CDDP (μM)
D
A2780s
A2780cp
% Input w/ p53 (HKII promoter binding)
IgG
Ab-p53
% Input w/ P-p53 (Ser15) Ab (HKII promoter binding)
P-p53 (Ser15)
CDDP (10μM)
% Input w/ P-p53 (Ser20) Ab (HKII promoter binding)
P-p53 (Ser20)
E
HKII promoter
ChIP
TATA
+1
-500 bp
-250 bp
-258
-104
TGGGCGATCACTTGAGGTTAGGAGTTTGAGACCAGCCTGGCCAACATGTCA
AAACCCTGTCTCTACTAAAAATATAAAAATTAGCTGGACATGGTGGTGAGTGC
CTATAATTTCAGCTATTTGGGAGGCTGAGGCAGGAGCAGAATCGCTTGAA

9. HKII is enriched in the nucleus in primary human OVCA cells with longer PFI.

Progression free interval (PFI) is used as a major indicator to determine chemoresponsiveness, predicting the prognosis in OVCA patients (Kurman and Shih Ie, 2008) Using primary human OVCA cells with varied PFI and subtype, we determined if CDDP induces HKII nuclear localization, associated with the prognosis of patients in the context of PFI (Fig.4.11). In high grade serous (HGS) subtype of the primary human OVCA cell (SNU-3561; PFI =19 months) as chemosensitive phenotype, HKII was already largely enriched in the nucleus in both control and CDDP treated group. In addition, A-8 cells with longer PFI (PFI = 39 months), CDDP treatment induced nuclear localization of HKII and significantly decreased mitochondrial HKII localization (Fig 4.11, * $P < 0.05$). In contrast, in A-39 (PFI < 6 months) as chemoresistant phenotype, HKII was highly localized in mitochondria, but not changed regardless of CDDP treatment. These data collectively suggest that both HKII nuclear localization as basal level and CDDP-induced HKII nuclear localization are possibly associated with the length of PFI and chemoresponsivess in OVCA patients.

Figure 4.11 Nuclear HKII localization is increased in chemosensitive high grade serous OVCA patients.

(A) Various primary OVCA human cells, SNU-3561 and ascites (A-8 & A-39) were cultured with CDDP (10μM, 24 h). Cellular localization of HKII (Red) as % of total cells with TOM20 (Green: mitochondrial Marker) and DAPI (Blue: Nucleus marker) were measured using confocal microscopy **(B)** Results were quantified using Image premier program and progression free interval (PFI) is shown in each cell. Results are expressed as mean ± SEM (n = 4) and analyzed by 2-way ANOVA and Bonferroni post hoc test (* $P < 0.05$, CTL vs. CDDP). Scale bar: 10 μm

Fig.4.11

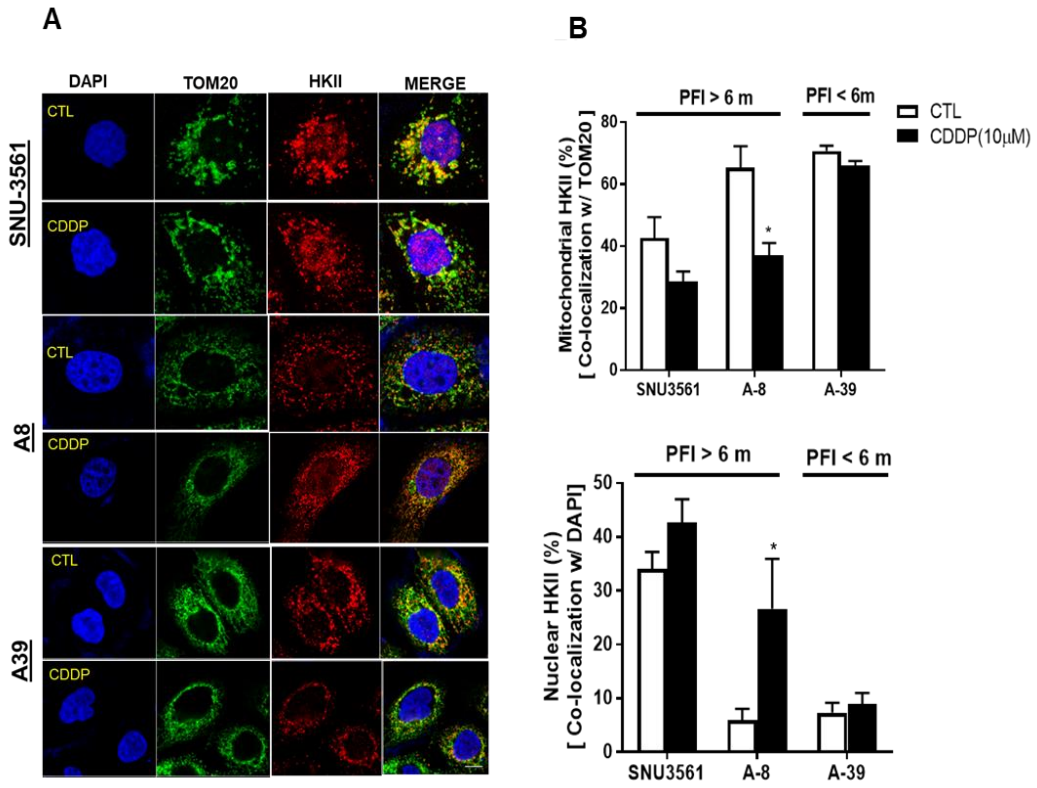
A
DAPI
TOM20
HKII
MERGE
SNU-3561
A8
A39
CTL
CDDP
B
PFI > 6 m
PFI < 6m
CTL
CDDP(10μM)
Mitochondrial HKII (%)
[Co-localization w/ TOM20]
SNU3561
A-8
A-39
Nuclear HKII (%)
[Co-localization w/ DAPI]

10. CDDP promotes HKII interaction with P-p53(Ser15)/AIF in the nucleus in chemosensitive OVCA cells.

We next sought to explore the molecular link between dysregulated metabolism and induction of apoptosis in chemosensitive OVCA cells. In previous findings, P-p53(Ser15) and HKII were co-localized in the nucleus in response to CDDP in chemosensitive A2780s cells but not in chemoresistant cells. Our group previously reported that CDDP promotes nuclear localization of AIF, the mediator of caspase-independent apoptosis, whereas Chen et al. demonstrated that HKII interacts with AIF in mitochondria (Chen et al., 2009; Farrand et al., 2014; Yang et al., 2008). In this context, we postulated that CDDP stimulates P-p53(Ser15) and promotes its recruitment with HKII and AIF, enabling translocation of this complex to the nucleus where HKII can be transcriptionally regulated by P-p53(Ser15) in chemosensitive cells, eliciting AIF-induced apoptosis. To better examine direct HKII-P-p53(Ser15) and HKII-AIF interactions, proximity ligation assay (PLA) was used and number of PLA signal per cell were quantified. In chemosensitive A2780s cells treated with CDDP (10 μM, 0-24 h), PLA signal of HKII-P-p53(Ser15) interaction at the nucleus were increased starting at 6 h and reached highest at 24 h treatment and significantly increased apoptotic response (Fig.4.12A & C; ** $P < 0.01$), but this interaction was largely attenuated in mitochondria at 3-6 h (Fig.4.12 A; * $P < 0.05$, ** $P < 0.01$) and recovered again at 24h, suggesting the intracellular trafficking of HKII-P-p53(Ser15) interaction from mitochondria to the nucleus. In contrast, HKII-P-p53(Ser15) in chemoresistant A2780cp exhibited minimal interaction in the nucleus, but this interaction is limitedly enriched in mitochondrial region at 24 h (Fig. 4.12 A & C; * $P < 0.05$), supporting that inhibition of nuclear translocation of HKII-P-p53(Ser15) occurred in A2780cp cells, associated with its minimal apoptotic response.

With the HKII-AIF interaction, PLA signal (HKII-AIF) in A2780s cell was increased in the nucleus but decreased in mitochondria (Fig. 4.12B & C; * $P < 0.05$) in response to prolonged duration of

CDDP (24 h). This result implies that P-p53(Ser15) led translocation of this interaction (HKII-AIF) from mitochondria to the nucleus as HKII-P-p53(Ser15) simultaneously did, suggesting cooperative interaction and co-movement of these molecules [P-p53(Ser15)-HKII-AIF]. Compared with A2780s cells, PLA signal (HKII-AIF) in A2780cp cells was weaker overall, mainly localized in mitochondria and was not largely changed in response to CDDP.

We next examined our previous finding is applied to other OVCA cells. We have examined that PLA interaction of HKII-P-p53(Ser15) in other variant OVCA cells including chemosensitive PA-1 cells (p53-wild type) and chemoresistant OVCAR3 cells (p53-mutant) (Fig. 4.13A). We observed that both nuclear and mitochondrial interaction of HKII-P-p53(Ser15) as PLA signal was increased in nuclei of chemosensitive PA-1 cells, and was associated with increased chemosensitivity. Conversely, only mitochondrial HKII-Pp53(Ser15) interaction was increased in chemoresistant OVCAR3 cells (Fig. 4.13A & B). It suggests that nuclear HKII-P-p53 interaction is associated with chemosensitivity in OVCA cells. In summary, these results support the notion that CDDP activated-P-p53(Ser15) facilitates 1) translocation of HKII by direct and transient interaction to facilitate its regulation; 2) regulation of HKII and glycolysis, and 2) AIF-induced apoptosis in OVCA cells.

Figure 4.12 HKII-P-p53(Ser15)-AIF interaction in the nucleus in chemosensitive OVCA cells.

A2780s and A2780cp cells were cultured with CDDP (10 μM, 24 h; DMSO as a vehicle) followed by proximity ligation assay (PLA). Interactions of **(A)** HKII-P-p53(Ser15) and **(B)** HKII-AIF in A2780s and A2780cp cells were assessed by PLA, using Duolink Image tool program from Sigma. Number of HKII-P-p53(Ser15) (A: red spot) and HKII-AIF (B: red spot) interactions in cellular localization [nucleus marker (Blue: DAPI), mitochondria marker (Green: TOM20), and PLA Signal (Red)] were counted and analyzed using Duolink Image tool. (**C**) OVCA cells treated same as above were also subjected to apoptosis measurement using Hoechst staining. Results are expressed as mean ± SEM (n = 4) and analyzed by 2-way ANOVA and Bonferroni post hoc test (* $P < 0.05$, ** $P < 0.01$, CTL vs. CDDP). Scale bar: 10 μm

Fig.4.12

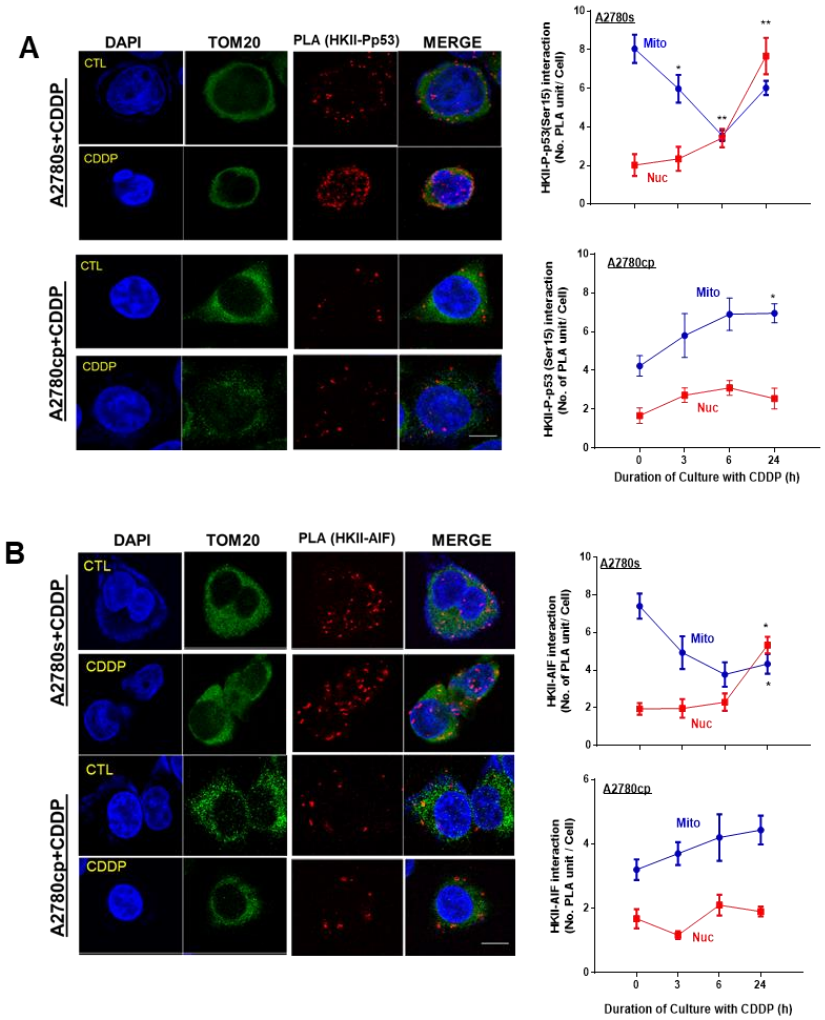
A
DAPI
TOM20
PLA (HKII-Pp53)
MERGE
CTL
CDDP
A2780s+CDDP
A2780cp+CDDP
A2780s
A2780cp
Mito
Nuc
HKII-P-p53(Ser15) interaction (No. PLA unit/ Cell)
HKII-P-p53 (Ser15) interaction (No. of PLA unit/ Cell)
Duration of Culture with CDDP (h)
B
DAPI
TOM20
PLA (HKII-AIF)
MERGE
HKII-AIF interaction (No. of PLA unit/ Cell)
HKII-AIF interaction (No. PLA unit / Cell)
Duration of Culture with CDDP (h)
C
CTL
CDDP(10μM)
Apoptosis (%)
***
A2780s
A2780cp

Figure 4.13 Nuclear HKII-P-p53(Ser15) interaction is associated with chemosensitivity in OVCA cells.

(**A**) Chemosensitive PA-1 (p53-wild-type, endometrioid) and chemoresistant OVCAR-3 (p53-mutant, high grade serous) cells were cultured with or without CDDP (10 μM, 24 h; DMSO as a vehicle). Interactions of HKII-P-p53(Ser15) (PLA unit: red spot) with counterstaining of localization [nucleus marker (Blue: DAPI) and mitochondria marker (Green: TOM20)] in other OVCA cells were analyzed using Duolink Image tool. (**B**) PA-1 and OVCAR-3 cells were cultured in the same condition above were subjected to apoptosis measurement using Hoechst staining. Results are expressed as mean ± SEM (n = 3) and analyzed by 2-way ANOVA and Bonferroni post hoc test (** $P < 0.01$, CTL vs. CDDP). Scale bar: 10 μm

Fig.4.13

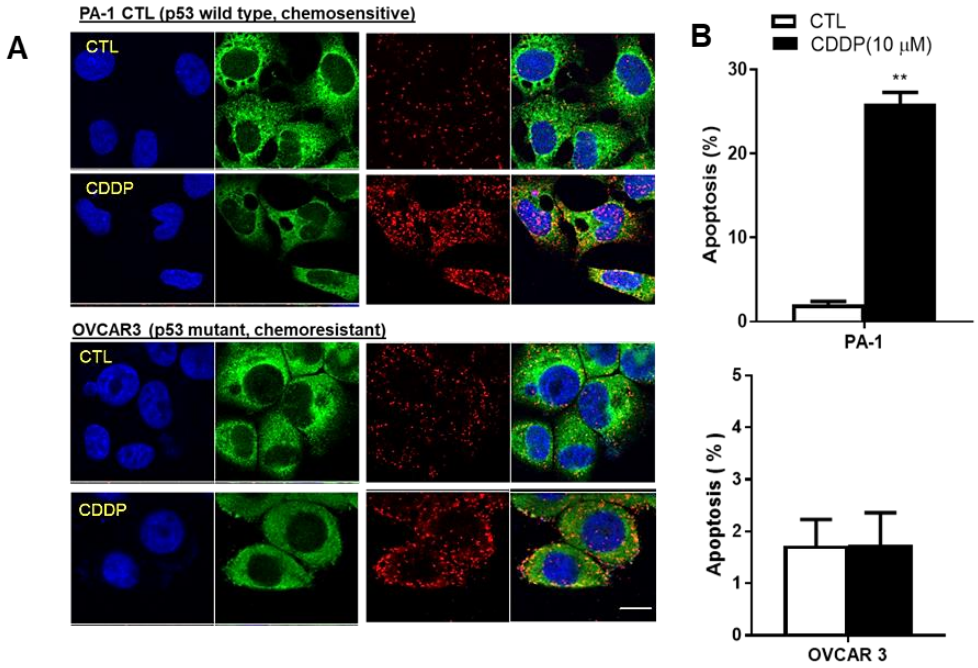
A
PA-1 CTL (p53 wild type, chemosensitive)
CTL
CDDP
OVCAR3 (p53 mutant, chemoresistant)
CTL
CDDP
B
CTL
CDDP(10 μM)
Apoptosis (%)
30
20
10
0
**
PA-1
Apoptosis (%)
5
4
3
2
1
0
OVCAR 3

11. CDDP increases nuclear HKII-Pp53(Ser15) interaction in chemosensitive primary human cells.

Based on our previous studies in OVCA cell lines, we then examined the interaction and intracellular trafficking of HKII-P-p53(Ser15) by PLA assay in various cultures of primary human cells collected from patients with OVCA with the varied length of progression free interval (PFI). (Fig.4.14 and Table.1). After CDDP treatment (10 μM, 24 h), the nuclear intracellular trafficking and interaction of HKII-P-p53(Ser15) (PLA unit: Red signal) were highly increased in chemosensitive SNU-3561 with longer PFI (PFI = 19 months), but this response was significantly attenuated in chemoresistant 2068 cell with shorter PFI (PFI = 0 months) (Fig.4.14A). When we compared the correlation between increased nuclear PLA unit as the interaction of HKII-P-p53(Ser15) and chemosensitivity *in vitro* as CDDP-induced apoptosis by Pearson correlation analysis, we observed a positive correlation (Fig. 4.14B, r = 0.88, **** $P = 0.0007$). In addition, chemosensitivity *in vitro* as determined is correlated with chemosensitivity *in vivo*, determined by PFI (Fig. 4.14C, r = 0.68, $P = 0.03$).

We then categorized these treated primary human cells into chemosensitive (PFI ≥ 6 months) and chemoresistant (PFI < 6 months) (Oncology, 2016, August). We categorized these treated primary human cells into chemosensitive (PFI > 6 m) and chemoresistant (PFI ≤ 6 months). We observed significantly lower nuclear PLA units, HKII-P-p53(Ser15) in chemoresistant primary human OVCA cells (PFI ≤ 6 months; cells: 2066, 2068, 2170; Fig. 4.14D) compared with that of chemosensitive 2149 cells (PFI = 25 months), (*left panel*, Fig. 4.14D, * $P < 0.05$, ** $P < 0.01$). Next, we examined the correlation between the increased interaction of HKII-P-p53(Ser15) (nuclear PLA unit) and PFI and observed the positive correlation (*right panel*, Fig.4.14D, r = 0.73, $P = 0.011$). In summary, interaction and intracellular trafficking of HKII-P-p53(Ser15) occurred in the nucleus in chemosensitive primary OVCA human cells (PFI > 6 months), but not in

chemoresistant primary human OVCA cells (PFI ≤ 6 months), suggesting nuclear intracellular trafficking of HKII-P-p53 (Ser15) may function as a determinant of chemosensitivity.

Table 4.1 Demographic information of patients for primary human OVCA Cells

Table 4.1 illustrates the clinical characteristics of the patients recruited for primary cultures of human OVCA cells from Ottawa Hospital Research Institute (OHRI) and Seoul National University Hospital (SNUH). The majority of collected tumors were primarily high-grade serous (HGS) with one clear cell (CC) subtype. Most of the tumors were at stage III and IV, although some received neo-adjuvant treatment that precluded accurate staging. Genexol and Lipoxo are the brand name of Paclitaxel and liposomal Doxorubicin, respectively. The majority of patients had disease progression or recurrence within 6 months, while four patients had a PFI of longer than 6 months. Some of the primary human cells were previously exposed to chemotherapy before its collection. Information of exact procedure of surgery was limitedly provided except for the record that tumors were removed in primary or relapse cases.

Table 4.1 Demographic Information of patients for primary human cells

No.	Source	Sub type	Stage	PFI (Months) /Sensitivity	Survival status	Collected stage & Institute /Chemotherapy list
SNU 3561	Pleural fluid	HGS	4B	19/Sensitive	Alive	Primary removal surgery at SNUH 1. Genexol-Carboplatin Recurrence 2. Genexol-Carboplatin
A8	Ascites	HGS	3C	39/Sensitive	Alive	Primary removal surgery at SNUH 1. Paclitaxel-Carboplatin
A39	Ascites	CC	Unknown	PFI < 6 /Sensitive	Deceased	Second removal surgery at SNUH 1. Taxol-Carboplatin 2. Belotecan
2068	Ascites	HGS	3c	0/ Resistant	Deceased	Second removal surgery at SNUH 1.Carboplatin & Taxol 2 Carboplatin
2149	Ascites	HGS	1c	25/ Sensitive	Alive	Second removal surgery at SNUH 1.Carboplatin & Taxol 2.Carboplatin & Taxol
2159	Ascites	HGS	Neo adjuvant	0/ Resistant	Deceased	Second removal surgery at SNUH 1. Carboplatin 2. LipoDox
2161	Ascites	HGS	Neo adjuvant	10/ Intermediate resistant	Unknown	Second removal surgery at SNUH 1. Carboplatin & Taxol
2164	Ascites	HGS	Neo adjuvant	0/ Resistant	Deceased	1. Carboplatin & Taxol 2. Lipo Dox
2165	Ascites	HGS	3c	5/ Resistant	Alive	Second removal surgery at SNUH 1. Carboplatin & Taxol 2. LipoDox
2166	Ascites	HGS	Neo Adjuvant	4/ Resistant	Deceased	Second removal surgery at SNUH 1. Carboplatin & Taxol 2. LipoDox 3. Paclitaxel
2170	Ascites	HGS	3b	4/ Resistant	Deceased	Second revmoval surgery at SNUH 1. Carboplatin & Taxol 2. Carboplatin

Figure 4.14 CDDP promotes interaction and intracellular trafficking of HKII-P-p53(Ser 15) to the nucleus of chemosensitive primary human OVCA cells.

(A) Various primary human OVCA cells including SNU 3561 and 2068 collected from patients were treated with or without CDDP (10 μM, 24 h; DMSO as a vehicle), and analyzed by increased PLA units [interaction of HKII-P-p53 (Ser15); Red] in the nucleus with counterstaining of TOM20 (Green, mitochondrial marker), DAPI (Blue: nucleus marker), using Duolink Image program. **(B)** The correlation between the increased rate of PLA unit, nuclear HKII-Pp53(Ser15) interaction and chemosensitivity *in vitro* was analyzed. Chemosensitivity *in vitro* as CDDP-induced apoptosis was assessed using Hoechst staining. **(C)** The correlation between chemosensitivity *in vitro* and PFI as chemosensitivity *in vivo* was analyzed. **(D)** (Left panel) Primary human OVCA cells treated above were categorized based on the length of PFI (PFI > 6 months and PFI ≤ 6 months) and increased PLA signal, nuclear HKII-P-p53(Ser15) interaction in these cells were compared with chemosensitive primary human OVCA cells, 2149 (PFI = 40 months). (Right panel) The correlation between increased PLA unit, [nuclear HKII-P-p53 (Ser15) interaction] and PFI was analyzed. Results are expressed as mean ± SEM (n = 5) and analyzed by 2-way ANOVA and Bonferroni post hoc test. (* $P < 0.05$, ** $P < 0.01$, CTL vs. CDDP). The correlations were analyzed using Pearson correlation (r) method. Scale bar: 10 μm

Fig.4.14

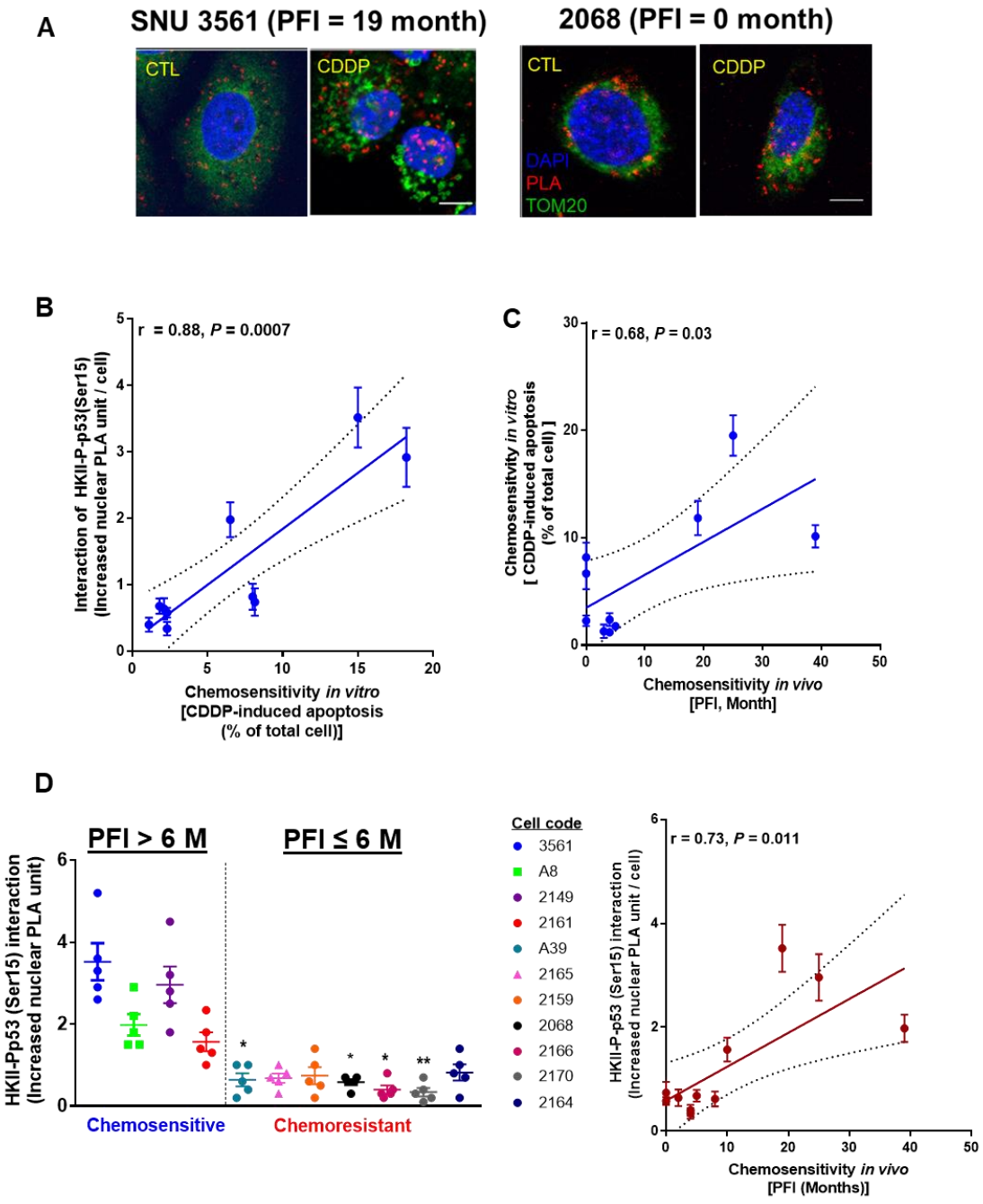
A
SNU 3561 (PFI = 19 month)
2068 (PFI = 0 month)
CTL
CDDP
CTL
CDDP
DAPI
PLA
TOM20
B
r = 0.88, P = 0.0007
Interaction of HKII-P-p53(Ser15)
(Increased nuclear PLA unit / cell)
Chemosensitivity in vitro
[CDDP-induced apoptosis
(% of total cell)]
C
r = 0.68, P = 0.03
Chemosensitivity in vitro
[CDDP-induced apoptosis
(% of total cell)]
Chemosensitivity in vivo
[PFI, Month]
D
PFI > 6 M
PFI ≤ 6 M
HKII-Pp53 (Ser15) interaction
(Increased nuclear PLA unit)
Chemosensitive
Chemoresistant
Cell code
3561
A8
2149
2161
A39
2165
2159
2068
2166
2170
2164
r = 0.73, P = 0.011
HKII-P-p53 (Ser15) interaction
(Increased nuclear PLA unit / cell)
Chemosensitivity in vivo
[PFI (Months)]

12. Increased nuclear HKII-P-p53(Ser15) interaction functions as potential biomarker for chemosensitive OVCA.

To confirm whether nuclear HKII-P-p53(Ser15) interaction is also increased in the clinical sample *in vivo,* PLA signal was examined in paired pre- and post-chemotherapy tumor immunohistochemistry (IHC) sections obtained from the same OVCA patients with different epithelial histological subtypes of OVCA as indicated (Table 4.2). We then examined whether the nuclear HKII-P-p53(Ser15) interaction is associated with chemoresponsiveness, determined as PFI. When comparing the nuclear HKII-P-p53(Ser15) in post-chemotherapy relative to pre-chemotherapy samples from the same patient, we observed a notable increase in nuclear HKII-P-p53(Ser15) with a patient with longer PFI (40 months), but not in a patient with a shorter PFI (1 month, Fig. 4.15A). When we assessed the correlation between increased nuclear HKII-P-p53(Ser15) interaction (Increased PLA unit = post-chemotherapy – pre-chemotherapy) and PFI using Pearson correlation analysis, a strong correlation was observed (Fig. 4.15B, r = 0.72, $P < 0.0001$). However, the correlation between these PLA units and overall survival is less strong (Fig. 4.15C, r = 0.43, $P = 0.004$), which may be because the overall survival does not strongly correspond to PFI in this population of OVCA patients (r = 0.47, Fig. 4.15D). Finally, the long-term survival was examined using Kaplan-Meier curves. Patients with a higher nuclear HKII-P-p53(Ser15) interaction after chemotherapy had significantly better progression free survival than patients with lower nuclear HKII-P-p53(Ser15) interaction (Fig 4.15E, ** $P = 0.005$). In addition, there is a significant difference in the overall survival rate between patients with higher or lower nuclear HKII-P-p53 (Ser15) interaction (Fig. 4.15F, * $P = 0.008$). Collectively, these data suggest that increased nuclear HKII-P-p53(Ser15) interaction after chemotherapy is more likely associated with chemoresponsiveness and overall survival, particularly in epithelial subtypes of OVCA.

Table 4.2 Demographic information of patients for Immunohistochemistry

Table 4.2 illustrates the clinical characteristics of the patients recruited for ovarian tumor immunohistochemistry (IHC) sections for PLA studies (number of patients = 41, total 82 sections). The majority of patients were older than 50. The tumors were primarily high-grade serous ovarian tumors (88%), with 10% clear cell, and 2% endometrioid subtype. Most of the tumors (88%) were stage III and IV. Majority of patients had a recurrent disease with a PFI of longer than 6 months (80%), while 20% of patients progressed or had a recurrence within 6 months.

Table 4.2. Information of patients for recruited for primary human cells

Characteristics (patients, n=41) paired sections (82)	Range	Patient studied population	
		n/ Total	%
Age (years)	< 50	13/ 41	32
	51-60	18/ 41	44
	> 60	10/ 41	24
FIGO stage	I	4 / 41	10
	II	1 / 41	2
	III	32 / 41	78
	IV	4 / 41	10
Progression-free interval (PFI)	PFI > 12 m	25 /41	60
	6 m < PFI ≤ 12 m	8 / 41	20
	6 m ≤ PFI	8 / 41	20
Histologic sub-type	High grade serous	36 / 41	88
	Clear cell	4 / 41	10
	Endometrioid	1 / 41	2

Figure 4.15 Chemotherapy-induced nuclear interaction of HKII-P-p53(Ser15) is associated with chemoresponsiveness in OVCA patients.

(A) Paired pre- and post- chemotherapy ovarian tumor IHC sections from the same patients (n=41, total 82 sections) were collected, fixed with formalin, processed for antigen retrieval, and stained with HKII and P-p53(Ser15) antibodies. Number of HKII-P-p53(Ser15) interaction (PLA unit: red spot) and its cellular localization [nucleus marker (Blue: DAPI), mitochondria marker (Green: TOM20)] were assessed using confocal microscopy and Duolink Image Tool. **(B)** The correlation was analyzed between [increased PLA unit, nuclear (HKII-Pp53 (Ser15) interaction) = post-chemotherapy minus pre-chemotherapy] and PFI (n = 41) and **(C)** overall survival, (n = 40), respectively. (*One of the patients was excluded due to loss of contact for follow-up.) **(D)** The correlation was analyzed between progression free survival (PFS) and overall survival (OS). **(E)** (PFS) and **(F)** OS were examined using Kaplan–Meier curves according to increased nuclear PLA units. Hazard ratio (HR) and Confidence Interval (CI) were also analyzed. The correlation was analyzed using Pearson correlation (r) method. *P* value of Kaplan-Meier curves were analyzed log-rank test. Scale bar: 10 μm

Fig.4.15

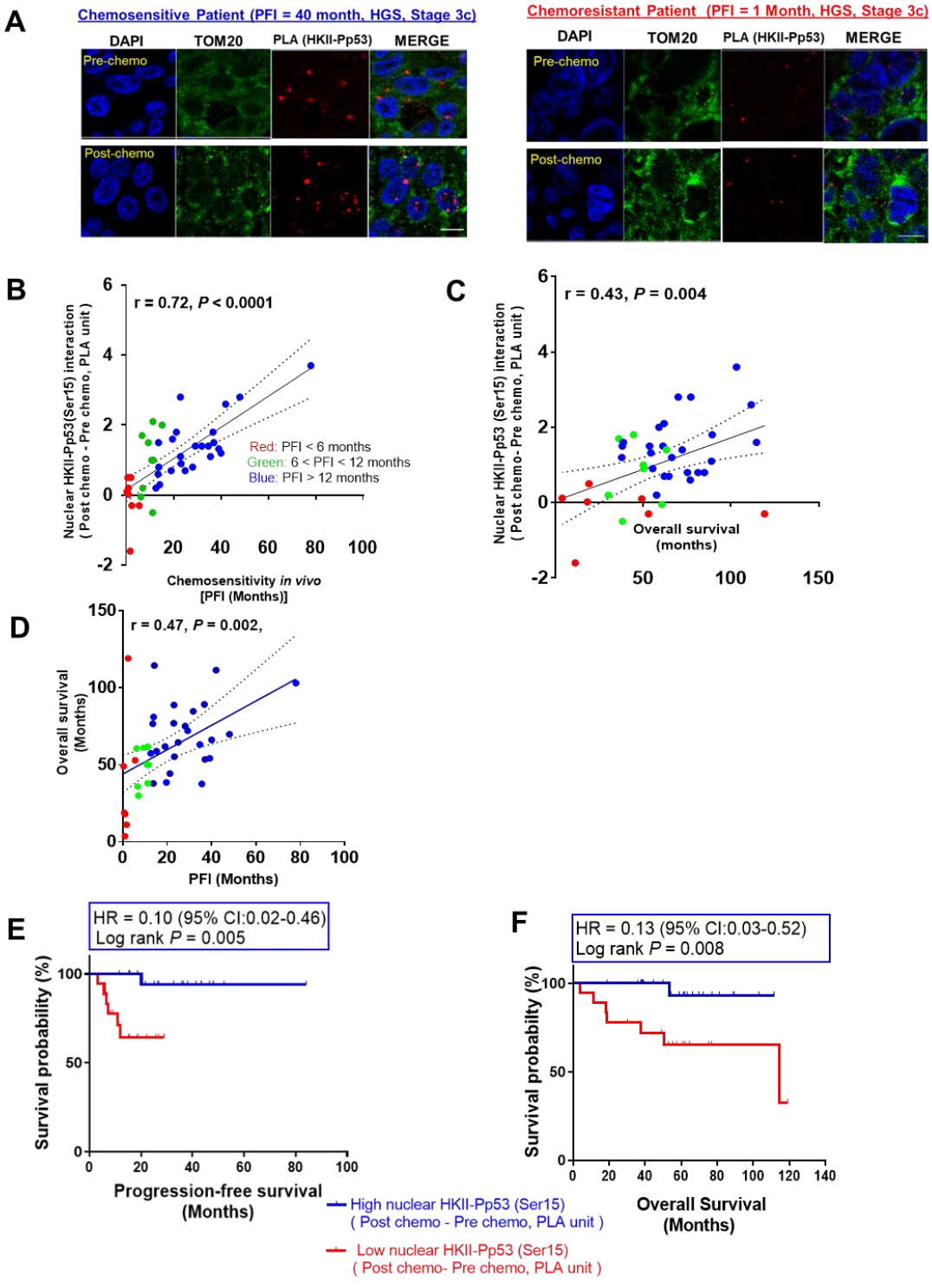
A
Chemosensitive Patient (PFI = 40 month, HGS, Stage 3c)
Chemoresistant Patient (PFI = 1 Month, HGS, Stage 3c)
DAPI
TOM20
PLA (HKII-Pp53)
MERGE
Pre-chemo
Post-chemo
B
r = 0.72, P < 0.0001
Nuclear HKII-Pp53(Ser15) interaction (Post chemo - Pre chemo, PLA unit)
Red: PFI < 6 months
Green: 6 < PFI < 12 months
Blue: PFI > 12 months
Chemosensitivity in vivo [PFI (Months)]
C
r = 0.43, P = 0.004
Nuclear HKII-Pp53 (Ser15) interaction (Post chemo- Pre chemo, PLA unit)
Overall survival (months)
D
r = 0.47, P = 0.002,
Overall survival (Months)
PFI (Months)
E
HR = 0.10 (95% CI:0.02-0.46)
Log rank P = 0.005
Survival probability (%)
Progression-free survival (Months)
F
HR = 0.13 (95% CI:0.03-0.52)
Log rank P = 0.008
Survival probability (%)
Overall Survival (Months)
High nuclear HKII-Pp53 (Ser15) (Post chemo - Pre chemo, PLA unit)
Low nuclear HKII-Pp53 (Ser15) (Post chemo- Pre chemo, PLA unit)

To confirm above observations and instead of using increased value (Increased PLA unit = post-chemotherapy – pre-chemotherapy), we assessed our findings based on the ratio of PLA signal between pre- and post- chemotherapy (post-chemotherapy /pre-chemotherapy). When we assessed the correlation between increased ratio of nuclear HKII-P-p53(Ser15) interaction (post-chemotherapy /pre-chemotherapy) and PFI using Pearson correlation analysis, a strong correlation was observed (Fig 4.16A, r = 0.69, $P < 0.0001$) and the correlation between these PLA units and overall survival was less strong (Fig. 4.16B, r = 0.40, $P = 0.03$), which may be because the overall survival does not strongly correspond to PFI in this population of OVCA patients as previously explained. When we classify the ratio value of HKII-P-p53(Ser15) based on the length of PFI (PFI ≤6 months, 6 < PFI < 12 months, PFI >12 months), we observed significant correlation between nuclear HKII-P-p53(Ser15) and PFI in chemosensitive patients group (Fig. 4.16 C, 6 < PFI < 12 months: r = 0.71; PFI > 12 months: r = 0.72), but not in chemoresistant patients (PFI ≤ 6 months, r = -0.015) suggesting the increased ratio of HKII-P-p53(Ser15) in post-chemo/pre-chemo is more closely associated with chemosensitivity in OVCA. Finally, the long-term survival was examined using Kaplan-Meier curves. Patients with a higher ratio of nuclear HKII-P-p53(Ser15) interaction after chemotherapy had significantly better progression free survival than patients with lower nuclear HKII-P-p53(Ser15) interaction (Fig 4.16D, * $P = 0.03$). In addition, there is a significant difference in the overall survival rate between patients with higher or lower nuclear HKII-P-p53 (Ser15) interaction (Fig. 4.16E, * $P = 0.03$).

Based on that we also examined how nuclear HKII-P-p53(Ser15) interaction either before or after chemotherapy may function as a prognostic indicator. With Hematoxylin and eosin staining, we first confirmed our sections collected from a different histological subtype of epithelial OVCA where the majority of them are high grade serous (88%) (Fig 4.17A, Table 4.2). We then assessed the prognostic value of HKII-P-p53 (Ser15) in either pre-chemotherapy or post- chemotherapy alone instead of using increased value. However, weaker correlation (r < 0.5) was observed both in

pre-chemotherapy alone (Fig 4.17B, r = - 0.38, P = 0.015) or post-chemotherapy alone (Fig 4.17C, r = 0.35, P = 0.03), suggesting that the increased nuclear HKII-P-p53(Ser15) interaction between pre-chemotherapy and post-chemotherapy are more important determinant for chemosensitivity.

Next, instead of assessing nuclear HKII-P-p53(Ser15) interaction, we assessed the correlation between increased mitochondrial HKII-P-p53(Ser15) interaction (Increased PLA unit, mitochondria = post-chemotherapy – pre-chemotherapy) and PFI using Pearson correlation analysis. But the association between HKII-P-p53(Ser15) in mitochondria region and both PFI (Fig. 4.17D, r = - 0.35, P = 0.02) and overall survival (Fig. 4.17E r = - 0.08, P = 0.63) were weak. However the negative correlation between mitochondrial HKII-P-p53(Ser15) and PFI possibly suggests us that HKII-P-p53(Ser15) because the association of HKII-P-p53 (Ser15) may translocate from mitochondria the nucleus or other sub-cellular organelles after post-chemotherapy in response to CDDP. We also examined the long-term survival using Kaplan-Meier curves. Patients with a lower increased mitochondrial HKII-P-p53 (Ser15) interaction had significantly better progression free survival than patients with higher mitochondrial HKII-P-p53(Ser15) interaction (Fig. 4.17F, * P = 0.047), but there is no significant difference in the overall survival rate between patients with higher or lower mitochondrial HKII-P-p53 (Ser15) interaction (Fig. 4.17G) suggesting increased nuclear HKII-P-p53(Ser15) interaction is stronger indicator for chemosensitivity.

Figure 4.16 CDDP increases the nuclear HKII-P-p53(Ser15) interaction in post-chemotherapy, associated with chemoresponsiveness in OVCA patients.

Same IHC samples for Fig. 4.15 were analyzed with different calculation method, **[Increased ratio of PLA unit, [nuclear HKII-P-p53 (Ser15) interaction) = post-chemotherapy / pre-chemotherapy]. (A)** The correlation was analyzed between increased ratio of PLA unit *in vivo* and PFI (n=41) and **(B)** overall survival (n=40). **(C)** IHC sections were classified in to three groups based on the length of PFI (PFI $\leq$ 6 months, 6 < PFI < 12 months, and PFI >12 months) and the correlation between PFI length and the increased ratio of nuclear HKII-P-p53(Ser15) interaction were assessed. **(D)** Progression-free survival and **(E)** overall survival were examined using Kaplan–Meier curves according to an increased ratio of nuclear PLA units. Hazard ratio (HR) and Confidence Interval (CI) were also analyzed. The correlation was analyzed using Pearson correlation (r) method. *P* value of Kaplan-Meier curves were analyzed log-rank test.

Fig.4.16

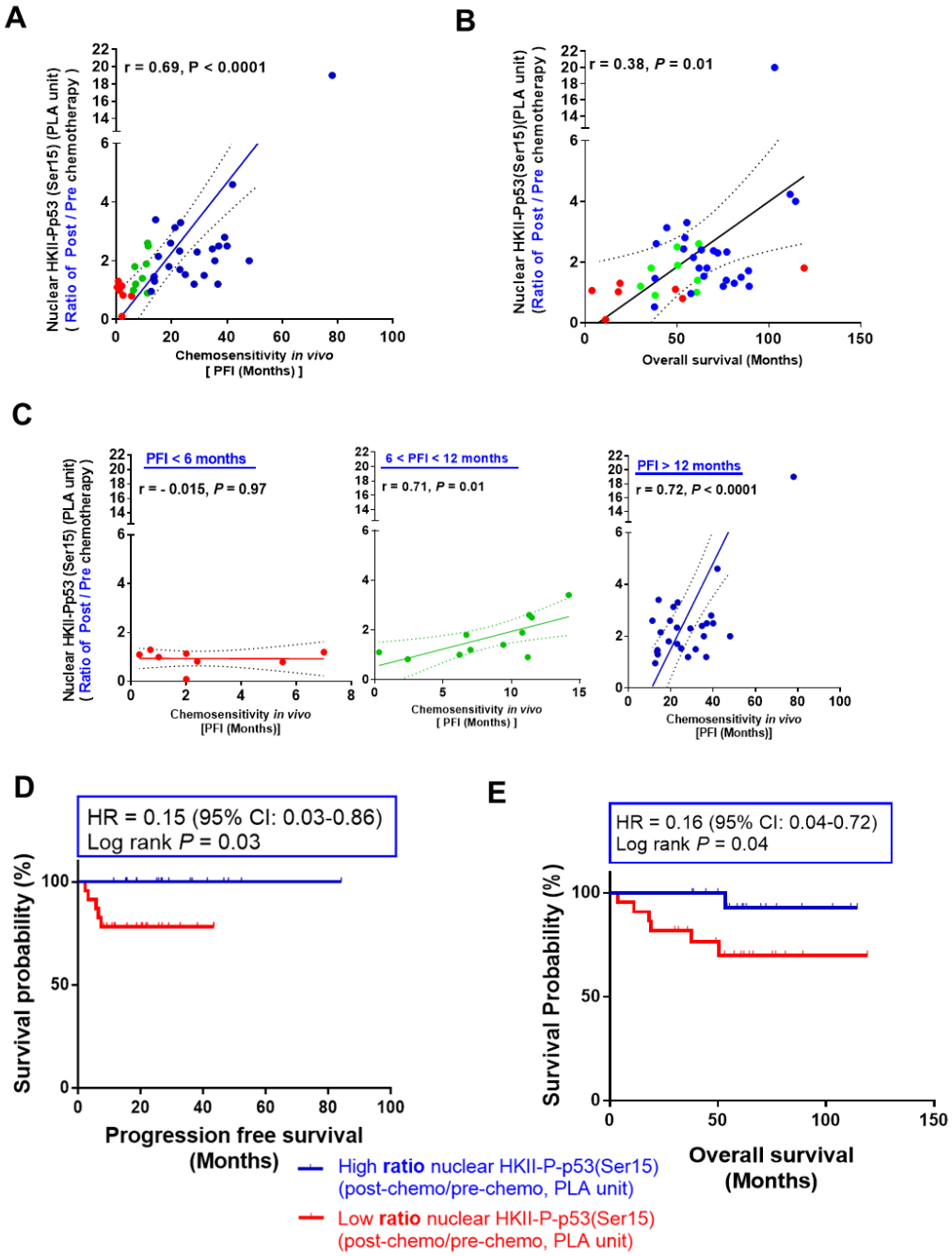
A
r = 0.69, P < 0.0001
Nuclear HKII-Pp53 (Ser15) (PLA unit)
(Ratio of Post / Pre chemotherapy)
Chemosensitivity in vivo
[PFI (Months)]
B
r = 0.38, P = 0.01
Nuclear HKII-Pp53(Ser15)(PLA unit)
(Ratio of Post / Pre chemotherapy)
Overall survival (Months)
C
PFI < 6 months
r = - 0.015, P = 0.97
6 < PFI < 12 months
r = 0.71, P = 0.01
PFI > 12 months
r = 0.72, P < 0.0001
Nuclear HKII-Pp53 (Ser15) (PLA unit)
(Ratio of Post / Pre chemotherapy)
Chemosensitivity in vivo
[PFI (Months)]
D
HR = 0.15 (95% CI: 0.03-0.86)
Log rank P = 0.03
Survival probability (%)
Progression free survival
(Months)
E
HR = 0.16 (95% CI: 0.04-0.72)
Log rank P = 0.04
Survival Probability (%)
Overall survival
(Months)
High ratio nuclear HKII-P-p53(Ser15)
(post-chemo/pre-chemo, PLA unit)
Low ratio nuclear HKII-P-p53(Ser15)
(post-chemo/pre-chemo, PLA unit)

Figure 4.17 Evaluation of prognostic value of HKII-P-p53 (Ser15) in OVCA patients

(**A**) Hematoxylin and eosin staining of each section with varied epithelial OVCA subtype were obtained. HKII-P-p53(Ser15) in either in only pre- or post- chemotherapy sections were examined. The correlation between PFI and prognostic value of nuclear HKII-P-p53(Ser15) in either **(B)** Pre-chemotherapy or **(C)** post- chemotherapy alone were examined. **(D)** Number of HKII-P-p53(Ser15) interaction (PLA unit: red spot) in mitochondria [nucleus marker (Blue: DAPI), mitochondria marker (Green: TOM20)] were analyzed using confocal microscopy and Duolink Image Tool. The correlation was analyzed between [Increased PLA unit, **mitochondria** (HKII-Pp53(Ser15) interaction) = post-chemotherapy minus pre-chemotherapy] and chemosensitivity *in vivo* (PFI, n = 41) and **(E)** overall survival (n = 40). The correlation was analyzed using Pearson correlation (r) method. **(F)** Progression free survival and **(G)** overall survival was examined using Kaplan – Meier curves according to mitochondria. Hazard ratio (HR) and Confidence Interval (CI) were also analyzed. The correlation was analyzed using Pearson correlation (r) method. *P* value of Kaplan-Meier curves were analyzed log-rank test.

Fig.4.17

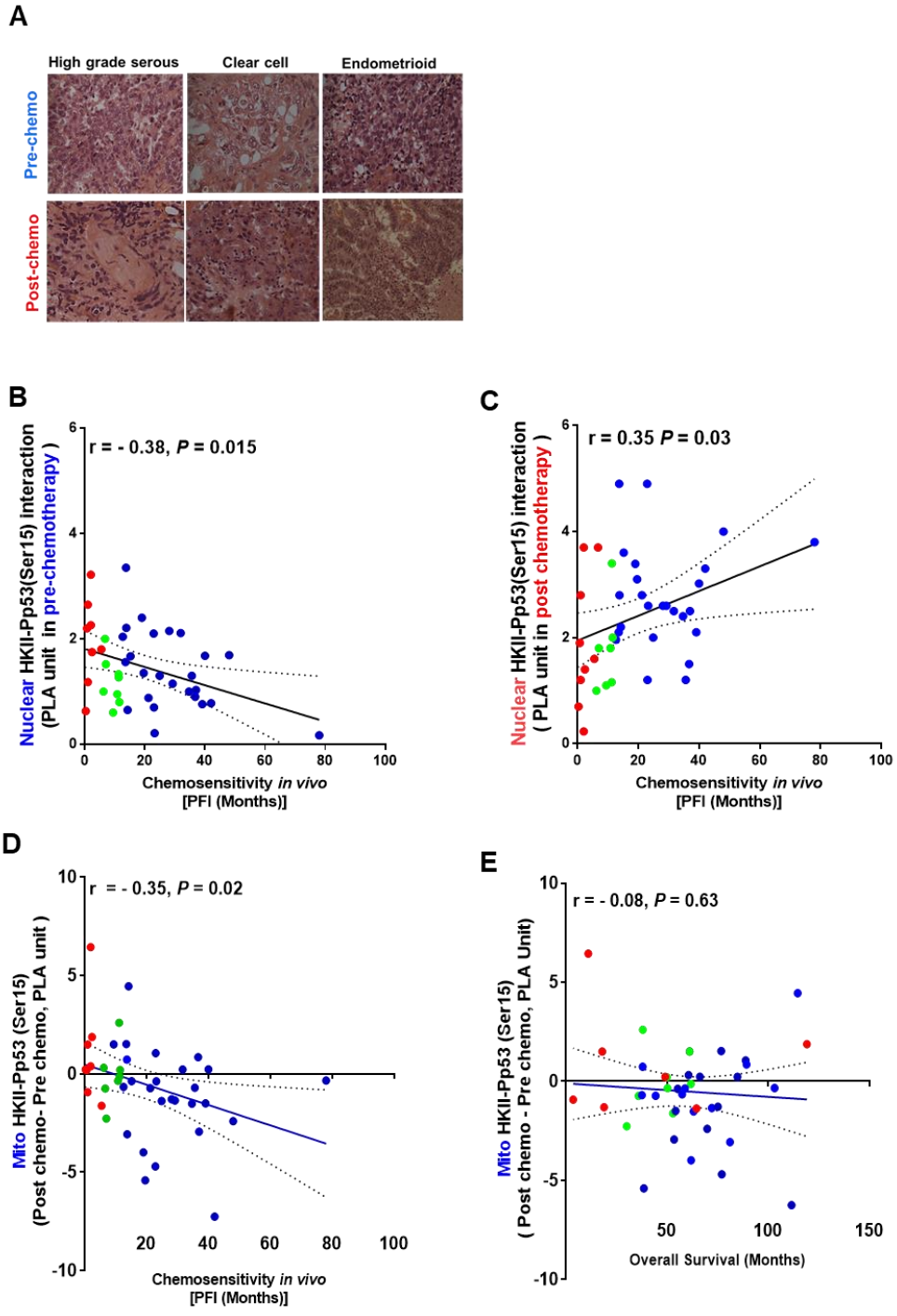
A
High grade serous
Clear cell
Endometrioid
Pre-chemo
Post-chemo
B
r = - 0.38, P = 0.015
Nuclear HKII-Pp53(Ser15) interaction (PLA unit in pre-chemotherapy)
Chemosensitivity in vivo [PFI (Months)]
C
r = 0.35 P = 0.03
Nuclear HKII-Pp53(Ser15) interaction (PLA unit in post chemotherapy)
Chemosensitivity in vivo [PFI (Months)]
D
r = - 0.35, P = 0.02
Mito HKII-Pp53 (Ser15) (Post chemo- Pre chemo, PLA unit)
Chemosensitivity in vivo [PFI (Months)]
E
r = - 0.08, P = 0.63
Mito HKII-Pp53 (Ser15) (Post chemo - Pre chemo, PLA Unit)
Overall Survival (Months)

Fig.4.17

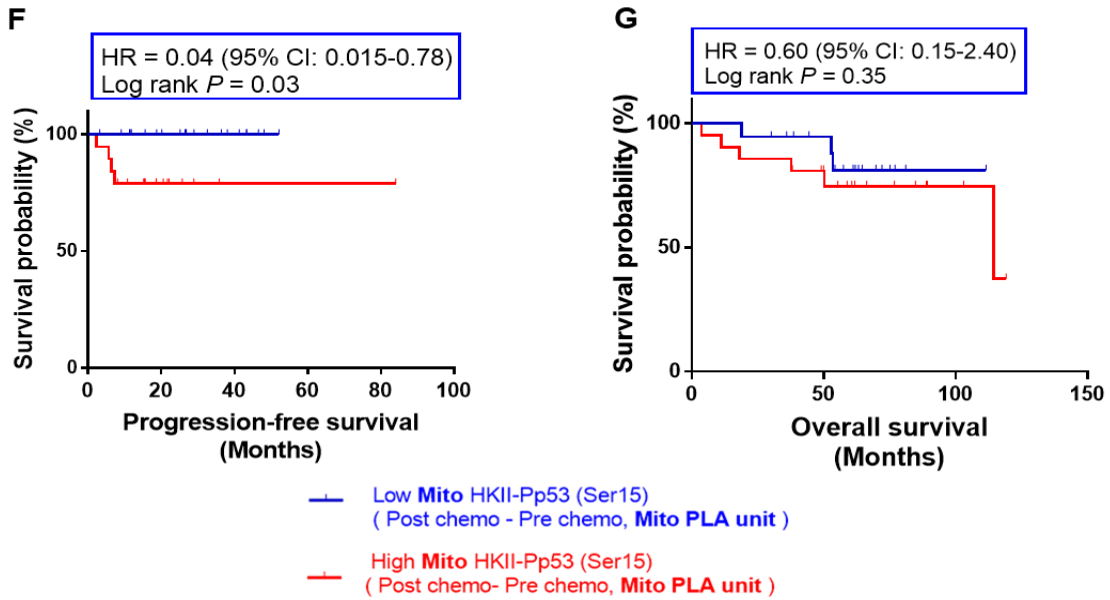
F
HR = 0.04 (95% CI: 0.015-0.78)
Log rank P = 0.03
Survival probability (%)
100
50
0
0
20
40
60
80
100
Progression-free survival
(Months)
G
HR = 0.60 (95% CI: 0.15-2.40)
Log rank P = 0.35
Survival probability (%)
100
50
0
0
50
100
150
Overall survival
(Months)
Low Mito HKII-Pp53 (Ser15)
(Post chemo - Pre chemo, Mito PLA unit)
High Mito HKII-Pp53 (Ser15)
(Post chemo- Pre chemo, Mito PLA unit)

Chapter 5. Discussion

5. 1 Overview & Significance

OVCA is the fifth leading cause of cancer deaths in women (Siegel et al., 2017). Chemoresistance is a major hurdle for effective treatment in OVCA. The mechanisms of chemoresistance are multifactorial, partly due to dysregulation of apoptosis (mutation of tumor suppressors and hyperactive oncogenes) and increased metabolism (Abdullah and Chow 2013). Elevated glycolysis (Warburg effect) is required for cancer cell survival and tumorigenesis (Mathupala et al., 2001; Wolf et al., 2011). However, it remains unknown if and how tumor metabolism affect the cell survival of chemoresistant OVCA cells. Previous studies suggested the role of key glycolytic enzyme HKII in metastasis and tumor formation beyond its metabolic function, but whether HKII is associated with chemoresistance needs to be further elucidated.

The aim of the proposed thesis is to establish a role of tumor metabolism in chemoresistant OVCA. The main objective of the present study was to investigate the role of HKII in aerobic glycolysis, chemoresistance, and its regulatory mechanism in cell survival of chemoresistant OVCA. We first examined the role of HKII in mitochondrial-mediated apoptosis in OVCA. CDDP induced distinctive responses in protein level and intracellular localization of HKII and metabolic responses in chemosensitive and chemoresistant OVCA cells. In addition, we demonstrated a novel regulatory mechanism of p53 for HKII: 1) the interaction and intracellular trafficking of activated P-p53(Ser15) and HKII in the nucleus are required for CDDP-induced apoptosis; 2) Upon entry to the nucleus, activated P-p53(Ser15) binds to the promoter of HKII for transcriptional suppression of HKII in chemosensitive OVCA cells.

Specifically, in chemosensitive OVCA cells, CDDP-induced phosphorylated-p53 (P-p53 Ser15), facilitates and recruits HKII and apoptosis inducing factor (AIF), enabling their translocation from mitochondria to the nucleus, where P-p53 (Ser15) transcriptionally suppresses

HKII, and nuclear accumulation of AIF induces apoptosis. Conversely, with the lack of p53 activation in chemoresistant OVCA cells, HKII and AIF are strongly bound in the mitochondria, and HKII activity is maintained **(Fig 5.1 Hypothetical model)**. The present study supports the notion that p53 is not only responsible for the apoptotic response but regulates key molecules involved in tumor metabolism. Finally, using various clinical samples (human OVCA cell lines, primary OVCA cells, and ovarian tumor sections) in OVCA patients, we have determined that nuclear HKII-p-P53(Ser15) interaction in OVCA may function as a potential determinant biomarker of chemosensitivity in epithelial OVCA.

Figure 5.1 Hypothetical model illustrating the role and regulation of HKII in OVCA cells.

(A) <u>In chemosensitive OVCA cells,</u> (1) CDDP treatment leads to activation of p53 at site of Ser 15. and (2) CDDP induces formation HKII- AIF complex in mitochondria; (3) CDDP-induced P-p53 facilitates translocation of HKII-AIF from mitochondria to the nucleus; (4) P-p53(Ser15) suppresses HKII gene expression by binding to the HKII promoter region; and (5) nuclear AIF induces apoptosis; **(B) <u>In chemoresistant OVCA cells,</u>** (1) CDDP fails to activate p53 (2) HKII and AIF are strongly bound in mitochondria, resulting in maintaining HKII enzymatic activity (3) As a result, P-p53 induced decrease of HKII expression and AIF-induced apoptosis areattenuated.

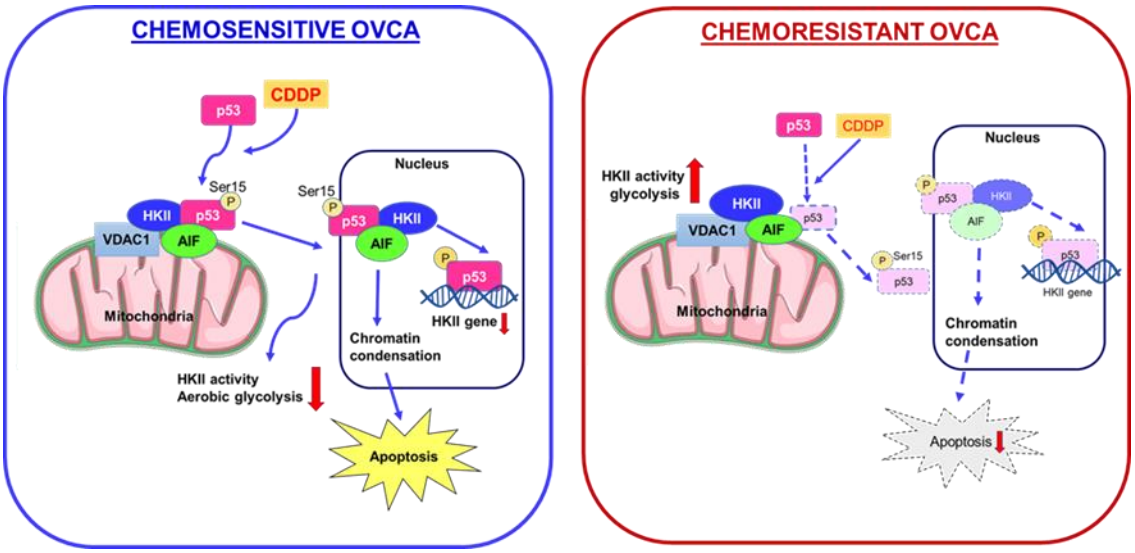
CHEMOSENSITIVE OVCA
p53
CDDP
Ser15
P
HKII
p53
VDAC1
AIF
Mitochondria
Nucleus
Ser15
P
p53
HKII
AIF
P
p53
HKII gene
Chromatin condensation
HKII activity
Aerobic glycolysis
Apoptosis
CHEMORESISTANT OVCA
p53
CDDP
HKII activity
glycolysis
HKII
VDAC1
AIF
p53
Mitochondria
Nucleus
P
p53
HKII
AIF
P
p53
HKII gene
P
Ser15
p53
Chromatin condensation
Apoptosis

5.2 Experimental Advantages for Utilizing Isogenic Cancer Cell Line Pairs

The present studies used matched pairs of a chemosensitive parental cell line (A2780s) and its isogenic resistant counterpart (A2780cp) OVCA cell lines. The chemosensitive A2780s cells were obtained from serous cystadenocarcinoma OVCA (Bao, DiSaia, Sinkovics et al. 1972, Fraser, Bai et al. 2008) and A2780cp cells were developed by long-term exposure (14 - 21 days) in chemosensitive cells to increasing concentration of CDDP. The availability of these cell lines enables us to investigate the molecular mechanism of chemoresistance in the comparison between chemosensitive and chemoresistant phenotype. Since the resistant cell lines has the same genetic background as it's parental sensitive cells, any distinctive differences at the molecular level and CDDP responsiveness may be associated with chemoresistance. Using these paired cell lines, we can examine the distinctive differences in molecular pathogenesis in chemosensitive and chemoresistant cells, CDDP effect on the level of protein, mRNA abundance, metabolic differences, and its subsequent molecular changes during gain and loss of function of specific genes. These different responses are not from the heterogeneity of cell-specific characteristics, and therefore these findings could be more informative to better understand the chemoresistance in OVCA cells.

5.3 Experimental Advantages of Primary Human OVCA cells

The present studies have used primary human OVCA cells and ascites fluids collected from patient tumors in advanced stages (III/IV) OVCA during surgical de-bulking. The primary human cells are collected from human ovarian tumor or ascites. Primary human OVCA cells were collected during 2005-2017 and the clinical record of critical information (stages, histologic subtypes, OS and PFI, clinical outcomes such as recurrence, relapse, and complication and treatment record) are available to allow for a better understanding of the status and prognosis of OVCA patients (Hennessy et al., 2009; Rosen et al., 2009). Although human IHC sections from the patient tumor are valuable resources, a limitation is that the sections cannot be further treated. With tumor sections, it is difficult to acquire pre- and post-chemotherapy samples from the same treated tumor

area and therefore drug responses, and molecular/mechanistic studies such as intracellular trafficking cannot be examined. Conversely, primary human OVCA cells could be treated with chemotherapeutic agents *in vitro* for studies on the cellular and molecular responses and its signaling cascades in the context of its clinical outcome. PFI corresponds to chemosensitivity in OVCA *in vivo*. Studies with primary human OVCA cells may provide clinical relevance and valuable insight.

5.4 Experimental Advantages for Clinical Samples

The present studies used clinical samples as IHC sections collected from paired pre- and post-chemotherapy tumor in OVCA patients. Pre- samples are collected during the biopsy process in primary debulking surgery and post-samples are collected in case of recurrence second debulking surgery. IHC slides were collected during 2005-2017 along with the clinical record of patients (stages, histologic subtypes, overall survival, PFI, clinical outcome such as recurrence, relapse, and complication, and treatment record).

Clinical samples from patients allow us to better understand the responses to chemotherapy regimen and different molecular expression in varied groups of OVCA patients with different stage, histologic subtypes, and PFI. Considering that chemotherapy regimen in clinics is usually not CDDP, but frequently combination with Paclitaxel and Carboplatin, IHC slides from patients in this study were treated with a not only single chemotherapeutic agent, but to various chemotherapies.

The length of PFI is a determinant in response to chemotherapy and predicting clinical outcome. Previous studies indicate that longer PFI corresponds to better responses in chemotherapy in OVCA, whereas shorter PFI corresponds to chemoresistance or even cancer death (Hennessy et al., 2009). In the present studies, we examine how *in vitro* data is compatible with clinical samples to compare the similarities and differences.

5.5 Dysregulation of Apoptosis

Apoptosis is a response to CDDP-induced cell death, which involves the expression of specific pro-apoptotic cell death genes and down-regulation of survival counterparts. The mechanism of CDDP resistance is multifactorial and complex including altered expression of regulatory tumor suppressor proteins and oncogenes involved in signal transduction cascade which exerts apoptosis. Understanding the dysregulated apoptotic pathway and its underlying mechanisms of chemoresistance may provide insight for the development of better therapeutic strategies. Based on extensive research in the field, some of the critical determinants such as defects of p53 and activation of Akt have been considered as general mechanisms of the representative chemoresistant phenotype. In mitochondrial-mediated apoptosis, chemoresistance often involved the aberrant expression of the anti-apoptotic Bcl-2 family which regulates the integrity of other OMM and mitochondrial dynamics.

Our laboratory has delineated the molecular mechanisms of chemoresistance in OVCA cancer cells, which include overexpression and hyperactivation of Akt, dysfunction of p53 and its subsequent effect, altered expression of Bcl-2 family members, stabilized p53-associated Parkin-like cytoplasmic protein (PARC) and PPM1D, increased levels of FLIP and Gelsolin, and the involvement of mitochondrial fission/fusion proteins (Abedini et al., 2014; Ali et al., 2012; Kong et al., 2014). The present thesis highlights the role of tumor glycolysis metabolism (Warburg effect) in the etiology of chemoresistance in OVCA. Altered mitochondrial energy metabolic pathways have been implicated in the dysregulation of intrinsic apoptosis pathway and chemoresistance.

5.6 Energy Metabolism & Chemoresistance

In this study, we observed the role of the key glycolytic enzyme HKII in tumor metabolism and chemoresistance in OVCA. Accelerated glycolysis is a key hallmark of tumorigenesis (Mathupala et al., 2006; Mathupala et al., 2001; Warburg, 1956). Accumulating evidence

demonstrates that HKII is associated with tumorigenesis, proliferation, and survival of multiple types of cancer, including lung cancer, glioblastoma, breast cancer, and prostate cancer (Mathupala et al., 2001; Patra et al., 2013; Wang et al., 2014). Patra et al. demonstrated that deletion of HKII significantly decreased tumor burden and prolonged the survival without a side effect in a mouse model, suggesting that HKII is a critical factor involved in tumor progression (Patra et al., 2013). Suh et al. reported that high HKII protein expression is closely associated with lower progression free survival rate than lower overall survival rate in OVCA human IHC samples (Suh et al., 2014).

Our *in vitro* results, however, showed that high expression of HKII is a necessary but not sufficient determinant of chemoresistance, and that CDDP-induced HKII downregulation is important for determining chemosensitivity (Fig. 4.1). We demonstrated that CDDP induced HKII downregulation in protein and mRNA abundance level, but not in chemoresistant cells where apoptosis was minimal. In addition, immunofluorescence study indicated that nuclear localization of HKII was observed in both basal and CDDP-treated chemosensitive cells, whereas HKII was highly localized in mitochondria in chemoresistant cells (Fig. 4.4 & 4.5). These findings were consistently observed not only in cancer cell lines, but also primary human OVCA cells and IHC sections (Fig. 4.14 & 4.15).

It has been previously reported that the glycolytic enzymes PFK1 and PKM2 are associated with chemoresistance in cancer (Wang et al., 2017; Zhou et al., 2012), a finding consistent with our current studies showing that CDDP also decreased the protein content of these enzymes (Fig. 4.1). Although our studies do not exclude the possible involvement of these enzymes in chemoresistant OVCA, CDDP-induced, P-p53(Ser15)-mediated interaction with HKII, HKII down-regulation, and nuclear localization seem to be important.

Mito-HKII may function as a key metabolic enzyme to execute Warburg effect and to fulfill for energy demand in chemoresistant cells, leading to cell survival. Our result supported this notion, showing that the detachment of HKII from OMM decreased its enzymatic function as downregulated glycolysis metabolism (decreased OCR, ECAR, ATP and HK activity; Fig. 4.3). Detached HKII from mitochondria lost its enzymatic function as a consequence, since it may lose accessibility of its substrate glucose and the product ATP as confirmed in our gain- and loss-of-function study (Fig. 4.6 - 4.8). Mito-HKII in the chemoresistant cell may allow cells to acquire energy for cell survival even in the presence of chemotherapy, whereas CDDP-induced nuclear HKII causes impaired energy metabolism, insufficient energy supply and facilitation of apoptosis.

5.7 The Role of HKII in Intrinsic Apoptosis Pathway

Mito-HKII functions to shield cells from apoptosis by preventing the opening of mPTP and regulating MOMP (Neary and Pastorino, 2013; Wolff et al., 2008). However, the role of HKII in apoptosis and in chemoresistance needs to be further investigated. Notably, our data indicate that HKII depletion does not sensitize p53-defect chemoresistant cells to CDDP, but the presence of a functional p53 is required for the induction of apoptosis (Fig. 4.9). However, HKII depletion may contribute to the decreased proliferation of chemoresistant OVCA cells. How HKII depletion and CDDP together may affect metastasis, but not apoptosis of chemoresistant OVCA needs to be further explored. Based on our study, the reversal of chemoresistance can be achieved by inhibiting the HKII when functional p53 is present. Thus, in OVCA cells expressing mutant p53, HKII depletion may have minimal effect on cell death due to defective p53. In tumors harboring a wild type p53, suppression of HKII could lead to a reversal of chemoresistance. These results suggest that OVCA patients harboring a functional p53 could potentially benefit from drug targeting metabolism in OVCA. In patients harboring defective p53, glycolysis inhibitor may stall the progression or proliferation of cancer.

Akt is a key regulator of CDDP sensitivity. p-HKII promotes stable association of HKII with mitochondria (Gottlob et al., 2001; Miyamoto et al., 2008). Precisely how Akt mediated mito-HKII is associated with chemoresistance in OVCA needs to be further examined. Our study also demonstrated that mito-HKII level is affected by Akt depletion and p53 reconstitution (Fig. 4.8). In addition, mito-HKII is enriched in different subtype of chemoresistant OVCA cells as well as primary human OVCA cells; high mito -HKII is enriched in chemoresistant primary human OVCA cells with shorter PFI, and high nuclear HKII in chemosensitive OVCA cells with longer PFI, associated with chemosensitivity (Fig. 4.11).

HKII plays important roles in mitochondrial protection. As previously mentioned, apoptosis induction and mPTP formation by the pro-apoptotic family members Bax/Bak are prevented, largely due to pre-occupied Bax binding site by HKII (Majewski et al., 2004a; Roberts et al., 2013). However, the role of HKII in mitochondrial dynamics remains unknown. It needs to be further investigated if HKII affects the maintenance of mitochondrial integrity and the structure of cristae controlling key mitochondrial dynamic molecules such as Optic Atrophy 1 (OPA1). OPA1 is a profusion inner mitochondrial membrane dynamin-related protein that also regulates cristae structure. Cristae structural alterations, changes in the ultrastructure of the inner mitochondrial membrane compartments, significantly contribute to apoptotic signaling (Frezza et al., 2006; Yamaguchi et al., 2008). OPA1 associates with itself to form oligomers. CDDP induced a long form of OPA1 processing as intact OPA1 is associated with chemoresistance (Kong et al., 2014; Tsuyoshi et al., 2017). In addition, pro-apoptotic Bax/Bak disrupts OPA1 oligomerization, inducing apoptosis (Yamaguchi et al., 2008). However, whether and how mito-HKII are involved in the interaction between Bax/Bak and OPA1 along with its oligomerization, subsequently affecting the maintenance of mitochondrial cristae (Frezza et al., 2006) need to be further investigated. In addition, whether disruption of OPA1 may affect mito-HKII and its metabolic activity needs to be further investigated.

5.8 Regulatory Roles of p53 on HKII and Its Mediated Metabolism

The present study demonstrates the regulatory roles of p53 in intracellular trafficking and transcription of HKII. These processes mediate HKII regulation and glycolysis more effectively. Phosphorylation and activation of p53 are required for its stability and induction of apoptosis (Ogawara et al., 2002; Ou et al., 2005). We observed that the presence of functional p53 is required for HKII nuclear localization where HKII is transcriptionally regulated in chemosensitive OVCA cells, but this phenomenon is compromised in p53-defect chemoresistant cells (Fig. 4.6 & Fig. 4.10).

We show the transcriptional regulatory role of p53 in HKII in OVCA. Wang et al. previously demonstrated that p53/PTEN are involved in the expression of HKII in prostate cancer cells (Wang et al., 2014). Present study further emphasizes not only the expression, but activation of p53 for HKII regulation. Our group previously demonstrated that p53 phosphorylation at Serine 15 but not Serine 20 is required for CDDP-induced apoptosis (Fraser, Bai et al. 2008). ChIP assay provides a mechanistic view that P-p53(Ser15) but not P-p53(Ser20) is involved in the suppression of HKII transcription via promoter binding (Fig. 4.10).

p53 regulates HKII and its mediated glycolysis. Using gain- and loss-in-function approaches, we observed that p53 facilitates the regulation of HKII-mediated glycolysis metabolism (Fig. 4.6 & 4.8). When p53 is knocked down in chemosensitive A2780s cells, glycolysis metabolism was not decreased regardless of CDDP treatment. Conversely, p53 overexpression in A2780cp cells decreased glycolysis and HK activity upon CDDP treatment, suggesting the regulatory role of p53 in glycolytic metabolism.

This study for the first time has demonstrated a role of the nuclear HKII-P-p53(Ser15) interaction in epithelial OVCA. Although previous clinical studies focused on either HKII expression or p53 expression alone in multiple cancers including OVCA, the clinical relevance and mechanistic view between these molecules were limitedly addressed. Mechanistically, HKII-P-

p53(Ser15) nuclear intracellular trafficking implies that P-p53(Ser15) binding to HKII promoter is required for its transcriptional regulation.

Regarding intracellular trafficking, P-p53(Ser15) may facilitate HKII nuclear localization, but this mechanism needs to be further elucidated. Nuclear localization signal resides in the sequence of HKII. Also, HKII localization in both nucleus and cytoplasm have been reported (Neary and Pastorino, 2010; Pastorino et al., 2002). However, its specific causes for the induction of HKII localization in different cellular organelle have not as yet been reported. Our findings support that activation of p53 [P-p53(Ser15)] is required for detachment of HKII from mitochondria and its nuclear localization. We and others previously demonstrated that P-p53(Ser15) targets mitochondria during apoptosis (Wolff et al., 2008; Yang et al., 2008). PLA studies indicate that CDDP induces HKII-Pp53 (Ser15) interaction and intracellular trafficking into the nucleus, but this is compromised in chemoresistant cells (Fig. 4.12 & Fig. 4.13). This possibly suggests that defect of p53 may inhibit this nuclear interaction between HKII-Pp53(Ser15). Our studies showed that P-p53(Ser15) is more highly localized in the nucleus in chemosensitive than that in chemoresistant OVCA cells (Fig 4.4B). This intracellular trafficking may be required for further transcriptional regulation of HKII in the nucleus.

Precisely how this intracellular trafficking and regulation are associated with apoptosis is yet unknown. One possible mechanism is AIF-induced apoptosis. Our group and others showed that CDDP induced AIF-mediated apoptosis and AIF nuclear translocation from mitochondria (Farrand et al., 2013; Yang et al., 2008). Our study shows that HKII-Pp53(Ser15) interact with AIF and forms a complex which eventually moves to the nucleus, resulting in AIF-induced apoptosis (Fig. 4.12B). Another mechanism may be the interaction between HKII-P-p53(Ser15) and pro-apoptotic protein, Bak. It is also possible that CDDP induces the formation of P-p53(Ser15) with Bak complex at the mitochondria, increases permeabilization of OMM, resulting in intrinsic apoptosis in OVCA cells (Kong et al., 2014).

Our findings expand and implement *in vitro* results to the translational studies using primary human cells and IHC sections from patients in OVCA. Based on accumulating evidence, longer PFI corresponds to better responses to recurrence therapy in OVCA. CDDP induces high enrichment of nuclear interaction of HKII-P-p53(Ser15) in both primary human cells and tumor sections with a clinically defined platinum-sensitive group (PFI > 12 months), but this signal is attenuated and limitedly localized in the mitochondrial region in the clinically defined platinum-resistant group (PFI ≤ 6 months) (Fig. 4.14 & Fig. 4.15). Clinically, more common chemotherapy regimen are platinum-containing carboplatin and Paclitaxel since carboplatin is reported to have better toxicity profile (Ho et al., 2016). Although we have used CDDP in vitro cell line study, the mechanism of molecular action between CDDP and carboplatin are the same and reported to have similar clinical outcome including OS. This study used IHC sections and primary cells treated with carboplatin and Paclitaxel and therefore our study is not limited to determine action of CDDP.

Our study demonstrated that increased nuclear HKII-P-p53(Ser15) interaction is highly associated with better clinical outcome. (Fig. 4.15). For example, when we categorized the group of patients depending on PFI, we have observed strong correlation between high nuclear HKII-P-p53(Ser15) and longer PFI (Fig. 4.16B). We also observed a higher correlation between increased nuclear HKII-P-p53(Ser15) and PFI than with overall survival. It is possible that overall survival can be affected by other factors such as age, outcome of surgery, and other complications (Fig. 4.15D). Interestingly, some of resistant patients in our samples collected live longer than 5 years regardless of their chemoresponsiveness. In addition, increased nuclear HKII-P-p53(Ser15) interaction is stronger determinant for chemosensitivity than increased mitochondrial HKII-P-p53(Ser15) interaction (Fig. 4.17D). It also possibly supports the suggested mechanism for translocation of complex from HKII-P-p53(Ser15)-AIF from mitochondria to the nucleus as shown the correlation between mitochondrial HKII-P-P53(Ser15) and PFI is a negative value.

Nuclear HKII-P-p53(Ser15) interaction can be used as a potential bio marker for determining chemosensitivity. To our knowledge, the present study is the first report to investigate nuclear HKII-P-p53(Ser15) interaction for predicting clinical outcomes. These findings can be used for patients given not only adjuvant chemotherapy but also for neoadjuvant chemotherapy, in which that patient is treated with chemotherapy first followed by debulking surgery. In addition, since we used our IHC sections treated with other chemotherapies in addition to platinum-containing drug, the present studies can be expanded to investigate the nuclear HKII-P-p53(Ser15) effect not only with platinum-containing drugs, but also other chemotherapeutic agents (e.g., Paclitaxel & Doxorubicin).

In light of the limited samples examined particularly in subtypes of high grade serous, whether the possible utility of HKII-P-p53(Ser15) interaction as a predictor of chemosensitivity in other histological subtype of epithelial OVCA needs to be further investigated (e.g., clear cell & endometrioid). In clear cell carcinoma with distinctive metabolic phenotype, the poor clinical outcome with frequent recurrence is reported as more severe OVCA than high grade serous (Skirnisdottir et al., 2005). Although our findings showed that nuclear HKII-P-p53(Ser15) interaction was largely increased in clear cell carcinoma with longer PFI, we need to validate these findings with increased sample numbers of clear cells. Collectively, these findings provide clinical relevance and suggest a potential role of nuclear HKII-P-p53(Ser15) interaction as a biomarker associated with chemosensitivity.

5.9 Future Research Directions

A. Patient Derived Tumor Xenograft Model (PDX)

As an alternative emerging preclinical model, patient-derived xenografts (PDX) may provide clinical insights and a better understanding of chemoresistant tumor and its targeted therapy *in vivo* system (Tentler et al., 2012; Topp et al., 2014). PDX are animal models of cancer, where

tissue or tumor cells isolated from ascites of pleural fluids from patients are implanted into an immunodeficient mouse, simulating the natural growth of cancer, the progression of cancer, and responses to chemotherapy. In xenograft using cancer cell lines, genomic characteristic and heterogeneity of cancer cells could be changed during multiple passages. When implanted into immunodeficient mice, cell lines frequently do not develop tumors and the result of successfully grown tumor does not necessarily reflect the original tumor and results in a genetic divergence, unlike the heterogeneous population of cells frequently observed in the patient tumor (Williams et al., 2013).

Cell line-xenografts often fail to predict the actual drug responses occurred in the primary tumors (Hutchinson and Kirk, 2011). However, within PDX models, patients' tumors grow in the physiologically-relevant tumor microenvironment, similar to the patient's primary tumor site. The advantage of PDX models includes preservation of histologic appearance, retaining molecular fidelity of original tumor in regard to genomic characteristics and intratumoral heterogeneity (Liu et al., 2017). PDX models are beneficial to understand chemoresistant system because various therapies can be tested, and pre- and post-treatment data can be acquired from the xenograft tissue.

For future direction, ovarian PDXs will be implemented to study the involvement of HKII associated with chemoresistance and effect on glycolysis inhibitor. Ovarian PDXs will be established by injecting tumor or ascites collected from patients intraperitoneally in non-obese diabetic (NOD)- severely compromised immune deficient (SCID) nude mice. Based on our *in vitro* studies and clinical record, we will subcutaneously inject chemosensitive phenotype of SNU-3561 (PFI =19 months) and chemoresistant phenotype, A39 (PFI < 6 months) into the right flank. Animals will be examined three times per week for the appearance of palpable tumors or abdominal distention for the assessment of tumor development. To examine the effect on co-treatment of CDDP (1.8 mg/kg/week) and the glycolysis inhibitor Metformin (10 mg/kg/day), CDDP and Metformin will be intraperitoneally administered in two cycles.

At the termination of the study at the day of 40, tumor volumes will be measured for tumor growth, animals will be sacrificed, and a necropsy will be conducted to collect tumor specimens for IHC staining. Tumor histology will be examined using histoscan to verify the tumor integrity and successive transplantations. The influence of CDDP and Metformin on tumor progression (volume) and apoptosis will be assessed to validate the previous finding of HKII involvement in tumor progression. Tumors harvested from these animals will be processed for IHC analysis, using HKII and P-p53(Ser15) antibodies to determine its cellular localization. We expect that tumor growth in PDX model with SNU-3561 will be smaller compared with that from PDX with A-39. For the apoptosis measurement, we expect that tumor volume will be significantly reduced in Metformin and CDDP treatment together in SNU-3561, but not in A-39 model. In addition, using IHC and PLA, the nuclear interaction of HKII and P-p53(Ser15) could be observed by PDX model. If our hypothesis is correct, the nuclear interaction of HKII and P-p53(Ser15) will be significantly increased in SNU-3561 upon CDDP treatment, but not PDX model with A-39. These PDX model will provide insight for chemosensitivity, target identification, and the validation of therapeutic combination in OVCA. Future direction using clinically relevant PDX tumor models will provide compelling evidence and insight to chemosensitivity and possible treatment scenario.

B. Targeting metabolism for cancer therapy

1) Candidates for targeting tumor metabolism

For the numerous aforementioned reasons, targeting glucose metabolism has been considered as a promising therapeutic target. However, side effects and barriers to effective treatments have led to several unsuccessful clinical trials (Table. 5.1).

2-DG, Lonidamine (LND), and 3-Bromopyruvate (3-BP) are used as HK inhibitors. 2-DG, a glucose analogue, is used as a competitive HK inhibitor. Research in both *in vitro* & *in vivo* demonstrates that concomitant use of 2-DG with an inhibitor of lysosomal permeabilization

increased its anti-tumor action, inducing mitochondrial damage & necrotic cell death (Kosic et al., 2016). Besides, 2-DG with PPARα agonist, Fenofibrate leads to cancer cell death by inducing ER stress (Liu et al., 2016). Despite these promising results, 2-DG clinical trial has been stopped in phase I since it results in intolerable low glucose concentration level (hyporglycemia) and a reduction in white blood cell count in leukemia patients (Landau et al., 1958). Also, it causes some toxicity when it is concurrently treated with radiotherapy in glioma patients (Dwarakanath et al., 2009). With regards to safety and efficacy, the minimal concentration of 2-DG with use of concomitant chemotherapeutic agent or development of other glucose analog inhibitor for better target specificity could be considered.

Considering that HKII has variable isoforms and HKI is also highly expressed in normal cells, the demand for target specificity for HKII is urgently needed in regard to the safety and efficacy. Other drugs such as 3-BP and Methyl jasmonate, which are known to specifically detach HKII from VDAC of mitochondria, showed anti-neoplastic effects *in vitro* and *in vivo* mouse tumor models (Goldin et al., 2008; Jae et al., 2009). In OVCA xenograft, 3-BP decreased tumor growth and prolonged survival length (Ha et al., 2018). These drugs have been shown to facilitate mitochondria-mediated apoptosis, whereas the target of these drugs covers a broad spectrum, inhibiting additional enzymes GAPDH and Lactate Dehydrogenase A (LDHA).

LND (indazole-3-carboxylic acid) inhibits aerobic glycolysis and HKII in hypoxic conditions. Since its combined therapy with temozolomide showed anti-tumor effects in brain cancer, clinical trials for combination approaches are ongoing (Suh et al., 2014). In advanced OVCA, LND has been shown to be active and tolerable when combined with DNA damaging agents (CDDP) and Paclitaxel in phase II clinical trial (De Lena et al., 2001). Although its results are promising, whether LND will revert chemoresistance in OVCA needs to be further tested clinically.

3-(3-Pyrinidyl)-1-(4- Pyrinidyl)-2-propane-1-one (3-PO) inhibits PKFB3 family which is the key enzyme regulating F2,6 BP and the activity of phosphofructokinase 1 (PFK1; a rate-limiting step of glycolysis). 3-PO shows a suppressive effect in glycolytic flux and growth of cancer cells *in vitro* and *in vivo* (Clem et al., 2013). These compounds and their derivatives are currently in clinical trials to test the efficacy and safety.

Dichloroacetate (DCA) was originally used for hereditary lactic acidosis (Galluzzi et al., 2013; Wong et al., 2008); and DCA is now an anti-cancer drug targeting metabolism. DCA inhibits PDK1, stimulating the activity of PDH and shifting from glycolysis and lactate production to mitochondrial respiration. DCA induces apoptosis in endometrioid cancer (Wong et al., 2008). Combined treatment of DCA and Metformin elicited a synergistic effect in the suppression of OVCA growth (Li et al., 2016). Also, when given with the anti-angiogenesis inhibitor bevacizumab (Avastin), DCA enhances anti-tumor effects in brain cancer through reversing hypoxic adaptation. Considering that bevacizumab has recently approved (2016) for recurrent platinum-sensitive OVCA, concomitant use of bevacizumab with DCA may broaden its indications to include chemoresistant OVCA (Kumar et al., 2013). Clinically, this drug shows successful efficacy as durable remission for four years in glioblastoma and resistant non-Hodgkin lymphoma, but further clinical studies with combined therapy need to be conducted in other solid tumors (Michelakis et al., 2010; Strum et al., 2013).

In addition, repurposing Metformin, the first-line medication for type 2 diabetes, has gained considerable interest as potential cancer treatments (Kasznicki et al., 2014). Metformin inhibits mitochondrial complex I and targeting mitochondrial Bcl-2 family of anti-apoptotic proteins in cancers. Metformin has also been shown to directly inhibit HKI and HKII as a competitive inhibitor by mimicking its product G-6-P (Salani et al., 2013) (Marini et al., 2013). Detachment of HKII from mitochondria and suppression of glucose consumption by Metformin has been reported (Marini et al., 2013). Accumulating evidence suggests Metformin having anti-tumor activity (Chen

et al., 2016; Galluzzi et al., 2013; Gwak et al., 2017; Li et al., 2016) and antagonizing cancer cell proliferation by suppressing flow of glucose- and glutamine-derived metabolic intermediates, leading to decreased citrate production and lipid biosynthesis (Griss et al., 2015). Recent research demonstrates that anti-tumor activity is increased when Metformin is used in combination with p53 stabilizers (Chen et al., 2016). Currently, Metformin and combined CDDP and carboplatin therapy are at the initial phase (patient recruitment) of a clinical trial in multiple solid tumors, including OVCA, worldwide (USA, UK, Netherland, Australia, and Norway) (Health, 2018). (Kasznicki et al., 2014)

AT-101 (Gossypol), a Bcl-xL inhibitor, has also been shown to target LDH. It is currently in phase I clinical trial as combined therapy with other apoptotic inducing chemotherapy agents (Docetaxel, CDDP, and Carboplatin) for relapsed leukemia and Laryngeal cancer. Though Imatinib (Gleevec) has not been in clinical trial targeting metabolism, it has recently been shown to also inhibit glycolysis activity (Galluzzi et al., 2013). Thus, implementation of pre-approved drug or broadening the indications of current drugs targeting metabolism are on-going. Based on the outcome of clinical trials, targeting metabolism only appears insufficient, but promising synergistic anti-tumor effect could be realized when it is used combination with conventional chemotherapy.

In addition to inhibition of tumor metabolism, restriction of nutrition has been considered as a plausible option in cancer control. The Ketogenic Diet (low carbohydrate, high fat, and adequate protein) under certain settings may suppress tumor growth and increase chemosensitivity (Lee and Longo, 2011; Lee et al., 2012). The combination of a ketogenic diet with the hyper-oxygen condition also showed an anti-tumor effect in mice (Lee et al., 2012). However, chemotherapy frequently develops muscle wasting and cachexia (weakness and wasting of the body mass due to severe chronic illness), and patients undergoing chemotherapy are thereby recommended to consume elevated calories and protein. In tumor bearing mice, high calorie food consumption increased survival, even in the absence of chemotherapy (Poff et al., 2013). Still, dietary

interventions in tandem with traditional therapeutics are still under development and possible side effects, such as hypoglycemia, should be considered seriously (Niakan, 2010).

2) Challenges & Strategies for targeting tumor metabolism

The major barrier to the development of drugs that target metabolism is that many of them failed to specifically inhibit metabolic enzymes associated with cancer. Due to co-existence of multiple metabolic isoforms, many small molecule inhibitors for targeting metabolism can cause side effects since it may inhibit essential glycolysis and metabolic pathway required for a physiological condition. Also, targeting a single metabolic pathway could lead to increased compensation by another metabolic pathway. Therefore, one needs to investigate the systematic effect of these drugs, including potential side and toxic effects on kidney or other body organs, the clearance rate of this drug, and its half-life.

Table 5.1 List of drug candidates targeting metabolic pathway

Table shows chemotherapeutic drugs targeting metabolism under development process. It describes targeting enzymes and pathway, current stage of pre-clinical and clinical trials, side effects, and potential application in OVCA.

Table 5. 1 Current drug development & clinical trial process for drugs targeting metabolism

Drug	Targets	Pathway	Clinical trial	Effects in cancer cells/ Clinical information	Application in OVCA
2-Deoxy-D-glucose (2-DG)	HK	Glycolysis	Phase I discontinued due to side effects	Hyperglycemia was observed as major adverse events.	2-DG and glutaminolysis inhibitor aminooxyacetate (AOA) synergistically inhibited cell growth of OVCA (Sun et al., 2017).
3-Bromopyruvate (3-BP)			Pre-clinical	3-BP also inhibits GAPDH & LDHA (Shoshan, 2012)	Co-treatment of 2-DG and 3-BP induced apoptosis in OVCA cells (Sun et al., 2017). 3-BP inhibits HKII and attenuates tumor progression in OVCA (Ha et al., 2018).
Lonidamine (LND)			Phase II (Europe)	LND potentiates the chemotherapy responses in the prostate, breast mouse xenograft model.	LND potentiates the responses of doxorubicin in mouse xenograft model (Nath et al., 2015). LND and CDDP show tolerability & activity in advanced OVCA (De Lena et al., 2001).
Methyl jasmonate			Pre-Clinical	Methyl jasmonate induced apoptosis and necrosis in liver cancer (Li et al., 2017a).	Methyl jasmonate treatment in OVCA has not been conducted *in vitro* & *in vivo*.
Dichloroacetate (DCA)	PDK1	Krebs Cycle	Pre-Clinical	DCA is prescribed for lactic acidosis.	DCA & Metformin together shows suppression of tumor in OVCA (Li et al., 2016).
AT-101 (Gossypol)	LDH Bcl-xL	BCL-xL	Phase I & II (US FDA) (Head & neck cancer)	AT-101 shows no significant efficacy when it was treated with docetaxel in head & neck cancer (Swiecicki et al., 2016). Clinical trial (Phase I) is on- going process in resistant leukemia & laryngeal cancer. AT-101 potentiates the responses of gefitinib in lung cancer in vitro.	In vitro, co-treatment of AT-101 and CDDP shows apoptosis in chermoresistant OVCA cells (Karaca et al., 2013).
Metformin	Mitochondria Complex I	Mitochondrial Respiration	Pre-clinical (US FDA) *Recruite patients	Metformin is prescribed for the treatment of type 2 diabetes. Metformin is effective in decrease size of the solid tumor in a mouse model.	Metformin induced cyclin D1 degradation & G1 cell cycle arrest in OVCA cells (Gwak et al., 2017). Currently in process of recruiting patients of OVCA for clinical trials (US FDA).

5.10 Conclusion

The current thesis provides significant contributions regarding the cellular and molecular mechanisms of CDDP resistance and tumor metabolism in OVCA cells. In this study, we investigate this regulatory role of P-p53 on HKII and its mediated cellular metabolism, associated with chemosensitivity in OVCA. The novel observations in this study include: p53 regulates HKII in two mechanistic processes as 1) intracellular trafficking of HKII and P-p53 (Ser15) in the nucleus and 2) transcriptional suppression of p53 on HKII via promoter binding. In addition, this study demonstrates for the first time that both interaction of P-p53(Ser15) and HKII in the nucleus are required for regulating aerobic glycolysis and chemosensitivity. As shown in our hypothetical model **(Fig. 5.1)**, we observed that 1) CDDP activates p53 and facilitated the formation of a P-p53(Ser15)-HKII-AIF complex in chemosensitive OVCA cells; 2) translocation of the P-p53(Ser15)-HKII-AIF complex from the mitochondria to the nucleus, 3) HKII can be transcriptionally regulated by P-p53(Ser15), resulting in chemosensitivity and AIF-induced apoptosis in OVCA cells; and 4) These biochemical and cellular mechanisms are however deregulated in chemoresistant cells. In our translational research with clinical samples, HKII-P-p53(Ser15) interaction in the nucleus is associated with chemosensitive OVCA in different epithelial subtypes of OVCA, suggesting its potential role as potential biomarker.

In conclusion, we have shown that intracellular trafficking and transcriptional regulation of HKII with activated p53 are essential for the regulation of glycolytic metabolism and chemosensitivity of OVCA. Our studies enable us to better understand the link between glycolysis metabolism and chemosensitivity in OVCA. Furthermore, as shown in our translational research identification of this mechanism provide insight that interaction of HKII-P-p53(Ser15) may function as a potential biomarker for improved clinical outcome in chemoresistant OVCA and decision on more effective therapy.

Chapter 6. References

1. Abedini, M. R., Muller, E. J., Brun, J., Bergeron, R., Gray, D. A., and Tsang, B. K. (2008). Cisplatin induces p53-dependent FLICE-like inhibitory protein ubiquitination in ovarian cancer cells. Cancer research *68*, 4511-4517.
2. Abedini, M. R., Qiu, Q., Yan, X., and Tsang, B. K. (2004). Possible role of FLICE-like inhibitory protein (FLIP) in chemoresistant ovarian cancer cells in vitro. Oncogene *23*, 6997-7004.
3. Abedini, M. R., Wang, P. W., Huang, Y. F., Cao, M., Chou, C. Y., Shieh, D. B., and Tsang, B. K. (2014). Cell fate regulation by gelsolin in human gynecologic cancers. Proceedings of the National Academy of Sciences of the United States of America *111*, 14442-14447.
4. Agarwal, R., and Kaye, S. B. (2003). Ovarian cancer: strategies for overcoming resistance to chemotherapy. Nature reviews Cancer *3*, 502-516.
5. Ahmad, A., Ahmad, S., Schneider, B. K., Allen, C. B., Chang, L. Y., and White, C. W. (2002). Elevated expression of hexokinase II protects human lung epithelial-like A549 cells against oxidative injury. American journal of physiology Lung cellular and molecular physiology *283*, L573-584.
6. Ahn, K. J., Hwang, H. S., Park, J. H., Bang, S. H., Kang, W. J., Yun, M., and Lee, J. D. (2009). Evaluation of the role of hexokinase type II in cellular proliferation and apoptosis using human hepatocellular carcinoma cell lines. Journal of nuclear medicine : official publication, Society of Nuclear Medicine *50*, 1525-1532.
7. Ali, A. Y., Abedini, M. R., and Tsang, B. K. (2012). The oncogenic phosphatase PPM1D confers cisplatin resistance in ovarian carcinoma cells by attenuating checkpoint kinase 1 and p53 activation. Oncogene *31*, 2175-2186.
8. Altomare, D. A., Wang, H. Q., Skele, K. L., De Rienzo, A., Klein-Szanto, A. J., Godwin, A. K., and Testa, J. R. (2004). AKT and mTOR phosphorylation is frequently detected in ovarian cancer and can be targeted to disrupt ovarian tumor cell growth. Oncogene *23*, 5853-5857.
9. Andrzejewski, S., Klimcakova, E., Johnson, R. M., Tabaries, S., Annis, M. G., McGuirk, S., Northey, J. J., Chenard, V., Sriram, U., Papadopoli, D. J., *et al.* (2017). PGC-1alpha Promotes Breast Cancer Metastasis and Confers Bioenergetic Flexibility against Metabolic Drugs. Cell metabolism *26*, 778-787 e775.
10. Anglesio, M. S., Wiegand, K. C., Melnyk, N., Chow, C., Salamanca, C., Prentice, L. M., Senz, J., Yang, W., Spillman, M. A., Cochrane, D. R., *et al.* (2013). Type-specific cell line models for type-specific ovarian cancer research. PloS one *8*, e72162.
11. Annibaldi, A., and Widmann, C. (2010). Glucose metabolism in cancer cells. Curr Opin Clin Nutr Metab Care *13*, 466-470.
12. Antoun, S., Atallah, D., Tahtouh, R., Alaaeddine, N., Moubarak, M., Khaddage, A., Ayoub, E. N., Chahine, G., and Hilal, G. (2018). Different TP53 mutants in p53 overexpressed epithelial ovarian carcinoma can be associated both with altered and unaltered glycolytic and apoptotic profiles. Cancer cell international *18*, 14.
13. Arts, H. J., Katsaros, D., de Vries, E. G., Massobrio, M., Genta, F., Danese, S., Arisio, R., Scheper, R. J., Kool, M., Scheffer, G. L., *et al.* (1999). Drug resistance-associated markers P-glycoprotein, multidrug resistance-associated protein 1, multidrug resistance-associated protein 2, and lung resistance protein as prognostic factors in ovarian carcinoma. Clinical cancer research : an official journal of the American Association for Cancer Research *5*, 2798-2805.
14. Ashcroft, M., Taya, Y., and Vousden, K. H. (2000). Stress signals utilize multiple pathways to stabilize p53. Molecular and cellular biology *20*, 3224-3233.

15. Assaily, W., and Benchimol, S. (2006). Differential utilization of two ATP-generating pathways is regulated by p53. Cancer cell *10*, 4-6.
16. Atlas, C., Aad, G., Abbott, B., Abdallah, J., Abdinov, O., Aben, R., Abolins, M., AbouZeid, O. S., Abramowicz, H., Abreu, H., *et al.* (2016). Search for direct top squark pair production in final states with two tau leptons in pp collisions at [Formula: see text] TeV with the ATLAS detector. The European physical journal C, Particles and fields *76*, 81.
17. Banin, S., Moyal, L., Shieh, S., Taya, Y., Anderson, C. W., Chessa, L., Smorodinsky, N. I., Prives, C., Reiss, Y., Shiloh, Y., and Ziv, Y. (1998). Enhanced phosphorylation of p53 by ATM in response to DNA damage. Science *281*, 1674-1677.
18. Banno, K., Kisu, I., Yanokura, M., Masuda, K., Ueki, A., Kobayashi, Y., Hirasawa, A., and Aoki, D. (2013). Hereditary gynecological tumors associated with Peutz-Jeghers syndrome (Review). Oncology letters *6*, 1184-1188.
19. Barthel, A., Okino, S. T., Liao, J., Nakatani, K., Li, J., Whitlock, J. P., Jr., and Roth, R. A. (1999). Regulation of GLUT1 gene transcription by the serine/threonine kinase Akt1. The Journal of biological chemistry *274*, 20281-20286.
20. Beaufort, C. M., Helmijr, J. C., Piskorz, A. M., Hoogstraat, M., Ruigrok-Ritstier, K., Besselink, N., Murtaza, M., van, I. W. F., Heine, A. A., Smid, M., *et al.* (2014). Ovarian cancer cell line panel (OCCP): clinical importance of in vitro morphological subtypes. PloS one *9*, e103988.
21. Bell, D. A. (2005). Origins and molecular pathology of ovarian cancer. Modern pathology : an official journal of the United States and Canadian Academy of Pathology, Inc *18 Suppl 2*, S19-32.
22. Bellacosa, A., de Feo, D., Godwin, A. K., Bell, D. W., Cheng, J. Q., Altomare, D. A., Wan, M., Dubeau, L., Scambia, G., Masciullo, V., *et al.* (1995). Molecular alterations of the AKT2 oncogene in ovarian and breast carcinomas. International journal of cancer *64*, 280-285.
23. Benedet, J. L., Bender, H., Jones, H., 3rd, Ngan, H. Y., and Pecorelli, S. (2000). FIGO staging classifications and clinical practice guidelines in the management of gynecologic cancers. FIGO Committee on Gynecologic Oncology. International journal of gynaecology and obstetrics: the official organ of the International Federation of Gynaecology and Obstetrics *70*, 209-262.
24. Berkers, C. R., Maddocks, O. D., Cheung, E. C., Mor, I., and Vousden, K. H. (2013). Metabolic regulation by p53 family members. Cell metabolism *18*, 617-633.
25. Berridge, M. J., Lipp, P., and Bootman, M. D. (2000). The versatility and universality of calcium signalling. Nature reviews Molecular cell biology *1*, 11-21.
26. Borst, P., Evers, R., Kool, M., and Wijnholds, J. (2000). A family of drug transporters: the multidrug resistance-associated proteins. Journal of the National Cancer Institute *92*, 1295-1302.
27. Breckenridge, D. G., Germain, M., Mathai, J. P., Nguyen, M., and Shore, G. C. (2003). Regulation of apoptosis by endoplasmic reticulum pathways. Oncogene *22*, 8608-8618.
28. Bryson, J. M., Coy, P. E., Gottlob, K., Hay, N., and Robey, R. B. (2002). Increased hexokinase activity, of either ectopic or endogenous origin, protects renal epithelial cells against acute oxidant-induced cell death. The Journal of biological chemistry *277*, 11392-11400.
29. Canada, O. C. (2014). Supporting awareness and research. In, (Ovarian Cancer Canada).
30. CanadianCancerSociety (2017). Canadian Cancer Statistics Publication. In, (Toronto, Ontario: Canadian Cancer Society).
31. Cannistra SA, G. D., Recht A. (2015). Cancer: Principles and Practice of Oncology. (10th Edition), Vol 76, 10 edn (Philadelphia, PA, USA: Lippincott Williams & Wilkins).

32. Cardone, M. H., Roy, N., Stennicke, H. R., Salvesen, G. S., Franke, T. F., Stanbridge, E., Frisch, S., and Reed, J. C. (1998). Regulation of cell death protease caspase-9 by phosphorylation. Science *282*, 1318-1321.
33. Catanzaro, D., Gaude, E., Orso, G., Giordano, C., Guzzo, G., Rasola, A., Ragazzi, E., Caparrotta, L., Frezza, C., and Montopoli, M. (2015). Inhibition of glucose-6-phosphate dehydrogenase sensitizes cisplatin-resistant cells to death. Oncotarget *6*, 30102-30114.
34. Cepeda, V., Fuertes, M. A., Castilla, J., Alonso, C., Quevedo, C., and Perez, J. M. (2007). Biochemical mechanisms of cisplatin cytotoxicity. Anticancer Agents Med Chem *7*, 3-18.
35. Chan, F. K., Chun, H. J., Zheng, L., Siegel, R. M., Bui, K. L., and Lenardo, M. J. (2000). A domain in TNF receptors that mediates ligand-independent receptor assembly and signaling. Science *288*, 2351-2354.
36. Chang, S. J., and Bristow, R. E. (2012). Evolution of surgical treatment paradigms for advanced-stage ovarian cancer: redefining 'optimal' residual disease. Gynecologic oncology *125*, 483-492.
37. Cheaib, B., Auguste, A., and Leary, A. (2015). The PI3K/Akt/mTOR pathway in ovarian cancer: therapeutic opportunities and challenges. Chinese journal of cancer *34*, 4-16.
38. Chen, C., Pore, N., Behrooz, A., Ismail-Beigi, F., and Maity, A. (2001). Regulation of glut1 mRNA by hypoxia-inducible factor-1. Interaction between H-ras and hypoxia. The Journal of biological chemistry *276*, 9519-9525.
39. Chen, L., Ahmad, N., and Liu, X. (2016). Combining p53 stabilizers with metformin induces synergistic apoptosis through regulation of energy metabolism in castration-resistant prostate cancer. Cell cycle *15*, 840-849.
40. Chen, Z., Zhang, H., Lu, W., and Huang, P. (2009). Role of mitochondria-associated hexokinase II in cancer cell death induced by 3-bromopyruvate. Biochimica et biophysica acta *1787*, 553-560.
41. Cheng, J. Q., Jiang, X., Fraser, M., Li, M., Dan, H. C., Sun, M., and Tsang, B. K. (2002). Role of X-linked inhibitor of apoptosis protein in chemoresistance in ovarian cancer: possible involvement of the phosphoinositide-3 kinase/Akt pathway. Drug resistance updates : reviews and commentaries in antimicrobial and anticancer chemotherapy *5*, 131-146.
42. Cheung, E. C., Ludwig, R. L., and Vousden, K. H. (2012). Mitochondrial localization of TIGAR under hypoxia stimulates HK2 and lowers ROS and cell death. Proceedings of the National Academy of Sciences of the United States of America *109*, 20491-20496.
43. Cheung, E. C., and Vousden, K. H. (2010). The role of p53 in glucose metabolism. Current opinion in cell biology *22*, 186-191.
44. Chris M.J. Conklin, C. B. G. (2013). Differential diagnosis and clinical relevance of ovarian carcinoma subtypes. Expert Review of Obstetrics and Gynecology *8*, 67-82.
45. Christofk, H. R., Vander Heiden, M. G., Harris, M. H., Ramanathan, A., Gerszten, R. E., Wei, R., Fleming, M. D., Schreiber, S. L., and Cantley, L. C. (2008). The M2 splice isoform of pyruvate kinase is important for cancer metabolism and tumour growth. Nature *452*, 230-233.
46. Clem, B. F., O'Neal, J., Tapolsky, G., Clem, A. L., Imbert-Fernandez, Y., Kerr, D. A., 2nd, Klarer, A. C., Redman, R., Miller, D. M., Trent, J. O., *et al.* (2013). Targeting 6-phosphofructo-2-kinase (PFKFB3) as a therapeutic strategy against cancer. Molecular cancer therapeutics *12*, 1461-1470.
47. Cook, L. S., Pestak, C. R., Leung, A. C., Steed, H., Nation, J., Swenerton, K., Gallagher, R., Magliocco, A., Kobel, M., Brooks-Wilson, A., and Le, N. (2017). Combined oral contraceptive use before the first birth and epithelial ovarian cancer risk. British journal of cancer *116*, 265-269.
48. Cools, M., Wolffenbuttel, K. P., Drop, S. L., Oosterhuis, J. W., and Looijenga, L. H. (2011). Gonadal development and tumor formation at the crossroads of male and female sex

determination. Sexual development : genetics, molecular biology, evolution, endocrinology, embryology, and pathology of sex determination and differentiation *5*, 167-180.
49. Corona, J. C., Gimenez-Cassina, A., Lim, F., and Diaz-Nido, J. (2010). Hexokinase II gene transfer protects against neurodegeneration in the rotenone and MPTP mouse models of Parkinson's disease. Journal of neuroscience research *88*, 1943-1950.
50. Covens, A., Carey, M., Bryson, P., Verma, S., Fung Kee Fung, M., and Johnston, M. (2002). Systematic review of first-line chemotherapy for newly diagnosed postoperative patients with stage II, III, or IV epithelial ovarian cancer. Gynecologic oncology *85*, 71-80.
51. Croce, C. M. (2008). Oncogenes and cancer. The New England journal of medicine *358*, 502-511.
52. Crul, M., van Waardenburg, R. C., Beijnen, J. H., and Schellens, J. H. (2002). DNA-based drug interactions of cisplatin. Cancer treatment reviews *28*, 291-303.
53. Dabholkar, M., Bostick-Bruton, F., Weber, C., Bohr, V. A., Egwuagu, C., and Reed, E. (1992). ERCC1 and ERCC2 expression in malignant tissues from ovarian cancer patients. Journal of the National Cancer Institute *84*, 1512-1517.
54. Dang, C. V. (2012). Links between metabolism and cancer. Genes & development *26*, 877-890.
55. Danial, N. N., and Korsmeyer, S. J. (2004). Cell death: critical control points. Cell *116*, 205-219.
56. Datta, S. R., Dudek, H., Tao, X., Masters, S., Fu, H., Gotoh, Y., and Greenberg, M. E. (1997). Akt phosphorylation of BAD couples survival signals to the cell-intrinsic death machinery. Cell *91*, 231-241.
57. De Lena, M., Lorusso, V., Latorre, A., Fanizza, G., Gargano, G., Caporusso, L., Guida, M., Catino, A., Crucitta, E., Sambiasi, D., and Mazzei, A. (2001). Paclitaxel, cisplatin and lonidamine in advanced ovarian cancer. A phase II study. European journal of cancer *37*, 364-368.
58. Denault, J. B., and Boatright, K. (2004). Apoptosis in Biochemistry and Structural Biology. 3-8 February 2004, Keystone, CO, USA. IDrugs *7*, 315-317.
59. DeWaal, D., Nogueira, V., Terry, A. R., Patra, K. C., Jeon, S. M., Guzman, G., Au, J., Long, C. P., Antoniewicz, M. R., and Hay, N. (2018). Hexokinase-2 depletion inhibits glycolysis and induces oxidative phosphorylation in hepatocellular carcinoma and sensitizes to metformin. Nature communications *9*, 446.
60. Di Tucci, C., Casorelli, A., Morrocchi, E., Palaia, I., Muzii, L., and Panici, P. B. (2017). Fertility management for malignant ovarian germ cell tumors patients. Critical reviews in oncology/hematology *120*, 34-42.
61. Dubeau, L. (2008). The cell of origin of ovarian epithelial tumours. The Lancet Oncology *9*, 1191-1197.
62. Dwarakanath, B. S., Singh, D., Banerji, A. K., Sarin, R., Venkataramana, N. K., Jalali, R., Vishwanath, P. N., Mohanti, B. K., Tripathi, R. P., Kalia, V. K., and Jain, V. (2009). Clinical studies for improving radiotherapy with 2-deoxy-D-glucose: present status and future prospects. Journal of cancer research and therapeutics *5 Suppl 1*, S21-26.
63. Ebell, M. H., Culp, M. B., and Radke, T. J. (2016). A Systematic Review of Symptoms for the Diagnosis of Ovarian Cancer. American journal of preventive medicine *50*, 384-394.
64. Edwards, S. L., Brough, R., Lord, C. J., Natrajan, R., Vatcheva, R., Levine, D. A., Boyd, J., Reis-Filho, J. S., and Ashworth, A. (2008). Resistance to therapy caused by intragenic deletion in BRCA2. Nature *451*, 1111-1115.
65. Ehmann, F., Caneva, L., and Papaluca, M. (2014). European Medicines Agency initiatives and perspectives on pharmacogenomics. British journal of clinical pharmacology *77*, 612-617.

66. Eilers, M., and Eisenman, R. N. (2008). Myc's broad reach. Genes & development *22*, 2755-2766.
67. Elmore, S. (2007). Apoptosis: a review of programmed cell death. Toxicol Pathol *35*, 495-516.
68. Enomoto, T., Weghorst, C. M., Inoue, M., Tanizawa, O., and Rice, J. M. (1991). K-ras activation occurs frequently in mucinous adenocarcinomas and rarely in other common epithelial tumors of the human ovary. The American journal of pathology *139*, 777-785.
69. Erster, S., Mihara, M., Kim, R. H., Petrenko, O., and Moll, U. M. (2004). In vivo mitochondrial p53 translocation triggers a rapid first wave of cell death in response to DNA damage that can precede p53 target gene activation. Molecular and cellular biology *24*, 6728-6741.
70. Farrand, L., Byun, S., Kim, J. Y., Im-Aram, A., Lee, J., Lim, S., Lee, K. W., Suh, J. Y., Lee, H. J., and Tsang, B. K. (2013). Piceatannol enhances cisplatin sensitivity in ovarian cancer via modulation of p53, X-linked inhibitor of apoptosis protein (XIAP), and mitochondrial fission. The Journal of biological chemistry *288*, 23740-23750.
71. Farrand, L., Kim, J. Y., Byun, S., Im-aram, A., Lee, J., Suh, J. Y., Lee, K. W., Lee, H. J., and Tsang, B. K. (2014). The diarylheptanoid hirsutenone sensitizes chemoresistant ovarian cancer cells to cisplatin via modulation of apoptosis-inducing factor and X-linked inhibitor of apoptosis. The Journal of biological chemistry *289*, 1723-1731.
72. Foran, P. G., Fletcher, L. M., Oatey, P. B., Mohammed, N., Dolly, J. O., and Tavare, J. M. (1999). Protein kinase B stimulates the translocation of GLUT4 but not GLUT1 or transferrin receptors in 3T3-L1 adipocytes by a pathway involving SNAP-23, synaptobrevin-2, and/or cellubrevin. The Journal of biological chemistry *274*, 28087-28095.
73. Franke, T. F., Kaplan, D. R., Cantley, L. C., and Toker, A. (1997). Direct regulation of the Akt proto-oncogene product by phosphatidylinositol-3,4-bisphosphate. Science *275*, 665-668.
74. Fraser, M., Bai, T., and Tsang, B. K. (2008). Akt promotes cisplatin resistance in human ovarian cancer cells through inhibition of p53 phosphorylation and nuclear function. Int J Cancer *122*, 534-546.
75. Fraser, M., Leung, B., Jahani-Asl, A., Yan, X., Thompson, W. E., and Tsang, B. K. (2003). Chemoresistance in human ovarian cancer: the role of apoptotic regulators. Reproductive biology and endocrinology : RB&E *1*, 66.
76. Frezza, C., Cipolat, S., Martins de Brito, O., Micaroni, M., Beznoussenko, G. V., Rudka, T., Bartoli, D., Polishuck, R. S., Danial, N. N., De Strooper, B., and Scorrano, L. (2006). OPA1 controls apoptotic cristae remodeling independently from mitochondrial fusion. Cell *126*, 177-189.
77. Gallion, H., Christopherson, W. A., Coleman, R. L., DeMars, L., Herzog, T., Hosford, S., Schellhas, H., Wells, A., and Sevin, B. U. (2006). Progression-free interval in ovarian cancer and predictive value of an ex vivo chemoresponse assay. International journal of gynecological cancer : official journal of the International Gynecological Cancer Society *16*, 194-201.
78. Galluzzi, L., Kepp, O., Vander Heiden, M. G., and Kroemer, G. (2013). Metabolic targets for cancer therapy. Nature reviews Drug discovery *12*, 829-846.
79. Galluzzi, L., Senovilla, L., Vitale, I., Michels, J., Martins, I., Kepp, O., Castedo, M., and Kroemer, G. (2012a). Molecular mechanisms of cisplatin resistance. Oncogene *31*, 1869-1883.
80. Galluzzi, L., Vitale, I., Abrams, J. M., Alnemri, E. S., Baehrecke, E. H., Blagosklonny, M. V., Dawson, T. M., Dawson, V. L., El-Deiry, W. S., Fulda, S., *et al.* (2012b). Molecular definitions of cell death subroutines: recommendations of the Nomenclature Committee on Cell Death 2012. Cell death and differentiation *19*, 107-120.

81. Gasparri, M. L., Bardhi, E., Ruscito, I., Papadia, A., Farooqi, A. A., Marchetti, C., Bogani, G., Ceccacci, I., Mueller, M. D., and Benedetti Panici, P. (2017). PI3K/AKT/mTOR Pathway in Ovarian Cancer Treatment: Are We on the Right Track? Geburtshilfe und Frauenheilkunde *77*, 1095-1103.
82. Gatenby, R. A., Gawlinski, E. T., Gmitro, A. F., Kaylor, B., and Gillies, R. J. (2006). Acid-mediated tumor invasion: a multidisciplinary study. Cancer research *66*, 5216-5223.
83. Gatenby, R. A., and Gillies, R. J. (2004). Why do cancers have high aerobic glycolysis? Nature reviews Cancer *4*, 891-899.
84. Godwin, A. K., Meister, A., O'Dwyer, P. J., Huang, C. S., Hamilton, T. C., and Anderson, M. E. (1992). High resistance to cisplatin in human ovarian cancer cell lines is associated with marked increase of glutathione synthesis. Proceedings of the National Academy of Sciences of the United States of America *89*, 3070-3074.
85. Gogvadze, V., Orrenius, S., and Zhivotovsky, B. (2006). Multiple pathways of cytochrome c release from mitochondria in apoptosis. Biochimica et biophysica acta *1757*, 639-647.
86. Gogvadze, V., Orrenius, S., and Zhivotovsky, B. (2008). Mitochondria in cancer cells: what is so special about them? Trends in cell biology *18*, 165-173.
87. Goldin, N., Arzoine, L., Heyfets, A., Israelson, A., Zaslavsky, Z., Bravman, T., Bronner, V., Notcovich, A., Shoshan-Barmatz, V., and Flescher, E. (2008). Methyl jasmonate binds to and detaches mitochondria-bound hexokinase. Oncogene *27*, 4636-4643.
88. Gorman, A. M., McGowan, A., O'Neill, C., and Cotter, T. (1996). Oxidative stress and apoptosis in neurodegeneration. J Neurol Sci *139 Suppl*, 45-52.
89. Gottlob, K., Majewski, N., Kennedy, S., Kandel, E., Robey, R. B., and Hay, N. (2001). Inhibition of early apoptotic events by Akt/PKB is dependent on the first committed step of glycolysis and mitochondrial hexokinase. Genes & development *15*, 1406-1418.
90. Griss, T., Vincent, E. E., Egnatchik, R., Chen, J., Ma, E. H., Faubert, B., Viollet, B., DeBerardinis, R. J., and Jones, R. G. (2015). Metformin Antagonizes Cancer Cell Proliferation by Suppressing Mitochondrial-Dependent Biosynthesis. PLoS biology *13*, e1002309.
91. Gross, A., McDonnell, J. M., and Korsmeyer, S. J. (1999). BCL-2 family members and the mitochondria in apoptosis. Genes & development *13*, 1899-1911.
92. Guo, C., Ludvik, A. E., Arlotto, M. E., Hayes, M. G., Armstrong, L. L., Scholtens, D. M., Brown, C. D., Newgard, C. B., Becker, T. C., Layden, B. T., *et al.* (2015). Coordinated regulatory variation associated with gestational hyperglycaemia regulates expression of the novel hexokinase HKDC1. Nature communications *6*, 6069.
93. Gwak, H., Kim, Y., An, H., Dhanasekaran, D. N., and Song, Y. S. (2017). Metformin induces degradation of cyclin D1 via AMPK/GSK3beta axis in ovarian cancer. Molecular carcinogenesis *56*, 349-358.
94. Ha, J. H., Radhakrishnan, R., Jayaraman, M., Yan, M., Ward, J. D., Fung, K. M., Moxley, K., Sood, A. K., Isidoro, C., Mukherjee, P., *et al.* (2018). LPA Induces Metabolic Reprogramming in Ovarian Cancer via a Pseudohypoxic Response. Cancer research *78*, 1923-1934.
95. Hanrahan, A. J., Schultz, N., Westfal, M. L., Sakr, R. A., Giri, D. D., Scarperi, S., Janakiraman, M., Olvera, N., Stevens, E. V., She, Q. B., *et al.* (2012). Genomic complexity and AKT dependence in serous ovarian cancer. Cancer discovery *2*, 56-67.
96. Harris, M. H., and Thompson, C. B. (2000). The role of the Bcl-2 family in the regulation of outer mitochondrial membrane permeability. Cell death and differentiation *7*, 1182-1191.
97. Hay, N. (2005). The Akt-mTOR tango and its relevance to cancer. Cancer cell *8*, 179-183.
98. Hay, N. (2016). Reprogramming glucose metabolism in cancer: can it be exploited for cancer therapy? Nature reviews Cancer *16*, 635-649.
99. Health, N. I. o. (2018). Clinical trial of metformin in ovarian cancer In, (8600 Rockville Pike, Bethesda, MD 20894 U.S. National Library of Medicine,).

100. Hennessy, B. T., Coleman, R. L., and Markman, M. (2009). Ovarian cancer. Lancet *374*, 1371-1382.
101. Ho, G. Y., Woodward, N., and Coward, J. I. (2016). Cisplatin versus carboplatin: comparative review of therapeutic management in solid malignancies. Critical reviews in oncology/hematology *102*, 37-46.
102. Horta, M., and Cunha, T. M. (2015). Sex cord-stromal tumors of the ovary: a comprehensive review and update for radiologists. Diagnostic and interventional radiology *21*, 277-286.
103. Hu, J., Lieb, J. D., Sancar, A., and Adar, S. (2016). Cisplatin DNA damage and repair maps of the human genome at single-nucleotide resolution. Proceedings of the National Academy of Sciences of the United States of America *113*, 11507-11512.
104. Hutchinson, L., and Kirk, R. (2011). High drug attrition rates--where are we going wrong? Nature reviews Clinical oncology *8*, 189-190.
105. Iida, Y., Aoki, K., Asakura, T., Ueda, K., Yanaihara, N., Takakura, S., Yamada, K., Okamoto, A., Tanaka, T., and Ohkawa, K. (2012). Hypoxia promotes glycogen synthesis and accumulation in human ovarian clear cell carcinoma. International journal of oncology *40*, 2122-2130.
106. Ischenko, I., Zhi, J., Moll, U. M., Nemajerova, A., and Petrenko, O. (2013). Direct reprogramming by oncogenic Ras and Myc. Proceedings of the National Academy of Sciences of the United States of America *110*, 3937-3942.
107. Ishida, S., Lee, J., Thiele, D. J., and Herskowitz, I. (2002). Uptake of the anticancer drug cisplatin mediated by the copper transporter Ctr1 in yeast and mammals. Proceedings of the National Academy of Sciences of the United States of America *99*, 14298-14302.
108. Ivan, M., Haberberger, T., Gervasi, D. C., Michelson, K. S., Gunzler, V., Kondo, K., Yang, H., Sorokina, I., Conaway, R. C., Conaway, J. W., and Kaelin, W. G., Jr. (2002). Biochemical purification and pharmacological inhibition of a mammalian prolyl hydroxylase acting on hypoxia-inducible factor. Proceedings of the National Academy of Sciences of the United States of America *99*, 13459-13464.
109. Jackson, J. R., Gilmartin, A., Imburgia, C., Winkler, J. D., Marshall, L. A., and Roshak, A. (2000). An indolocarbazole inhibitor of human checkpoint kinase (Chk1) abrogates cell cycle arrest caused by DNA damage. Cancer research *60*, 566-572.
110. Jae, H. J., Chung, J. W., Park, H. S., Lee, M. J., Lee, K. C., Kim, H. C., Yoon, J. H., Chung, H., and Park, J. H. (2009). The antitumor effect and hepatotoxicity of a hexokinase II inhibitor 3-bromopyruvate: in vivo investigation of intraarterial administration in a rabbit VX2 hepatoma model. Korean journal of radiology *10*, 596-603.
111. Jamieson, E. R., and Lippard, S. J. (1999). Structure, Recognition, and Processing of Cisplatin-DNA Adducts. Chemical reviews *99*, 2467-2498.
112. Jekunen, A. P., Hom, D. K., Alcaraz, J. E., Eastman, A., and Howell, S. B. (1994). Cellular pharmacology of dichloro(ethylenediamine)platinum(II) in cisplatin-sensitive and resistant human ovarian carcinoma cells. Cancer research *54*, 2680-2687.
113. Jin, Z., and El-Deiry, W. S. (2005). Overview of cell death signaling pathways. Cancer biology & therapy *4*, 139-163.
114. Kabir, F., and Wilson, J. E. (1994). Mitochondrial hexokinase in brain: coexistence of forms differing in sensitivity to solubilization by glucose-6-phosphate on the same mitochondria. Archives of biochemistry and biophysics *310*, 410-416.
115. Kaldawy, A., Segev, Y., Lavie, O., Auslender, R., Sopik, V., and Narod, S. A. (2016). Low-grade serous ovarian cancer: A review. Gynecologic oncology *143*, 433-438.
116. Kale, J., Osterlund, E. J., and Andrews, D. W. (2018). BCL-2 family proteins: changing partners in the dance towards death. Cell death and differentiation *25*, 65-80.
117. Karaca, B., Atmaca, H., Bozkurt, E., Kisim, A., Uzunoglu, S., Karabulut, B., Sezgin, C., Sanli, U. A., and Uslu, R. (2013). Combination of AT-101/cisplatin overcomes

chemoresistance by inducing apoptosis and modulating epigenetics in human ovarian cancer cells. Molecular biology reports *40*, 3925-3933.
118. Kasznicki, J., Sliwinska, A., and Drzewoski, J. (2014). Metformin in cancer prevention and therapy. Annals of translational medicine *2*, 57.
119. Kelland, L. R. (2000a). A new resistance mechanism to cisplatin? Drug resistance updates : reviews and commentaries in antimicrobial and anticancer chemotherapy *3*, 139-141.
120. Kelland, L. R. (2000b). Preclinical perspectives on platinum resistance. Drugs *59 Suppl 4*, 1-8; discussion 37-38.
121. Kerr, J. F., Wyllie, A. H., and Currie, A. R. (1972). Apoptosis: a basic biological phenomenon with wide-ranging implications in tissue kinetics. British journal of cancer *26*, 239-257.
122. Kim, J. W., and Dang, C. V. (2006). Cancer's molecular sweet tooth and the Warburg effect. Cancer research *66*, 8927-8930.
123. Kim, J. W., Gao, P., Liu, Y. C., Semenza, G. L., and Dang, C. V. (2007). Hypoxia-inducible factor 1 and dysregulated c-Myc cooperatively induce vascular endothelial growth factor and metabolic switches hexokinase 2 and pyruvate dehydrogenase kinase 1. Molecular and cellular biology *27*, 7381-7393.
124. Kim, J. W., Tchernyshyov, I., Semenza, G. L., and Dang, C. V. (2006). HIF-1-mediated expression of pyruvate dehydrogenase kinase: a metabolic switch required for cellular adaptation to hypoxia. Cell metabolism *3*, 177-185.
125. Kong, B., Wang, Q., Fung, E., Xue, K., and Tsang, B. K. (2014). p53 Is Required for Cisplatin-induced Processing of the Mitochondrial Fusion Protein L-Opa1 That Is Mediated by the Mitochondrial Metallopeptidase Oma1 in Gynecologic Cancers. The Journal of biological chemistry *289*, 27134-27145.
126. Kosic, M., Arsikin-Csordas, K., Paunovic, V., Firestone, R. A., Ristic, B., Mircic, A., Petricevic, S., Bosnjak, M., Zogovic, N., Mandic, M., *et al.* (2016). Synergistic Anticancer Action of Lysosomal Membrane Permeabilization and Glycolysis Inhibition. The Journal of biological chemistry *291*, 22936-22948.
127. Kotani, K., Carozzi, A. J., Sakaue, H., Hara, K., Robinson, L. J., Clark, S. F., Yonezawa, K., James, D. E., and Kasuga, M. (1995). Requirement for phosphoinositide 3-kinase in insulin-stimulated GLUT4 translocation in 3T3-L1 adipocytes. Biochemical and biophysical research communications *209*, 343-348.
128. Krasnov, G. S., Dmitriev, A. A., Lakunina, V. A., Kirpiy, A. A., and Kudryavtseva, A. V. (2013). Targeting VDAC-bound hexokinase II: a promising approach for concomitant anti-cancer therapy. Expert opinion on therapeutic targets *17*, 1221-1233.
129. Kumar, K., Wigfield, S., Gee, H. E., Devlin, C. M., Singleton, D., Li, J. L., Buffa, F., Huffman, M., Sinn, A. L., Silver, J., *et al.* (2013). Dichloroacetate reverses the hypoxic adaptation to bevacizumab and enhances its antitumor effects in mouse xenografts. Journal of molecular medicine *91*, 749-758.
130. Kurman, R. J., and Shih Ie, M. (2008). Pathogenesis of ovarian cancer: lessons from morphology and molecular biology and their clinical implications. International journal of gynecological pathology : official journal of the International Society of Gynecological Pathologists *27*, 151-160.
131. Kurman, R. J., and Shih Ie, M. (2010). The origin and pathogenesis of epithelial ovarian cancer: a proposed unifying theory. The American journal of surgical pathology *34*, 433-443.
132. Kurman, R. J., and Shih Ie, M. (2011). Molecular pathogenesis and extraovarian origin of epithelial ovarian cancer--shifting the paradigm. Human pathology *42*, 918-931.
133. Lambert, P. F., Kashanchi, F., Radonovich, M. F., Shiekhattar, R., and Brady, J. N. (1998). Phosphorylation of p53 serine 15 increases interaction with CBP. The Journal of biological chemistry *273*, 33048-33053.

134. Landau, B. R., Laszlo, J., Stengle, J., and Burk, D. (1958). Certain metabolic and pharmacologic effects in cancer patients given infusions of 2-deoxy-D-glucose. Journal of the National Cancer Institute *21*, 485-494.
135. Lawrenson, K., Sproul, D., Grun, B., Notaridou, M., Benjamin, E., Jacobs, I. J., Dafou, D., Sims, A. H., and Gayther, S. A. (2011). Modelling genetic and clinical heterogeneity in epithelial ovarian cancers. Carcinogenesis *32*, 1540-1549.
136. Lee, C., and Longo, V. D. (2011). Fasting vs dietary restriction in cellular protection and cancer treatment: from model organisms to patients. Oncogene *30*, 3305-3316.
137. Lee, C., Raffaghello, L., Brandhorst, S., Safdie, F. M., Bianchi, G., Martin-Montalvo, A., Pistoia, V., Wei, M., Hwang, S., Merlino, A., *et al.* (2012). Fasting cycles retard growth of tumors and sensitize a range of cancer cell types to chemotherapy. Science translational medicine *4*, 124ra127.
138. Lee, Y. Y., Choi, C. H., Do, I. G., Song, S. Y., Lee, W., Park, H. S., Song, T. J., Kim, M. K., Kim, T. J., Lee, J. W., *et al.* (2011). Prognostic value of the copper transporters, CTR1 and CTR2, in patients with ovarian carcinoma receiving platinum-based chemotherapy. Gynecologic oncology *122*, 361-365.
139. Leroy, B., Girard, L., Hollestelle, A., Minna, J. D., Gazdar, A. F., and Soussi, T. (2014). Analysis of TP53 mutation status in human cancer cell lines: a reassessment. Human mutation *35*, 756-765.
140. Li, B., Li, X., Ni, Z., Zhang, Y., Zeng, Y., Yan, X., Huang, Y., He, J., Lyu, X., Wu, Y., *et al.* (2016). Dichloroacetate and metformin synergistically suppress the growth of ovarian cancer cells. Oncotarget *7*, 59458-59470.
141. Li, J., Chen, K., Wang, F., Dai, W., Li, S., Feng, J., Wu, L., Liu, T., Xu, S., Xia, Y., *et al.* (2017a). Methyl jasmonate leads to necrosis and apoptosis in hepatocellular carcinoma cells via inhibition of glycolysis and represses tumor growth in mice. Oncotarget *8*, 45965-45980.
142. Li, J., Condello, S., Thomes-Pepin, J., Ma, X., Xia, Y., Hurley, T. D., Matei, D., and Cheng, J. X. (2017b). Lipid Desaturation Is a Metabolic Marker and Therapeutic Target of Ovarian Cancer Stem Cells. Cell stem cell *20*, 303-314 e305.
143. Li, Q., Gardner, K., Zhang, L., Tsang, B., Bostick-Bruton, F., and Reed, E. (1998). Cisplatin induction of ERCC-1 mRNA expression in A2780/CP70 human ovarian cancer cells. The Journal of biological chemistry *273*, 23419-23425.
144. Liefke, R., Oswald, F., Alvarado, C., Ferres-Marco, D., Mittler, G., Rodriguez, P., Dominguez, M., and Borggrefe, T. (2010). Histone demethylase KDM5A is an integral part of the core Notch-RBP-J repressor complex. Genes & development *24*, 590-601.
145. Lim, J. J., Han, C. Y., Lee, D. R., and Tsang, B. K. (2017). Ring Finger Protein 6 Mediates Androgen-Induced Granulosa Cell Proliferation and Follicle Growth via Modulation of Androgen Receptor Signaling. Endocrinology *158*, 993-1004.
146. Lin, M. Z., Marzec, K. A., Martin, J. L., and Baxter, R. C. (2014). The role of insulin-like growth factor binding protein-3 in the breast cancer cell response to DNA-damaging agents. Oncogene *33*, 85-96.
147. Liu, H., Kurtoglu, M., Leon-Annicchiarico, C. L., Munoz-Pinedo, C., Barredo, J., Leclerc, G., Merchan, J., Liu, X., and Lampidis, T. J. (2016). Combining 2-deoxy-D-glucose with fenofibrate leads to tumor cell death mediated by simultaneous induction of energy and ER stress. Oncotarget *7*, 36461-36473.
148. Liu, J. F., Palakurthi, S., Zeng, Q., Zhou, S., Ivanova, E., Huang, W., Zervantonakis, I. K., Selfors, L. M., Shen, Y., Pritchard, C. C., *et al.* (2017). Establishment of Patient-Derived Tumor Xenograft Models of Epithelial Ovarian Cancer for Preclinical Evaluation of Novel Therapeutics. Clinical cancer research : an official journal of the American Association for Cancer Research *23*, 1263-1273.

149. Loughery, J., Cox, M., Smith, L. M., and Meek, D. W. (2014). Critical role for p53-serine 15 phosphorylation in stimulating transactivation at p53-responsive promoters. Nucleic acids research *42*, 7666-7680.
150. Lovejoy, K. S., Todd, R. C., Zhang, S., McCormick, M. S., D'Aquino, J. A., Reardon, J. T., Sancar, A., Giacomini, K. M., and Lippard, S. J. (2008). cis-Diammine(pyridine)chloroplatinum(II), a monofunctional platinum(II) antitumor agent: Uptake, structure, function, and prospects. Proceedings of the National Academy of Sciences of the United States of America *105*, 8902-8907.
151. Ma, Y., Yu, C., Mohamed, E. M., Shao, H., Wang, L., Sundaresan, G., Zweit, J., Idowu, M., and Fang, X. (2016). A causal link from ALK to hexokinase II overexpression and hyperactive glycolysis in EML4-ALK-positive lung cancer. Oncogene *35*, 6132-6142.
152. Macheda, M. L., Rogers, S., and Best, J. D. (2005). Molecular and cellular regulation of glucose transporter (GLUT) proteins in cancer. Journal of cellular physiology *202*, 654-662.
153. Majewski, N., Nogueira, V., Bhaskar, P., Coy, P. E., Skeen, J. E., Gottlob, K., Chandel, N. S., Thompson, C. B., Robey, R. B., and Hay, N. (2004a). Hexokinase-mitochondria interaction mediated by Akt is required to inhibit apoptosis in the presence or absence of Bax and Bak. Molecular cell *16*, 819-830.
154. Majewski, N., Nogueira, V., Robey, R. B., and Hay, N. (2004b). Akt inhibits apoptosis downstream of BID cleavage via a glucose-dependent mechanism involving mitochondrial hexokinases. Molecular and cellular biology *24*, 730-740.
155. Manning, B. D., and Toker, A. (2017). AKT/PKB Signaling: Navigating the Network. Cell *169*, 381-405.
156. Marabese, M., Marchini, S., Marrazzo, E., Mariani, P., Cattaneo, D., Fossati, R., Compagnoni, A., Signorelli, M., Moll, U. M., Codegoni, A. M., and Broggini, M. (2008). Expression levels of p53 and p73 isoforms in stage I and stage III ovarian cancer. European journal of cancer *44*, 131-141.
157. Marchenko, N. D., Zaika, A., and Moll, U. M. (2000). Death signal-induced localization of p53 protein to mitochondria. A potential role in apoptotic signaling. The Journal of biological chemistry *275*, 16202-16212.
158. Marini, C., Salani, B., Massollo, M., Amaro, A., Esposito, A. I., Orengo, A. M., Capitanio, S., Emionite, L., Riondato, M., Bottoni, G., *et al.* (2013). Direct inhibition of hexokinase activity by metformin at least partially impairs glucose metabolism and tumor growth in experimental breast cancer. Cell cycle *12*, 3490-3499.
159. Mathupala, S. P., Ko, Y. H., and Pedersen, P. L. (2006). Hexokinase II: cancer's double-edged sword acting as both facilitator and gatekeeper of malignancy when bound to mitochondria. Oncogene *25*, 4777-4786.
160. Mathupala, S. P., Rempel, A., and Pedersen, P. L. (2001). Glucose catabolism in cancer cells: identification and characterization of a marked activation response of the type II hexokinase gene to hypoxic conditions. The Journal of biological chemistry *276*, 43407-43412.
161. Matoba, S., Kang, J. G., Patino, W. D., Wragg, A., Boehm, M., Gavrilova, O., Hurley, P. J., Bunz, F., and Hwang, P. M. (2006). p53 regulates mitochondrial respiration. Science *312*, 1650-1653.
162. Matulonis, U. A., Oza, A. M., Ho, T. W., and Ledermann, J. A. (2015). Intermediate clinical endpoints: a bridge between progression-free survival and overall survival in ovarian cancer trials. Cancer *121*, 1737-1746.
163. Mayo, L. D., Dixon, J. E., Durden, D. L., Tonks, N. K., and Donner, D. B. (2002). PTEN protects p53 from Mdm2 and sensitizes cancer cells to chemotherapy. The Journal of biological chemistry *277*, 5484-5489.

164. Mayo, L. D., and Donner, D. B. (2001). A phosphatidylinositol 3-kinase/Akt pathway promotes translocation of Mdm2 from the cytoplasm to the nucleus. Proceedings of the National Academy of Sciences of the United States of America *98*, 11598-11603.
165. MayoClinic (2014). Disease and Conditions Ovarian Cancer. In.
166. McCluggage, W. G. (2011). Morphological subtypes of ovarian carcinoma: a review with emphasis on new developments and pathogenesis. Pathology *43*, 420-432.
167. McLaughlin, J. R., Risch, H. A., Lubinski, J., Moller, P., Ghadirian, P., Lynch, H., Karlan, B., Fishman, D., Rosen, B., Neuhausen, S. L., *et al.* (2007). Reproductive risk factors for ovarian cancer in carriers of BRCA1 or BRCA2 mutations: a case-control study. The Lancet Oncology *8*, 26-34.
168. Michelakis, E. D., Sutendra, G., Dromparis, P., Webster, L., Haromy, A., Niven, E., Maguire, C., Gammer, T. L., Mackey, J. R., Fulton, D., *et al.* (2010). Metabolic modulation of glioblastoma with dichloroacetate. Science translational medicine *2*, 31ra34.
169. Mihara, M., Erster, S., Zaika, A., Petrenko, O., Chittenden, T., Pancoska, P., and Moll, U. M. (2003). p53 has a direct apoptogenic role at the mitochondria. Molecular cell *11*, 577-590.
170. Miyamoto, S., Murphy, A. N., and Brown, J. H. (2008). Akt mediates mitochondrial protection in cardiomyocytes through phosphorylation of mitochondrial hexokinase-II. Cell death and differentiation *15*, 521-529.
171. Miyashita, T., and Reed, J. C. (1995). Tumor suppressor p53 is a direct transcriptional activator of the human bax gene. Cell *80*, 293-299.
172. Moggs, J. G., Szymkowski, D. E., Yamada, M., Karran, P., and Wood, R. D. (1997). Differential human nucleotide excision repair of paired and mispaired cisplatin-DNA adducts. Nucleic acids research *25*, 480-491.
173. Moll, U. M., Chumas, J. C., Chalas, E., and Mann, W. J. (1990). Ovarian carcinoma arising in atypical endometriosis. Obstet Gynecol *75*, 537-539.
174. Moll, U. M., Wolff, S., Speidel, D., and Deppert, W. (2005). Transcription-independent pro-apoptotic functions of p53. Current opinion in cell biology *17*, 631-636.
175. Myint, K., Li, Y., Paxton, J., and McKeage, M. (2015). Multidrug Resistance-Associated Protein 2 (MRP2) Mediated Transport of Oxaliplatin-Derived Platinum in Membrane Vesicles. PloS one *10*, e0130727.
176. Nakamura, K., Bossy-Wetzel, E., Burns, K., Fadel, M. P., Lozyk, M., Goping, I. S., Opas, M., Bleackley, R. C., Green, D. R., and Michalak, M. (2000). Changes in endoplasmic reticulum luminal environment affect cell sensitivity to apoptosis. The Journal of cell biology *150*, 731-740.
177. Nakano, K., and Vousden, K. H. (2001). PUMA, a novel proapoptotic gene, is induced by p53. Molecular cell *7*, 683-694.
178. Narod, S. A., and Foulkes, W. D. (2004). BRCA1 and BRCA2: 1994 and beyond. Nature reviews Cancer *4*, 665-676.
179. Narod, S. A., Risch, H., Moslehi, R., Dorum, A., Neuhausen, S., Olsson, H., Provencher, D., Radice, P., Evans, G., Bishop, S., *et al.* (1998). Oral contraceptives and the risk of hereditary ovarian cancer. Hereditary Ovarian Cancer Clinical Study Group. The New England journal of medicine *339*, 424-428.
180. Nath, K., Nelson, D. S., Heitjan, D. F., Leeper, D. B., Zhou, R., and Glickson, J. D. (2015). Lonidamine induces intracellular tumor acidification and ATP depletion in breast, prostate and ovarian cancer xenografts and potentiates response to doxorubicin. NMR in biomedicine *28*, 281-290.
181. Neary, C. L., and Pastorino, J. G. (2010). Nucleocytoplasmic shuttling of hexokinase II in a cancer cell. Biochemical and biophysical research communications *394*, 1075-1081.

182. Neary, C. L., and Pastorino, J. G. (2013). Akt inhibition promotes hexokinase 2 redistribution and glucose uptake in cancer cells. Journal of cellular physiology *228*, 1943-1948.
183. Niakan, B. (2010). Spontaneous remission of cancer: steady and aggressive malignant growth faced with hypoxia or hypoglycemia. Medical hypotheses *75*, 505-506.
184. Ogawara, Y., Kishishita, S., Obata, T., Isazawa, Y., Suzuki, T., Tanaka, K., Masuyama, N., and Gotoh, Y. (2002). Akt enhances Mdm2-mediated ubiquitination and degradation of p53. The Journal of biological chemistry *277*, 21843-21850.
185. Okuda, T., Otsuka, J., Sekizawa, A., Saito, H., Makino, R., Kushima, M., Farina, A., Kuwano, Y., and Okai, T. (2003). p53 mutations and overexpression affect prognosis of ovarian endometrioid cancer but not clear cell cancer. Gynecologic oncology *88*, 318-325.
186. Oncology, A. S. o. C. (2016, August). Ovarian, Fallopian Tube, and Peritoneal Cancer. In, (Georgia, Atlanta, USA: American Society of Clinical Oncology).
187. Osthus, R. C., Shim, H., Kim, S., Li, Q., Reddy, R., Mukherjee, M., Xu, Y., Wonsey, D., Lee, L. A., and Dang, C. V. (2000). Deregulation of glucose transporter 1 and glycolytic gene expression by c-Myc. The Journal of biological chemistry *275*, 21797-21800.
188. Ou, Y. H., Chung, P. H., Sun, T. P., and Shieh, S. Y. (2005). p53 C-terminal phosphorylation by CHK1 and CHK2 participates in the regulation of DNA-damage-induced C-terminal acetylation. Molecular biology of the cell *16*, 1684-1695.
189. Park, S. Y., Jeong, M. S., and Jang, S. B. (2012). In vitro binding properties of tumor suppressor p53 with PUMA and NOXA. Biochemical and biophysical research communications *420*, 350-356.
190. Pastorino, J. G., Shulga, N., and Hoek, J. B. (2002). Mitochondrial binding of hexokinase II inhibits Bax-induced cytochrome c release and apoptosis. The Journal of biological chemistry *277*, 7610-7618.
191. Patra, K. C., Wang, Q., Bhaskar, P. T., Miller, L., Wang, Z., Wheaton, W., Chandel, N., Laakso, M., Muller, W. J., Allen, E. L., *et al.* (2013). Hexokinase 2 is required for tumor initiation and maintenance and its systemic deletion is therapeutic in mouse models of cancer. Cancer cell *24*, 213-228.
192. Pedersen, P. L. (2007). Warburg, me and Hexokinase 2: Multiple discoveries of key molecular events underlying one of cancers' most common phenotypes, the "Warburg Effect", i.e., elevated glycolysis in the presence of oxygen. Journal of bioenergetics and biomembranes *39*, 211-222.
193. Peter, M. E., Dhein, J., Ehret, A., Hellbardt, S., Walczak, H., Moldenhauer, G., and Krammer, P. H. (1995). APO-1 (CD95)-dependent and -independent antigen receptor-induced apoptosis in human T and B cell lines. International immunology *7*, 1873-1877.
194. Pfeiffer, T., and Morley, A. (2014). An evolutionary perspective on the Crabtree effect. Frontiers in molecular biosciences *1*, 17.
195. Poff, A. M., Ari, C., Seyfried, T. N., and D'Agostino, D. P. (2013). The ketogenic diet and hyperbaric oxygen therapy prolong survival in mice with systemic metastatic cancer. PloS one *8*, e65522.
196. Polster, B. M., Basanez, G., Etxebarria, A., Hardwick, J. M., and Nicholls, D. G. (2005). Calpain I induces cleavage and release of apoptosis-inducing factor from isolated mitochondria. The Journal of biological chemistry *280*, 6447-6454.
197. Prat, J., and Oncology, F. C. o. G. (2015). FIGO's staging classification for cancer of the ovary, fallopian tube, and peritoneum: abridged republication. Journal of gynecologic oncology *26*, 87-89.
198. Rao, R. V., Ellerby, H. M., and Bredesen, D. E. (2004). Coupling endoplasmic reticulum stress to the cell death program. Cell death and differentiation *11*, 372-380.
199. Ren, S. X., Cheng, A. S., To, K. F., Tong, J. H., Li, M. S., Shen, J., Wong, C. C., Zhang, L., Chan, R. L., Wang, X. J., *et al.* (2012). Host immune defense peptide LL-37 activates

caspase-independent apoptosis and suppresses colon cancer. Cancer research *72*, 6512-6523.

200. Reyes-Gonzalez, J. M., Armaiz-Pena, G. N., Mangala, L. S., Valiyeva, F., Ivan, C., Pradeep, S., Echevarria-Vargas, I. M., Rivera-Reyes, A., Sood, A. K., and Vivas-Mejia, P. E. (2015). Targeting c-MYC in Platinum-Resistant Ovarian Cancer. Molecular cancer therapeutics *14*, 2260-2269.
201. Richardson, R. B. (2013). p53 mutations associated with aging-related rise in cancer incidence rates. Cell cycle *12*, 2468-2478.
202. Riley, T., Sontag, E., Chen, P., and Levine, A. (2008). Transcriptional control of human p53-regulated genes. Nature reviews Molecular cell biology *9*, 402-412.
203. Roberts, D. J., and Miyamoto, S. (2014). Hexokinase II integrates energy metabolism and cellular protection: Akting on mitochondria and TORCing to autophagy. Cell death and differentiation.
204. Roberts, D. J., Tan-Sah, V. P., Ding, E. Y., Smith, J. M., and Miyamoto, S. (2014). Hexokinase-II positively regulates glucose starvation-induced autophagy through TORC1 inhibition. Molecular cell *53*, 521-533.
205. Roberts, D. J., Tan-Sah, V. P., Smith, J. M., and Miyamoto, S. (2013). Akt phosphorylates HK-II at Thr-473 and increases mitochondrial HK-II association to protect cardiomyocytes. The Journal of biological chemistry *288*, 23798-23806.
206. Robey, R. B., and Hay, N. (2006). Mitochondrial hexokinases, novel mediators of the antiapoptotic effects of growth factors and Akt. Oncogene *25*, 4683-4696.
207. Ros, S., and Schulze, A. (2013). Balancing glycolytic flux: the role of 6-phosphofructo-2-kinase/fructose 2,6-bisphosphatases in cancer metabolism. Cancer & metabolism *1*, 8.
208. Rose, P. G., Nerenstone, S., Brady, M. F., Clarke-Pearson, D., Olt, G., Rubin, S. C., Moore, D. H., Small, J. M., and Gynecologic Oncology, G. (2004). Secondary surgical cytoreduction for advanced ovarian carcinoma. The New England journal of medicine *351*, 2489-2497.
209. Rosen, D. G., Yang, G., Liu, G., Mercado-Uribe, I., Chang, B., Xiao, X. S., Zheng, J., Xue, F. X., and Liu, J. (2009). Ovarian cancer: pathology, biology, and disease models. Frontiers in bioscience *14*, 2089-2102.
210. Rust, H. L., and Thompson, P. R. (2011). Kinase consensus sequences: a breeding ground for crosstalk. ACS chemical biology *6*, 881-892.
211. Sakai, W., Swisher, E. M., Karlan, B. Y., Agarwal, M. K., Higgins, J., Friedman, C., Villegas, E., Jacquemont, C., Farrugia, D. J., Couch, F. J., *et al.* (2008). Secondary mutations as a mechanism of cisplatin resistance in BRCA2-mutated cancers. Nature *451*, 1116-1120.
212. Salani, B., Marini, C., Rio, A. D., Ravera, S., Massollo, M., Orengo, A. M., Amaro, A., Passalacqua, M., Maffioli, S., Pfeffer, U., *et al.* (2013). Metformin impairs glucose consumption and survival in Calu-1 cells by direct inhibition of hexokinase-II. Scientific reports *3*, 2070.
213. Sarbassov, D. D., Guertin, D. A., Ali, S. M., and Sabatini, D. M. (2005). Phosphorylation and regulation of Akt/PKB by the rictor-mTOR complex. Science *307*, 1098-1101.
214. Sasaki, H., Sheng, Y., Kotsuji, F., and Tsang, B. K. (2000). Down-regulation of X-linked inhibitor of apoptosis protein induces apoptosis in chemoresistant human ovarian cancer cells. Cancer research *60*, 5659-5666.
215. Sato, N., Tsunoda, H., Nishida, M., Morishita, Y., Takimoto, Y., Kubo, T., and Noguchi, M. (2000). Loss of heterozygosity on 10q23.3 and mutation of the tumor suppressor gene PTEN in benign endometrial cyst of the ovary: possible sequence progression from benign endometrial cyst to endometrioid carcinoma and clear cell carcinoma of the ovary. Cancer research *60*, 7052-7056.

216. Sato, S., and Itamochi, H. (2014). Neoadjuvant chemotherapy in advanced ovarian cancer: latest results and place in therapy. Therapeutic advances in medical oncology *6*, 293-304.
217. Sax, J. K., Fei, P., Murphy, M. E., Bernhard, E., Korsmeyer, S. J., and El-Deiry, W. S. (2002). BID regulation by p53 contributes to chemosensitivity. Nature cell biology *4*, 842-849.
218. Scheid, M. P., and Woodgett, J. R. (2001). PKB/AKT: functional insights from genetic models. Nature reviews Molecular cell biology *2*, 760-768.
219. Sekulic, A., Hudson, C. C., Homme, J. L., Yin, P., Otterness, D. M., Karnitz, L. M., and Abraham, R. T. (2000). A direct linkage between the phosphoinositide 3-kinase-AKT signaling pathway and the mammalian target of rapamycin in mitogen-stimulated and transformed cells. Cancer research *60*, 3504-3513.
220. Semenza, G. L. (2013). HIF-1 mediates metabolic responses to intratumoral hypoxia and oncogenic mutations. The Journal of clinical investigation *123*, 3664-3671.
221. Sheikh-Hamad, D., Cacini, W., Buckley, A. R., Isaac, J., Truong, L. D., Tsao, C. C., and Kishore, B. K. (2004). Cellular and molecular studies on cisplatin-induced apoptotic cell death in rat kidney. Archives of toxicology *78*, 147-155.
222. Shen, D. W., Fojo, A., Chin, J. E., Roninson, I. B., Richert, N., Pastan, I., and Gottesman, M. M. (1986). Human multidrug-resistant cell lines: increased mdr1 expression can precede gene amplification. Science *232*, 643-645.
223. Shen, D. W., Pouliot, L. M., Hall, M. D., and Gottesman, M. M. (2012). Cisplatin resistance: a cellular self-defense mechanism resulting from multiple epigenetic and genetic changes. Pharmacol Rev *64*, 706-721.
224. Shih, I. M., and Kurman, R. J. (2004). p63 expression is useful in the distinction of epithelioid trophoblastic and placental site trophoblastic tumors by profiling trophoblastic subpopulations. The American journal of surgical pathology *28*, 1177-1183.
225. Shoshan, M. C. (2012). 3-Bromopyruvate: targets and outcomes. Journal of bioenergetics and biomembranes *44*, 7-15.
226. Siddik, Z. H. (2003). Cisplatin: mode of cytotoxic action and molecular basis of resistance. Oncogene *22*, 7265-7279.
227. Siegel, R. L., Miller, K. D., and Jemal, A. (2017). Cancer Statistics, 2017. CA: a cancer journal for clinicians *67*, 7-30.
228. Simon, R., Radmacher, M. D., Dobbin, K., and McShane, L. M. (2003). Pitfalls in the use of DNA microarray data for diagnostic and prognostic classification. Journal of the National Cancer Institute *95*, 14-18.
229. Singer, G., Kurman, R. J., Chang, H. W., Cho, S. K., and Shih Ie, M. (2002). Diverse tumorigenic pathways in ovarian serous carcinoma. The American journal of pathology *160*, 1223-1228.
230. Singer, G., Oldt, R., 3rd, Cohen, Y., Wang, B. G., Sidransky, D., Kurman, R. J., and Shih Ie, M. (2003). Mutations in BRAF and KRAS characterize the development of low-grade ovarian serous carcinoma. Journal of the National Cancer Institute *95*, 484-486.
231. Singer, G., Stohr, R., Cope, L., Dehari, R., Hartmann, A., Cao, D. F., Wang, T. L., Kurman, R. J., and Shih Ie, M. (2005). Patterns of p53 mutations separate ovarian serous borderline tumors and low- and high-grade carcinomas and provide support for a new model of ovarian carcinogenesis: a mutational analysis with immunohistochemical correlation. The American journal of surgical pathology *29*, 218-224.
232. Skirnisdottir, I., Seidal, T., Gerdin, E., and Sorbe, B. (2002). The prognostic importance of p53, bcl-2, and bax in early stage epithelial ovarian carcinoma treated with adjuvant chemotherapy. International journal of gynecological cancer : official journal of the International Gynecological Cancer Society *12*, 265-276.

233. Skirnisdottir, I., Seidal, T., Karlsson, M. G., and Sorbe, B. (2005). Clinical and biological characteristics of clear cell carcinomas of the ovary in FIGO stages I-II. International journal of oncology *26*, 177-183.
234. Society, A. C. (2014a). Chemotherapy for ovarian cancer. In, (Georgia, Atlanta, USA: American Cancer Society).
235. Society, A. C. (2014b). What are the key statistics about ovarian cancer. In, (American Cancer Society).
236. Society, A. C. (2018). Key statistics for ovarian cnacer. In, A.C. Society, ed. (Atlanta, Georgia).
237. Soderberg, O., Gullberg, M., Jarvius, M., Ridderstrale, K., Leuchowius, K. J., Jarvius, J., Wester, K., Hydbring, P., Bahram, F., Larsson, L. G., and Landegren, U. (2006). Direct observation of individual endogenous protein complexes in situ by proximity ligation. Nature methods *3*, 995-1000.
238. St-Pierre, J., Drori, S., Uldry, M., Silvaggi, J. M., Rhee, J., Jager, S., Handschin, C., Zheng, K., Lin, J., Yang, W., *et al.* (2006). Suppression of reactive oxygen species and neurodegeneration by the PGC-1 transcriptional coactivators. Cell *127*, 397-408.
239. Staal, S. P., Hartley, J. W., and Rowe, W. P. (1977). Isolation of transforming murine leukemia viruses from mice with a high incidence of spontaneous lymphoma. Proceedings of the National Academy of Sciences of the United States of America *74*, 3065-3067.
240. Stokoe, D., Stephens, L. R., Copeland, T., Gaffney, P. R., Reese, C. B., Painter, G. F., Holmes, A. B., McCormick, F., and Hawkins, P. T. (1997). Dual role of phosphatidylinositol-3,4,5-trisphosphate in the activation of protein kinase B. Science *277*, 567-570.
241. Strum, S. B., Adalsteinsson, O., Black, R. R., Segal, D., Peress, N. L., and Waldenfels, J. (2013). Case report: Sodium dichloroacetate (DCA) inhibition of the "Warburg Effect" in a human cancer patient: complete response in non-Hodgkin's lymphoma after disease progression with rituximab-CHOP. Journal of bioenergetics and biomembranes *45*, 307-315.
242. Suh, D. H., Kim, M. A., Kim, H., Kim, M. K., Kim, H. S., Chung, H. H., Kim, Y. B., and Song, Y. S. (2014). Association of overexpression of hexokinase II with chemoresistance in epithelial ovarian cancer. Clin Exp Med *14*, 345-353.
243. Sun, L., Shukair, S., Naik, T. J., Moazed, F., and Ardehali, H. (2008). Glucose phosphorylation and mitochondrial binding are required for the protective effects of hexokinases I and II. Molecular and cellular biology *28*, 1007-1017.
244. Sun, L., Yin, Y., Clark, L. H., Sun, W., Sullivan, S. A., Tran, A. Q., Han, J., Zhang, L., Guo, H., Madugu, E., *et al.* (2017). Dual inhibition of glycolysis and glutaminolysis as a therapeutic strategy in the treatment of ovarian cancer. Oncotarget *8*, 63551-63561.
245. Susin, S. A., Lorenzo, H. K., Zamzami, N., Marzo, I., Snow, B. E., Brothers, G. M., Mangion, J., Jacotot, E., Costantini, P., Loeffler, M., *et al.* (1999). Molecular characterization of mitochondrial apoptosis-inducing factor. Nature *397*, 441-446.
246. Swiecicki, P. L., Bellile, E., Sacco, A. G., Pearson, A. T., Taylor, J. M., Jackson, T. L., Chepeha, D. B., Spector, M. E., Shuman, A., Malloy, K., *et al.* (2016). A phase II trial of the BCL-2 homolog domain 3 mimetic AT-101 in combination with docetaxel for recurrent, locally advanced, or metastatic head and neck cancer. Investigational new drugs *34*, 481-489.
247. Tabas, I., and Ron, D. (2011). Integrating the mechanisms of apoptosis induced by endoplasmic reticulum stress. Nature cell biology *13*, 184-190.
248. Tartaglia, L. A., Rothe, M., Hu, Y. F., and Goeddel, D. V. (1993). Tumor necrosis factor's cytotoxic activity is signaled by the p55 TNF receptor. Cell *73*, 213-216.
249. Taylor, R. C., Cullen, S. P., and Martin, S. J. (2008). Apoptosis: controlled demolition at the cellular level. Nature reviews Molecular cell biology *9*, 231-241.

250. Tentler, J. J., Tan, A. C., Weekes, C. D., Jimeno, A., Leong, S., Pitts, T. M., Arcaroli, J. J., Messersmith, W. A., and Eckhardt, S. G. (2012). Patient-derived tumour xenografts as models for oncology drug development. Nature reviews Clinical oncology *9*, 338-350.
251. Thorens, B., and Mueckler, M. (2010). Glucose transporters in the 21st Century. American journal of physiology Endocrinology and metabolism *298*, E141-145.
252. Tomita, Y., Marchenko, N., Erster, S., Nemajerova, A., Dehner, A., Klein, C., Pan, H., Kessler, H., Pancoska, P., and Moll, U. M. (2006). WT p53, but not tumor-derived mutants, bind to Bcl2 via the DNA binding domain and induce mitochondrial permeabilization. The Journal of biological chemistry *281*, 8600-8606.
253. Topp, M. D., Hartley, L., Cook, M., Heong, V., Boehm, E., McShane, L., Pyman, J., McNally, O., Ananda, S., Harrell, M., *et al.* (2014). Molecular correlates of platinum response in human high-grade serous ovarian cancer patient-derived xenografts. Molecular oncology *8*, 656-668.
254. Tsuyoshi, H., Wong, V. K. W., Han, Y., Orisaka, M., Yoshida, Y., and Tsang, B. K. (2017). Saikosaponin-d, a calcium mobilizing agent, sensitizes chemoresistant ovarian cancer cells to cisplatin-induced apoptosis by facilitating mitochondrial fission and G2/M arrest. Oncotarget *8*, 99825-99840.
255. Uekuri, C., Shigetomi, H., Ono, S., Sasaki, Y., Matsuura, M., and Kobayashi, H. (2013). Toward an understanding of the pathophysiology of clear cell carcinoma of the ovary (Review). Oncology letters *6*, 1163-1173.
256. van der Vos, K. E., and Coffer, P. J. (2011). The extending network of FOXO transcriptional target genes. Antioxidants & redox signaling *14*, 579-592.
257. Vander Heiden, M. G., Cantley, L. C., and Thompson, C. B. (2009). Understanding the Warburg effect: the metabolic requirements of cell proliferation. Science *324*, 1029-1033.
258. Vander Heiden, M. G., Chandel, N. S., Li, X. X., Schumacker, P. T., Colombini, M., and Thompson, C. B. (2000). Outer mitochondrial membrane permeability can regulate coupled respiration and cell survival. Proceedings of the National Academy of Sciences of the United States of America *97*, 4666-4671.
259. Vang, R., Shih Ie, M., and Kurman, R. J. (2009). Ovarian low-grade and high-grade serous carcinoma: pathogenesis, clinicopathologic and molecular biologic features, and diagnostic problems. Advances in anatomic pathology *16*, 267-282.
260. Vanhaesebroeck, B., and Alessi, D. R. (2000). The PI3K-PDK1 connection: more than just a road to PKB. The Biochemical journal *346 Pt 3*, 561-576.
261. Vanhaesebroeck, B., Guillermet-Guibert, J., Graupera, M., and Bilanges, B. (2010). The emerging mechanisms of isoform-specific PI3K signalling. Nature reviews Molecular cell biology *11*, 329-341.
262. Venkitaraman, A. R. (2002). Cancer susceptibility and the functions of BRCA1 and BRCA2. Cell *108*, 171-182.
263. Venkitaraman, A. R. (2014). Cancer suppression by the chromosome custodians, BRCA1 and BRCA2. Science *343*, 1470-1475.
264. Vergote, I., Trope, C. G., Amant, F., Kristensen, G. B., Ehlen, T., Johnson, N., Verheijen, R. H., van der Burg, M. E., Lacave, A. J., Panici, P. B., *et al.* (2010). Neoadjuvant chemotherapy or primary surgery in stage IIIC or IV ovarian cancer. The New England journal of medicine *363*, 943-953.
265. Vieira, H. L., Haouzi, D., El Hamel, C., Jacotot, E., Belzacq, A. S., Brenner, C., and Kroemer, G. (2000). Permeabilization of the mitochondrial inner membrane during apoptosis: impact of the adenine nucleotide translocator. Cell death and differentiation *7*, 1146-1154.
266. Vousden, K. H., and Lu, X. (2002). Live or let die: the cell's response to p53. Nature reviews Cancer *2*, 594-604.

267. Vousden, K. H., and Ryan, K. M. (2009). p53 and metabolism. Nature reviews Cancer *9*, 691-700.
268. Vyssokikh, M. Y., and Brdiczka, D. (2003). The function of complexes between the outer mitochondrial membrane pore (VDAC) and the adenine nucleotide translocase in regulation of energy metabolism and apoptosis. Acta biochimica Polonica *50*, 389-404.
269. Wang, D., and Lippard, S. J. (2005). Cellular processing of platinum anticancer drugs. Nature reviews Drug discovery *4*, 307-320.
270. Wang, G. L., Jiang, B. H., Rue, E. A., and Semenza, G. L. (1995). Hypoxia-inducible factor 1 is a basic-helix-loop-helix-PAS heterodimer regulated by cellular O2 tension. Proceedings of the National Academy of Sciences of the United States of America *92*, 5510-5514.
271. Wang, G. L., and Semenza, G. L. (1995). Purification and characterization of hypoxia-inducible factor 1. The Journal of biological chemistry *270*, 1230-1237.
272. Wang, L., Xiong, H., Wu, F., Zhang, Y., Wang, J., Zhao, L., Guo, X., Chang, L. J., Zhang, Y., You, M. J., *et al.* (2014). Hexokinase 2-mediated Warburg effect is required for PTEN- and p53-deficiency-driven prostate cancer growth. Cell Rep *8*, 1461-1474.
273. Wang, X., Zhang, F., and Wu, X. R. (2017). Inhibition of Pyruvate Kinase M2 Markedly Reduces Chemoresistance of Advanced Bladder Cancer to Cisplatin. Scientific reports *7*, 45983.
274. Warburg, O. (1956). On the origin of cancer cells. Science *123*, 309-314.
275. Webb, A. E., and Brunet, A. (2014). FOXO transcription factors: key regulators of cellular quality control. Trends in biochemical sciences *39*, 159-169.
276. West, K. A., Castillo, S. S., and Dennis, P. A. (2002). Activation of the PI3K/Akt pathway and chemotherapeutic resistance. Drug resistance updates : reviews and commentaries in antimicrobial and anticancer chemotherapy *5*, 234-248.
277. Williams, S. A., Anderson, W. C., Santaguida, M. T., and Dylla, S. J. (2013). Patient-derived xenografts, the cancer stem cell paradigm, and cancer pathobiology in the 21st century. Laboratory investigation; a journal of technical methods and pathology *93*, 970-982.
278. Wolf, A., Agnihotri, S., Micallef, J., Mukherjee, J., Sabha, N., Cairns, R., Hawkins, C., and Guha, A. (2011). Hexokinase 2 is a key mediator of aerobic glycolysis and promotes tumor growth in human glioblastoma multiforme. J Exp Med *208*, 313-326.
279. Wolff, S., Erster, S., Palacios, G., and Moll, U. M. (2008). p53's mitochondrial translocation and MOMP action is independent of Puma and Bax and severely disrupts mitochondrial membrane integrity. Cell Res *18*, 733-744.
280. Wong, J. Y., Huggins, G. S., Debidda, M., Munshi, N. C., and De Vivo, I. (2008). Dichloroacetate induces apoptosis in endometrial cancer cells. Gynecologic oncology *109*, 394-402.
281. Xie, H., Valera, V. A., Merino, M. J., Amato, A. M., Signoretti, S., Linehan, W. M., Sukhatme, V. P., and Seth, P. (2009). LDH-A inhibition, a therapeutic strategy for treatment of hereditary leiomyomatosis and renal cell cancer. Molecular cancer therapeutics *8*, 626-635.
282. Yamaguchi, R., Lartigue, L., Perkins, G., Scott, R. T., Dixit, A., Kushnareva, Y., Kuwana, T., Ellisman, M. H., and Newmeyer, D. D. (2008). Opa1-mediated cristae opening is Bax/Bak and BH3 dependent, required for apoptosis, and independent of Bak oligomerization. Molecular cell *31*, 557-569.
283. Yang, X., Fraser, M., Abedini, M. R., Bai, T., and Tsang, B. K. (2008). Regulation of apoptosis-inducing factor-mediated, cisplatin-induced apoptosis by Akt. British journal of cancer *98*, 803-808.

284. Yang, X., Fraser, M., Moll, U. M., Basak, A., and Tsang, B. K. (2006). Akt-mediated cisplatin resistance in ovarian cancer: modulation of p53 action on caspase-dependent mitochondrial death pathway. Cancer research *66*, 3126-3136.
285. Younes, M., Brown, R. W., Mody, D. R., Fernandez, L., and Laucirica, R. (1995). GLUT1 expression in human breast carcinoma: correlation with known prognostic markers. Anticancer research *15*, 2895-2898.
286. Yuan, Z. Q., Sun, M., Feldman, R. I., Wang, G., Ma, X., Jiang, C., Coppola, D., Nicosia, S. V., and Cheng, J. Q. (2000). Frequent activation of AKT2 and induction of apoptosis by inhibition of phosphoinositide-3-OH kinase/Akt pathway in human ovarian cancer. Oncogene *19*, 2324-2330.
287. Yun, J., Rago, C., Cheong, I., Pagliarini, R., Angenendt, P., Rajagopalan, H., Schmidt, K., Willson, J. K., Markowitz, S., Zhou, S., *et al.* (2009). Glucose deprivation contributes to the development of KRAS pathway mutations in tumor cells. Science *325*, 1555-1559.
288. Zhang, C., Liu, J., Liang, Y., Wu, R., Zhao, Y., Hong, X., Lin, M., Yu, H., Liu, L., Levine, A. J., *et al.* (2013). Tumour-associated mutant p53 drives the Warburg effect. Nature communications *4*, 2935.
289. Zhang, C., Zhang, D., and Cheng, J. X. (2015). Coherent Raman Scattering Microscopy in Biology and Medicine. Annual review of biomedical engineering *17*, 415-445.
290. Zhang, K., Chew, M., Yang, E. B., Wong, K. P., and Mack, P. (2001). Modulation of cisplatin cytotoxicity and cisplatin-induced DNA cross-links in HepG2 cells by regulation of glutathione-related mechanisms. Molecular pharmacology *59*, 837-843.
291. Zhang, Y., and Yang, J. H. (2013). Activation of the PI3K/Akt pathway by oxidative stress mediates high glucose-induced increase of adipogenic differentiation in primary rat osteoblasts. Journal of cellular biochemistry *114*, 2595-2602.
292. Zhao, H., and Piwnica-Worms, H. (2001). ATR-mediated checkpoint pathways regulate phosphorylation and activation of human Chk1. Molecular and cellular biology *21*, 4129-4139.
293. Zhao, Y., Butler, E. B., and Tan, M. (2013). Targeting cellular metabolism to improve cancer therapeutics. Cell death & disease *4*, e532.
294. Zheng, W., Feng, Q., Liu, J., Guo, Y., Gao, L., Li, R., Xu, M., Yan, G., Yin, Z., Zhang, S., *et al.* (2017). Inhibition of 6-phosphogluconate Dehydrogenase Reverses Cisplatin Resistance in Ovarian and Lung Cancer. Frontiers in pharmacology *8*, 421.
295. Zhou, M., Zhao, Y., Ding, Y., Liu, H., Liu, Z., Fodstad, O., Riker, A. I., Kamarajugadda, S., Lu, J., Owen, L. B., *et al.* (2010). Warburg effect in chemosensitivity: targeting lactate dehydrogenase-A re-sensitizes taxol-resistant cancer cells to taxol. Molecular cancer *9*, 33.
296. Zhou, Y., Lu, N., Qiao, C., Ni, T., Li, Z., Yu, B., Guo, Q., and Wei, L. (2016). FV-429 induces apoptosis and inhibits glycolysis by inhibiting Akt-mediated phosphorylation of hexokinase II in MDA-MB-231 cells. Molecular carcinogenesis *55*, 1317-1328.
297. Zhou, Y., Tozzi, F., Chen, J., Fan, F., Xia, L., Wang, J., Gao, G., Zhang, A., Xia, X., Brasher, H., *et al.* (2012). Intracellular ATP levels are a pivotal determinant of chemoresistance in colon cancer cells. Cancer research *72*, 304-314.

Chapter 7. Appendices

Appendix 1: Characterization of experimental OVCA cell lines

OVCA cell lines used are described depending on p53 status, other mutation sites, and chemosensitivity based on previous sequencing data and experiments for apoptotic measurement (Abedini et al., 2014; Fraser et al., 2008). Characterization of these cell lines are also verified in previous literatures (Anglesio et al., 2013; Leroy et al., 2014).

Appendix 1: Characterization of experimental cell lines

Cell line	**Tumor origin**	***TP53* status**	**Other**	**Chemosensitivity***
A2780s	Ovarian endometroid adenocarcinoma	Wild type	*PTEN/ARID1A*	Sensitive
A2780cp	Ovarian endometroid adenocarcinoma	Mutant V127F R260S	*PTEN/ARID1A*	Resistant
Hey	Ovarian serous cyst adenocarcinoma	Wild type	*KRAS*	Resistant
SKOV3	Ovarian endometroid adenocarcinoma	Null	*PI3KCIA/ARID1A*	Resistant
OVCAR-3	Ovarian endometroid adenocarcinoma	Mutant R248Q	None Detected	Resistant
PA-1	Ovarian endometroid adenocarcinoma	Wild type	None Detected	Sensitive
ES2	Ovarian clear cell carcinoma	Mutant S241F	*BRAF*	Resistant

Chapter 8. Curriculum Vitae

Chae Young Han

Ph. D Candidate, Department of Cellular and Molecular Medicine,

University of Ottawa, The Ottawa Hospital Research Institute, Ottawa, Ontario, Canada

EDUCATION

Sep 2013-Present	**Graduate student (Ph. D program), Cellular & Molecular Medicine** University of Ottawa, Ottawa, Canada Chronic Disease Program, Ottawa Hospital Research Institute Thesis advisor: Dr. Benjamin K Tsang Thesis: The Role of Hexokinase II in the Regulation of Glycolysis and Cisplatin Sensitivity in Ovarian Cancer
May 2011-Apr 2013	**Master of Science in Microbiology & Immunology** University of Western Ontario, London, Canada Thesis advisor: Dr. Sung O. Kim Thesis: Cellular adaptation of macrophages to anthrax lethal toxin-induced pyroptosis via epigenetic mechanism
Sep 2002- Sep 2005	**Bachelor of Science in Biology & Chemistry** Univ. of Illinois at Urbana-Champaign, Urbana, Illinois, USA
Mar 2000-Sep 2002	**Biotechnology** Seoul Women's University, Seoul, Korea (Transferred to University of Illinois)

PEER-REVIEWED PUBLICATIONS

Jung Jin Lim, **Chae Young Han**, Dong Ryul Lee, and Benjamin K. Tsang. RNF6 mediates androgen-induced granulosa cell proliferation and follicle growth via modulation of androgen receptor signaling. *Endocrinology* 158(4):993-1004 (2017)

Ha, S.D*, **Han, C.Y*, (Co-1st author),** Marie Reid. Chantelle. & Kim, S.O. HDAC8-mediated epigenetic reprogramming plays a key role in resistance to anthrax lethal toxin-induced pyroptosis in macrophages. *Journal of Immunology* 193(3):1333–1343(2014)

Ha, S.D, Park S.W, **Han, C.Y,** Nguyen, M. L. & Kim, S. O. Cellular adaptation to anthrax lethal toxin-induced mitochondrial cholesterol enrichment, hyperpolarization, and reactive

oxygen species generation through downregulating MLN64 in macrophages. *Mol. Cell. Biol.* **32**, 4846-4860 (2012).

Chae Young Han, David A. Patten, Richard B. Richardson, Mary-Ellen Harper, and Benjamin K Tsang, *Genes & Cancer* (In Press, 2018). Tumor metabolism regulating chemoresistance in ovarian cancer (Invited review)

MANUSCRIPT IN PREPARATIONS

1. **Chae Young Han**, David A Patten, Youngjin Han, Jung Jin Lim, Ja-Lok, Ku, Elizabeth A. Macdonald, Barbara Vanderhyden, Yong Sang Song, Mary-Ellen Harper, and Benjamin K. Tsang, **p53 regulates HK2 intracellular trafficking and gene expression in metabolic reprogramming and chemosensitivity in ovarian cancer**, Manuscript in preparation (Jan 2019)

2. **Chae Young Han**, David A Patten, Se Ik Kim, Jung Jin Lim, Michelle K Y Siu, Youngjin Han, Euridice Carmona, Robin Parks, Cheol Lee, Karen KL Chan , Ja-Lok, Ku, Elizabeth A. Macdonald, Barbara Vanderhyden, Anne Marie Mes-Masson, Hextan Y. S. Ngan, Annie Cheung, Yong Sang Song, Mary-Ellen Harper, and Benjamin K. Tsang, **Nuclear HKII-P-p53 interaction is a determinant for metabolic regulation and chemosensitivity as potential biomarker in ovarian cancer**, Manuscript in preparation (Dec2018)

3. Yize Zhang*, **Chae Young Han*** (**Co-1st author**), Fu Gang Duan, Xing-Xing Fan, Xiao-Jun Yao, Robin J Parks, Yi-Jun Tang, Mei-Fang Wang, Liang Liu, Benjamin K. Tsang, and Elaine Lai-Han Leung in collaboration with Macau University of Science and technology, **p53 regulates EGFR via modulation of reactive oxygen species production in chemoresistant non-small cell lung cancer**, submitted to *International Journal of Cancer* (Nov 2018)

HONORS & AWARDS

2018	Research travel grant (Univ. of Ottawa)
2017	FGPS & CMM Travel award (Univ. of Ottawa)
2014-2018	Admission Scholarship (Univ. of Ottawa)
2011-2013	Schulich & Western Graduate Research Scholarship (Univ. of Western Ontario)

ORAL PRESENTATIONS

Reproductive Biology Work-In-Progress Meeting (May 2017)**: Han CY**, Benjamin K Tsang. The Role of Hexokinase II in the regulation of aerobic glycolysis and cisplatin

sensitivity in ovarian carcinoma cells, Cancer Therapeutic Program, Ottawa Hospital Research Institute, General Campus

Cancer Group Work-In-Progress Meeting (Apr 2015-2017)**: Han CY**, Benjamin K Tsang. The Role of Hexokinase II in the regulation of aerobic glycolysis and cisplatin sensitivity in ovarian carcinoma cells, Cancer Therapeutic Program, Ottawa Hospital Research Institute, General Campus

POSTER PRESENTATIONS

Han CY, BK Tsang (Mar 2017). The role and regulation of Hexokinase II in aerobic glycolysis and cisplatin sensitivity in ovarian cancer cells. **Keystone symposium** (Tumor metabolism: mechanisms & targets), Whistler, BC, Canada

Han CY, BK Tsang (Nov. 2014-Nov. 2016). The role and regulation of Hexokinase II in aerobic glycolysis and cisplatin sensitivity in ovarian cancer cells. OHRI research day, Ottawa Hospital Research Institute

Han CY, Ha SD, Cherie Tan, & Kim SO (Nov. 2011-2012). Cellular adaptation of macrophages to anthrax lethal toxin-induced cytolysis through epigenetic mechanisms, Infection & Immunity Research Forum, University of Western Ontario

RESEARCH & LABORATORY EXPERIENCE

Sep 2013-Present	**Graduate student & Research Assistant (Ph.D Student)** Principal Investigator: Dr. Benjamin K Tsang, OHRI **To examine the role of Hexokinase II in the regulation of glycolysis and cisplatin sensitivity**
May 2011-Apr 2013	**Graduate Student (Master of Science)** Principal Investigator: Dr. Sung O Kim, Microbiology & Immunology, University of Western Ontario **To examine epigenetic mechanism of Anthrax lethal toxin on murine macrophage**
Dec 2002 – Jan 2005	**Undergraduate Research Assistant** Principal Investigator: Dr. Raymond Zielinski, Plant molecular biology, University of Illinois **To identify interacting proteins with Cam9 in Arabidopsis thaliana**

PROFESSIONAL EXPERIENCES

2010-2011 Clinical Safety Associate, Novartis (Seoul, South Korea)

2008-2010 Regulatory Affairs Associate, Hanmi Pharm. (Seoul, South Korea)

TEACHING EXPERIENCE

2015 –2017 Dr. Benjamin K. Tsang lab, Ottawa Hospital Research Institute
Mentoring master (international exchange program), graduate, summer undergraduate students

2008- 2010 Dr. Sung O. Kim Lab, Univ. of Western Ontario
Mentoring NSERC and undergraduate students

LEADERSHIP ROLE

2015-Present Lab safety officer

2014-Present Cell line maintenance and transportation (cells / sample shipment) officer

2014-2015 Procurement officer (product ordering / communication with vendors)

Apr, 2014 Member of organizing committee for the International Workshop on Women's Reproductive Health Research